LAWRENCE
LIVERMORE
NATIONAL
LABORATORY

UCRL-TR-218504

FY05 LDRD Final Report, A Revolution in Biological Imaging

H. N. Chapman, S. Bajt, R. Balhorn, A. Barty, D. Barsky, M. Bogan, S.-W. Chung, M. Frank, S. Hau-Riege, H. Ishii, R. London, S. Marchesini, A. Noy, B. Segelke, A. Szoke, H. Szoke, J. Trebes, A. Wootton, J. Hajdu, M. Bergh, C. Caleman, G. Huldt, S. Lejon, D. van der Spoel, M. Howells, H. He, J. Spence, K. Nugent, E. Ingerman

January 30, 2006

This work was performed under the auspices of the U.S. Department of Energy by University of California, Lawrence Livermore National Laboratory under Contract W-7405-Eng-48.

FY05 LDRD Final Report

A Revolution in Biological Imaging

LDRD Project Tracking Code: 02-ERD-047

Principal Investigator: Henry Chapman,

Co-Investigators:

Saša Bajt, Rodney Balhorn, Anton Barty, Daniel Barsky, Michael Bogan, Sung-Wook Chung, Matthias Frank, Stefan Hau-Riege, Hope Ishii, Richard London, Stefano Marchesini, Aleksandr Noy, Brent Segelke, Abraham Szőke, Hanna Szőke, Jim Trebes, Alan Wootton (LLNL); Janos Hajdu (University of Uppsala)

Collaborators:

Magnus Bergh, Calle Caleman, Gösta Huldt, Sara Lejon, David van der Spoel (Univeristy of Uppsala); Malcolm Howells, Haifeng He (LBNL); John Spence (Arizona State University); Keith Nugent (University of Melbourne); Eugene Ingerman (UC Davis)

Abstract

X-ray free-electron lasers (XFELs) are currently under development and will provide a peak brightness more than 10 orders of magnitude higher than modern synchrotrons. The goal of this project was to perform the fundamental research to evaluate the possibility of harnessing these unique x-ray sources to image single biological particles and molecules at atomic resolution. Using a combination of computational modelling and experimental verification where possible, we showed that it should indeed be possible to record coherent scattering patterns from single molecules with pulses that are shorter than the timescales for the degradation of the structure due to the interaction with those pulses. We used these models to determine the effectiveness of strategies to allow imaging using longer XFEL pulses and to design validation experiments to be carried out at interim ultrafast sources. We also developed and demonstrated methods to recover three-dimensional (3D) images from coherent diffraction patterns, similar to those expected from XFELs. Our images of micron-sized test objects are the highest-resolution 3D images of any noncrystalline material ever formed with x rays. The project resulted in 14 publications in peer-reviewed journals and four records of invention.

Table of Contents

1. BACKGROUND 3

1.1. FOURTH GENERATION LIGHT SOURCES 7
1.2. COMPARISION WITH EXISTING TECHNIQUES 9

2. RESEARCH AND RESULTS 13

2.1. BIOLOGICAL MODELING 14
2.2. HYDRODYNAMIC MODEL FOR X-RAY IRRADIATED BIOLOGICAL MOLECULES 14
2.3. EFFECT OF DAMAGE ON IMAGING AND CLASSIFICATION 18
2.3.1. Image Classification 18
2.3.2. Computer Requirements for Image Classification 20
2.3.3. Effect of Irradiation-Induced Damage on Image Quality 21
2.3.4. Convolution of Damage and Classification Models 23
2.3.5. Mapping of Resolution for Different Biological Molecules 23
2.4. DYNAMICS OF BULK MATERIALS 24
2.5. IMAGE RECONSTRUCTION 26
2.5.1. The Shrinkwrap Iterative Algorithm 27
2.5.2. Real-Space Algorithm 28
2.6. ALS EXPERIMENTS 28

3. EXIT PLAN 30

SUMMARY 32

ACKNOWLEDGEMENTS 33

REFERENCES 34

A. PUBLICATIONS FROM THE PROJECT 36

A.1. PAPERS TO PEER-REVIEWED JOURNALS 36
A.2. INVITED PRESENTATIONS 37
A.3. OTHER PRESENTATIONS 37
A.4. RECORDS OF INVENTION 38
A.5. TECHNICAL REPORTS 38

B. VUV-FEL PROPOSALS AND REVIEW 39

B.1. BIOLOGICAL IMAGING IN THE VUV-FEL (OVERVIEW) 42
B.2. COULOMB EXPLOSIONS OF BIOLOGICAL SAMPLES 43
B.3. DIFFRACTION IMAGING OF BIOLOGICAL SAMPLES 50
B.4. X-RAY INTERACTION WITH MATTER: OPTICS DAMAGE 56

C. LCLS 2004 LETTER OF INTENT 61

LETTER OF INTENT (CATEGORY A): IMAGING OF SINGLE PARTICLES AND BIOMOLECULES AT THE LINAC COHERENT LIGHT SOURCE (LCLS) 61

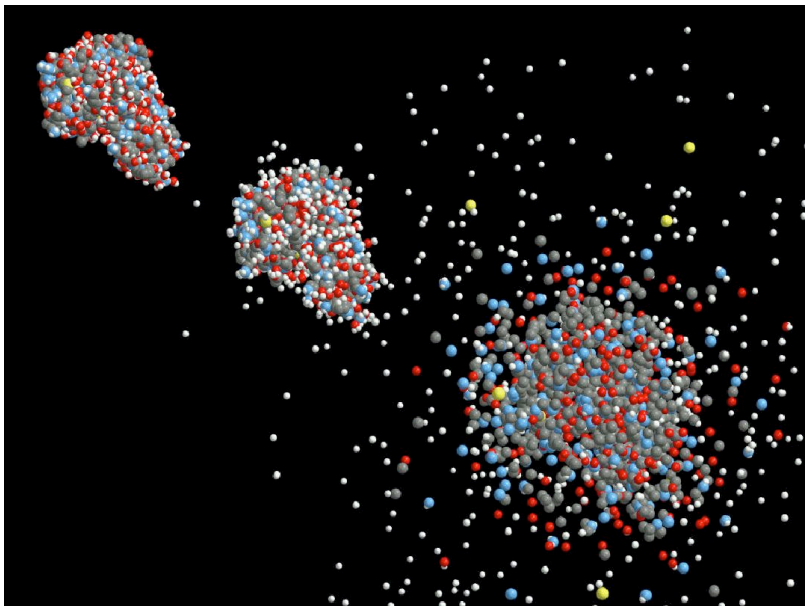

Figure 1. Three snapshots (before, during, and after) interaction of a 50 fs XFEL pulse with a lysozyme molecule (Neutze *et al*., 2000). The atomic coordinates were computed by molecular dynamics simulations. Even after half of the pulse has passed, the distortions are small. After the pulse, the explosion is well under way. The distortion of the molecule during the time of the pulse is considerably smaller for lower flux densities.

1. Background

The current development of fourth-generation light sources, essentially X-ray free electron lasers (XFELs), such as the Linac Coherent Light Source (LCLS) at the Stanford Linear Accelerator Center (SLAC), has sparked many ideas for new science that will be possible with 10 orders of magnitude higher peak X-ray brightness than what is currently available at synchrotrons. One of the most impressive and far-reaching XFEL experiments envisioned is the atomic resolution imaging of single molecules, single virus particles, or nanocrystals (Neutze *et al*, 2000). This ability will revolutionize life sciences by eliminating the need to crystallize biological material to determine its structure. The method relies on being able to record the large-angle diffraction patterns of these weakly scattering particles, which requires incident fluences many orders of magnitude beyond the steady-state radiation damage limit. However, by using XFEL pulses lasting 100 fs or less, such diffraction patterns can be recorded from the molecule or particle before radiation damage completely destroys it (see Figure 1). This is an extreme extension of an idea originating at LLNL and LANL of performing flash imaging to increase resolution by reducing the effects of radiation damage (Solem and Baldwin, 1982 and Solem and Chapline, 1984).

Crystallography is the most successful method for obtaining atomic resolution structure of biological materials (see Sec. 1.2). However, the very essence of crystallography is

also the cause of a large bottleneck in atomic resolution imaging of biological systems, namely the fundamental requirement of crystals. Many biologically important complexes are difficult or even impossible to crystallize. As a consequence, there are large and persistent vacancies in the understanding of the structural basis for the function of biological systems. Furthermore, some of the most important proteins in biology are notoriously difficult to crystallize. Only a handful of membrane protein structures (such as cell surface receptors which are the most common targets for pharmaceuticals) are known, for example, and high-resolution structural studies of large assemblies (for instance, molecular pathogens such as prion amyloid plaques which cause mad cow disease and Alzheimer's disease, molecular machines required for gene function such as the transcriptome, and cell signaling complexes that trigger the host pathogen response) are problematic. The success of crystallography lies in its ability to overcome radiation damage, by spreading the X-ray dose over many ($> 10^9$) identical copies of the molecule and taking advantage of the strong signal that arises from the coherent superposition of X-rays scattered from these elements. However, by performing measurements with ultrashort pulses, we can apply crystallographic techniques to non-repetitive and non-reproducible structures (e.g. cells, viruses, and single macromolecules). The radiation dose required for such "diffraction imaging" (Sayre and Chapman, 1995) will be orders of magnitude above the steady-state damage threshold of about 200–4000 photons/Å^2 (depending on sample size). Initial molecular dynamics calculations (Neutze *et al,* 2000) and our own hydrodynamic models (Sec. 2.2), indicate that, by using X-ray pulses of duration 100 fs or shorter, the tolerable radiation dose of large single molecules will increase by four orders of magnitude to 2×10^7 photons/Å^2. Smaller molecules, such as lysozyme molecules, will explode more quickly, and will require even shorter pulses to obtain the structural information before the motion degrades the resolution. The high-angle (high-resolution) scattering from a single molecule will be extremely weak since, unlike diffraction from a crystal, there will be no coherent addition of scattering from many identical unit cells. The proposed XFELs, with an increase in brightness of 10 orders of magnitude over synchrotron insertion devices, may provide enough photons per pulse to give a measurable atomic-resolution signal.

Atomic-resolution imaging of biological objects will necessarily be "lensless"; a diffraction pattern is recorded and a computer reconstruction algorithm performs the image formation step, replacing the role of a lens. Although the phase information of the diffraction pattern is not recorded, it is possible to reconstruct the complex image of a finite object from the far-field diffracted intensity. For single molecules and other non-periodic objects, the diffracted intensity is not confined to Bragg spots as it is for crystals (see Figure 4). This allows an "oversampling" of the diffraction pattern, and the collection of information not accessible in a crystallographic experiment (Sayre, 1952; Miao, 2000). This additional information is used to constrain the reconstruction of the phase. Studies of this reconstruction technique show that the more *a priori* information about the structure that can be added to the algorithm (e.g. positivity of electron density or constraints on the shape of the object), the better the reconstruction. To be useful, atomic-resolution imaging must be three-dimensional. A single diffraction pattern gives a single 2D view of a 3D object. A full 3D reconstruction can be achieved from diffraction patterns taken from many different orientations of the object. While it might be feasible

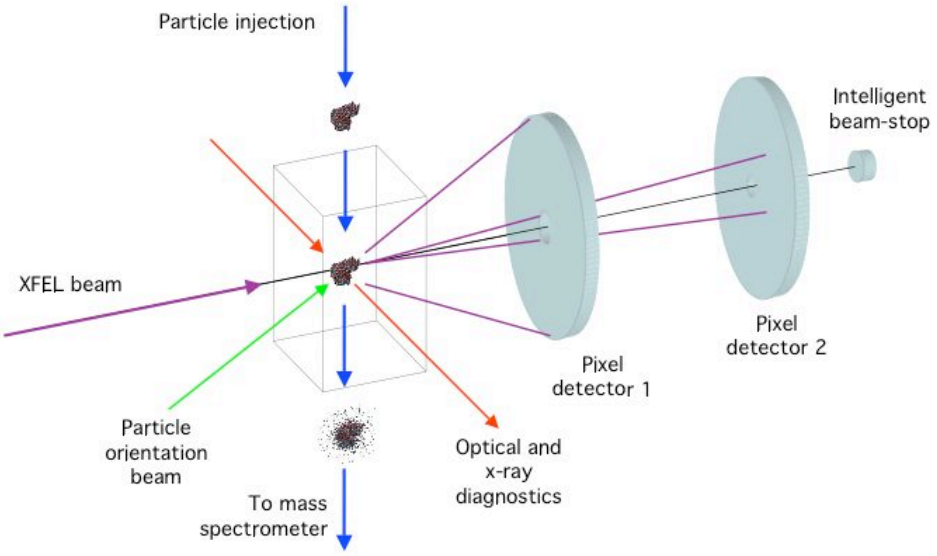

Figure 2. Schematic diagram of the single-particle diffraction imaging experiment at an XFEL. Angle-resolved detectors such as custom CCDs will record the coherent X-ray scattering. The diffraction patterns will be inverted to an image with powerful algorithms. The spatial resolution of the technique depends on the angular acceptance (ie, numerical aperture) of the detector.

to record a small number of views simultaneously with one pulse (after which the object is destroyed), a complete data set will require multiple views obtained from many identical copies of a biological object. With reproducible samples it will become possible to sort images to find those of similar orientation that can then be averaged. The averaging step will be important in order to improve signal to noise and hence improve resolution, and analysis of the problem becomes finding the minimum dose that is required not to image a particle, but to infer its orientation. Hence any method that can be employed to fix a particle's orientation will have a big impact on the technique.

Single-particle scattering experiments offer a host of challenges that need to be addressed before experiments at a 4^{th}-generation source are possible. These include: details of the classification of diffraction patterns and their reconstruction; an understanding of the interaction between the particle and an ultrashort X-ray pulse; methods for extreme focusing of high peak-power pulses and compressing them in time; developing the diagnostics and area detectors required; developing the methods for delivery systems of purified container-free samples, synchronized to the XFEL pulse; and methods to orient particles. In addition imaging methods need to be developed that can make use of longer and perhaps less intense pulses than will be initially available when fourth-generation sources are first brought online. Such methods, based on parallel imaging (using, for example, dip-pen lithography or nanocrystals) will be necessary to demonstrate the

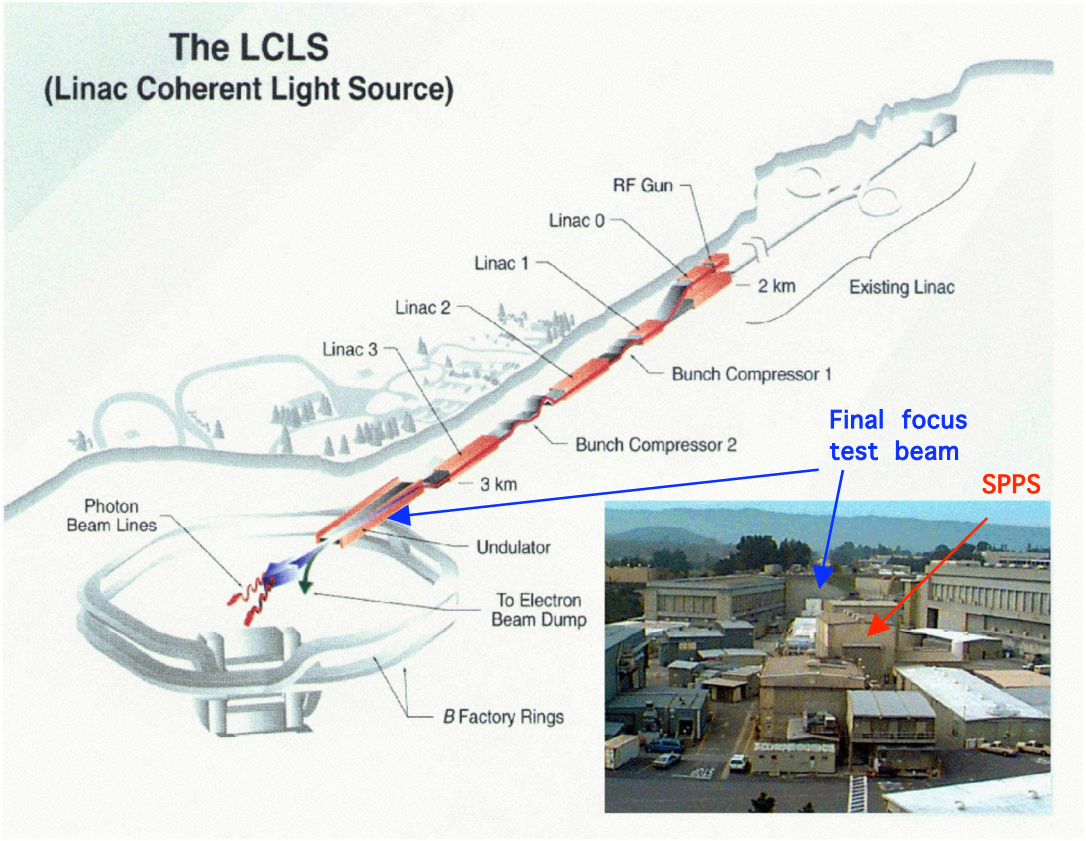

Figure 3. LCLS and SPPS. The Linac Coherent Light Source (LCLS) will be built at the Stanford Linear Accelerator Center (SLAC). The Sub-Picosecond Photon Source (SPPS) is a test source currently operational to enable early learning on Linac sources and short-pulse experiments. It has key features of the LCLS (pulse duration and X-ray wavelength), but it does not lase.

potential of the new sources and to enable the development of the techniques and diagnostics.

Reconstruction methods must be advanced beyond current state-of-the-art. In particular, methods must be developed to determine the relative orientations from low SNR diffraction patterns so they can be combined into 3D reciprocal space. The orientation classification and 3D reconstruction are dependent on each other, so iterative multi-scale, multi-resolution reconstruction algorithms will need to be developed, as well as efficient and parallel methods to perform orientation classification. Effects of experimental limitations need to be examined, such as missing information (e.g. low-resolution data obscured by the intense non-diffracting beam), low photon number statistics of diffraction patterns, homogeneity of samples, number of diffraction patterns, and accuracy of alignment.

The accuracy of the ultrafast simulations of structural damage is not well established, since up until now there has been no source available to experimentally access this short-pulse high-intensity X-ray regime. Experiments and more extended simulations need to

be performed to establish the requirements of the X-ray pulses and diagnostics, and the limitations of the technique. Methods for delivering extremely focused and time-compressed pulses need to be established and tested. The design of X-ray optical elements to perform these tasks will need to address the extreme peak power loading of XFEL pulses which will require new experimental and theoretical guidance. Another challenge along the path to single-particle imaging is sample preparation and handling. Since everything within the beam path will be imaged, including any sample holder or supporting membrane, the sample must be "container-free". It is envisioned that the sample will be sprayed into the XFEL pulse train, perhaps after being purified by passage through a mass spectrometer. Electrospray systems, or micromechanical systems similar to ink-jet nozzles, could be used to deliver the particles. External polarized laser fields could also be used to weakly orient particles. A schematic of the apparatus for XFEL single-particle diffraction imaging is shown in Figure 2. The imaging method relies upon a supply of molecules that are identical in structure, or nearly so. A large variability of structural conformations will cause blurring in the reconstructed image, or potentially prevent reconstruction. Comparisons between structures of molecules in solution, by NMR methods (Sec. 2.2), to crystal structures suggest that macromolecules are rigid, but this crucial point must be studied in detail using molecular dynamics simulations over long time scales.

1.1. Fourth Generation Light Sources

Fourth generation light sources are based on the free-electron laser, which is a general technique for producing coherent radiation from a relativistic electron beam. First generation sources operated parasitically at particle physics facilities, second generation sources are dedicated storage rings, and third generation sources are optimized for insertion devices—wigglers and undulators—which increase X-ray brightness. The free-electron laser (FEL) is based on a high-quality undulator, and requires high energy, low-emittance, and short pulse electron beams that can be generated in linear accelerators. Non-linear interaction between the electron bunches and X-ray emission within the undulator produces X-ray lasing that is coherent, extremely bright, tunable, short pulse (fs), and has peak powers 8 to 10 orders of magnitude higher than existing sources. Advances both in accelerator physics and short-pulse lasers have brought about the possibility of XFELs that operate in the 0.8 to 12 keV range. In this range, an FEL will operate in a single-pass mode called self-amplified spontaneous emission (SASE) (Nuhn, 2000; Pellegrini, 2002). Briefly and simplistically, a relativistic pulse of electrons is propagated through an FEL undulator. The electrons are accelerated by the periodic magnetic field of this device to give synchrotron radiation. The radiation field interacts with the electrons inducing a modulation of the electron density at the same wavelength as the radiation. This causes the electron pulse to form microbunches, with all electrons in a microbunch acting coherently. Once microbunching starts to occur, the effect will amplify itself as the electrons move through the undulator. When saturation is reached, each microbunch acts as a particle of total charge q of the microbunch.

There are many projects in XFEL development (Shen, 2001) (see Table 1). The two biggest are the Linac Coherent Light Source (LCLS) at Stanford (see Figure 3), and the TESLA FEL at DESY in Hamburg, Germany. The LCLS project is a collaboration

Facility	PLEIADES (LLNL Thomson source)	SPPS (at SLAC)	VUV-FEL	APS undulator beamline	XFEL
Operational date	2002	2003-2006	2005	1996	2008
Photon wavelength (Å)	0.1 to 1	0.1 to > 20	60	< 0.5 to 10	0.5 to 15
Pulse length (ps)	~0.1	~0.1	0.4	100	0.01 to 0.23
Beam dimension (μm)	20	200		100	100
Photons/pulse	$10^7 – 10^9$	2×10^8	$2x10^{13}$	$10^4 – 10^5$	$10^{12} – 10^{13}$
Peak Brightness (photons/(s.mm^2 .mrad^2.0.1%bw)	$10^{18} – 10^{20}$	2×10^{24}	10^{29}	10^{19}	10^{33}
Repetition rate (Hz)	10	30	7200 in 0.8 ms, then 88.2 ms break	6×10^6 and 6×10^3	120
Spatial coherence	No	no	Yes	No	Yes
Polarization	No	Linear or circular	Linear	Linear or circular	Linear
Bandwidth (ΔE/E) (%)	10	0.1	0.1	0.1	0.2

Table 1. A comparison of light source parameters. The XFEL will have sufficient peak brightness and short enough pulses for single-molecule imaging at Angstrom wavelengths. Other sources will be invaluable to test techniques and to validate models.

between several DOE laboratories (including LLNL) and is expected to be operating in 2008. The initial specifications of the LCLS are pulses of 230 fs duration with 10^{12} to 10^{13} photons per pulse and photon energies tunable between 0.8 and 24 keV (up to 8 keV in the first harmonic). The energy in a single coherent pulse is ~ 1 mJ which is about 10^{10} greater than what can be achieved in a coherent mode of a third-generation undulator. The LCLS will operate at 100 Hz repetition, and at the exit of the FEL the beam will have a transverse dimension of ~100 μm and a divergence of ~1 μrad. XFEL beams will be so intense that single-pulse specimen and x-ray optics damage become overriding issues. While the extreme intensity enables diffraction signals to be recorded from single molecules in a single pulse, methods need to be created to work with these sources. Plans for future upgrades of the LCLS, driven primarily by the needs of the biological imaging experiment, provide provision for pulse durations less than 1 fs (Cornacchia, 2004).

Other fourth-generation sources are under investigation. X-ray free-electron lasers based on single-pass Linacs such as the LCLS will not be able to provide the MHz repetition rates of synchrotrons due to the amount of power this would consume. The Energy

Recovery Linac (ERL) is a proposed alternative synchrotron radiation source that uses a linac to produce sub-ps electron pulses to generate sub-ps synchrotron pulses (Bilderback, 2001). Although the electron beam is brought to full energy in a single pass of the linac, it is bent back to the entrance of the linac by weak magnets, much like a storage ring. Interspersed in the ring will be undulators to provide the synchrotron radiation. The path of the ring will be chosen so that the electrons are injected back into the linac out of phase to the accelerated beam. In this case the linac acts as a decelerator, so the electron beam transfers energy back to the RF field of the linac. The low-energy electrons will then be dumped, but as much as 99.97% of the energy could be recovered into the linac, allowing it to run at high duty cycle. The proposed ERL will provide pulses on the order of 100 fs, with 10^7 photons per pulse. The source will enable pump-probe experiments at 100 fs resolution, averaged over many pulses. Unlike XFELs, these sources will not be able to exceed the steady-state radiation damage limit. Although the sample will be able to survive the interaction with a single pulse, the need for many, perfectly aligned particles (crystals) is not bypassed. These sources will not have the peak brightness to record diffraction patterns from single molecules but may be extremely useful for X-ray microscopy.

The first attempt to inject short electron pulses into an undulator is the Sub-Picosecond Photon Source (SPPS), a current experiment at SLAC. The SPPS uses the current SLAC linac and will provide early learning for the advanced accelerator physics required for LCLS as well as for short-pulse X-ray experiments. The source produces 100 fs pulses at 1.3 Å wavelength with 10^7 photons per pulse and a 10 Hz repetition rate. The SPPS has proved useful for testing damage models, for performing some of the first femtosecond X-ray diffraction experiments, and for the development and testing of short-pulse X-ray diagnostics.

1.2. Comparison with Existing Techniques

The flash-imaging method using XFELs will open up high-resolution imaging of a range of biologically relevant "objects," ranging from small molecular compounds acting as substrates or ligands, to macromolecules (e.g. enzymes), very large assemblies of macromolecules, to whole cells. Comparisons with other techniques are based on the issue of radiation damage which sets the fundamental limit of resolution for biological material, be that radiation electromagnetic (e.g. X-rays) or particles such as electrons. Damage is caused by the deposition of energy into the sample. Cryogenic cooling can slow down the deterioration of the sample, but it cannot eliminate damage-induced sample motion within the time needed to complete conventional measurements (Henderson, 1990; 1995). For example, the resolution limit for X-ray microscopy of cells at cryogenic temperature is thought to be worse than 100 Å. Obviously, the resolution of an X-ray microscope based at an XFEL could be much better than this, since the image formation would take place over timescales faster than the manifestation of damage. Since the sample is unlikely to survive its encounter with the X-ray pulse, it will be only possible to record single projection (i.e. 2D) images of nonreproducible samples such as cells.

Technique	Atomic resolution	Does not require crystallization	Time resolution	3D	Not Limited to small samples	Not Limited to large samples	Sample in natural state	Non-destructive
XFEL imaging	✓	✓	✓	✓	✓	✓		
Crystallography	✓		✓	✓	✓	✓		
TEM	✓	✓		✓	✓			
NMR	✓	✓	✓	✓		✓		✓
AFM		✓						✓
X-ray microscopy		✓		✓	✓	✓	✓	✓
Optical microscopy		✓		✓	✓	✓		✓

Table 2. XFEL lensless imaging will enable the highest resolution imaging of molecules and complexes that cannot be crystallized. Single-shot XFEL X-ray microscopy could provide the highest resolution 2D or stereo images of a cell in its natural state.

Current atomic-resolution imaging techniques for biological material are essentially methods to overcome radiation damage by spreading the dose over many identical samples. This is true for X-ray crystallography and for cryo-electron microscopy. NMR spectroscopy is limited by signal-to-noise ratio and by the difficulty of reconstruction. The most successful technique is X-ray crystallography which can achieve better than 1-Å resolution, even in large molecules by spreading the dose over 10^9 or more identical unit cells that scatter coherently to produce a diffraction pattern (see Figure 4). Like diffraction imaging, crystallography is lensless. However, since the amount of information that can be recorded (limited to Bragg peaks) is less than adequate to perform a direct reconstruction, much additional structural information must be provided. For simple systems at high resolution, just the knowledge of the positivity of the electron density and/or atomicity can fill the information void. For macromolecules, a good initial guess (based on similar structures) is needed in addition to techniques such as multiple anomalous dispersion, whereby patterns are recorded at wavelengths in the vicinity of an absorption edge. Despite this difficulty, this technique accounts for more than 80% of newly determined structures that are deposited into the Protein Databank (http://www.rcsb.org/pdb/). The majority of structures solved today are from diffraction data collected at synchrotrons, and there are beamlines being developed with completely automated measurements, including the mounting of the sample. Given a high-quality crystal, data collection and the solution to the structure can be obtained in a matter of days. As noted above, it is the crystallization of material that is the limitation of the technique.

Three-dimensional electron cryo-microscopy, combined with advanced image reconstruction methods, is rapidly developing, but currently the maximum resolution achievable is limited to about 7 Å (Bottcher, 2002) in structures without high symmetry (see Figure 5). The method does share some similar ideas with XFEL diffraction

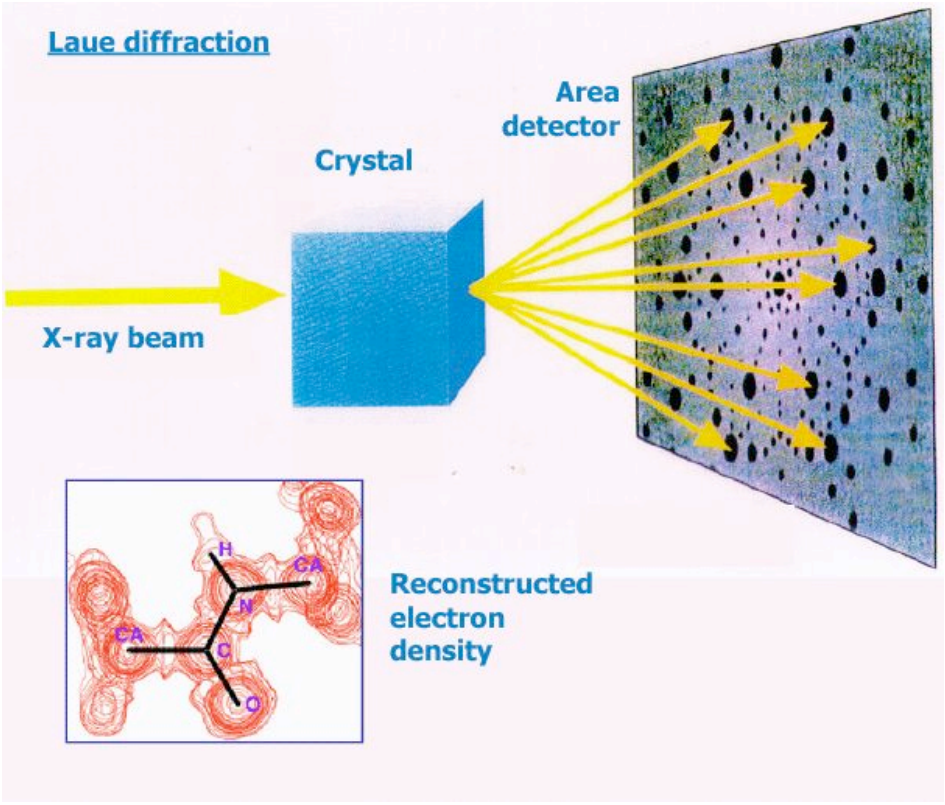

Figure 4. X-ray crystallography. The diffraction pattern from a three-dimensional periodic repeat of a molecule (a crystal) is the Fourier transform of the electron density of that molecule, sampled at the Bragg peaks (or reciprocal lattice vectors). When the phases of these Fourier-space samples are obtained (see e.g. Lamzin and Perrakis, 2000) the electron density spatial distribution can be recovered. Resolutions approaching 0.5 Å have been achieved permitting even hydrogen atoms and bond structures to be seen.

imaging, namely averaging over thousands of images to improve signal to noise and imaging with the lowest possible dose required to orient the image. The current resolution limit does appear to be technological, which, although it has advanced only slowly over the last decade, should be overcome. One fundamental limitation that applies to electron imaging and not to X-rays is that electrons, being Fermions, are not amenable to compression in time and space. Thus, there are limits to ultrafast measurements with electrons (to overcome damage and to obtain time-resolved measurements) since the information carried by the electron pulse would tend to thermalize while the pulse is still in flight (Siwick, 2002). However, the diffraction imaging method to be developed in this project could be applied directly to ultrafast electron diffraction of strongly scattering samples and even to a gas of aligned molecules (Spence, 2004).

Atomic resolution structural information can be elicited from small biological molecules by NMR spectroscopy which is used to solve the structure of most of the remaining 20% of molecules in the Protein Databank (PDB). For NMR, the low signal demands

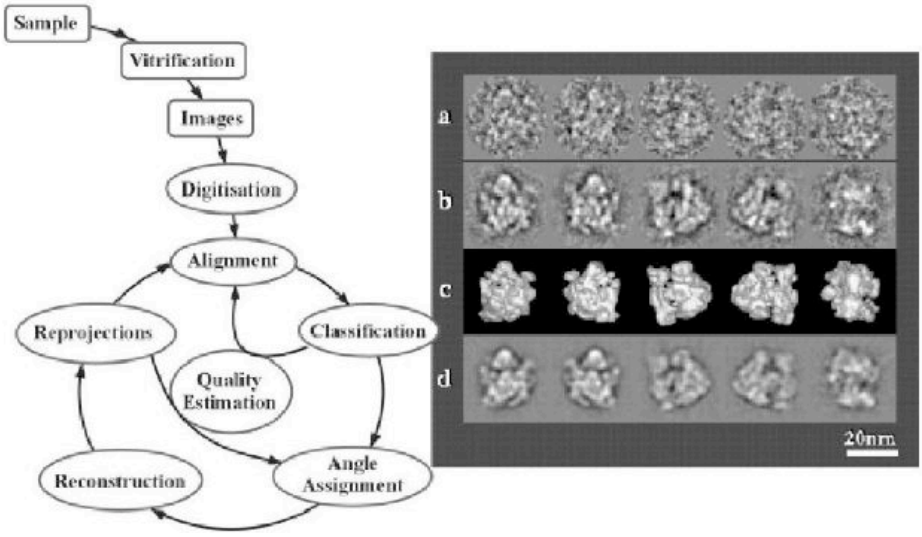

Figure 5. Single-particle cryo electron microscopy. Flow diagram and examples of ribosome particles embedded in vitreous ice and imaged in a TEM. Single noisy images (a) are classified into groups of similar 3D orientation then averaged within a class (b). A 3D model is developed (c) and made consistent with data by computing projections of the model (d). Much of the classification, averaging, and orientation techniques can be modified and applied to the case of diffraction imaging. Source: Hajdu and Weckert, 2001.

recording an average signal from a large number of molecules; its advantage is that the molecules are fully functional and in solution. Basically, the result of an NMR analysis is a set of estimates of distances between specific pairs of atoms (those with non-zero spin, usually just ^{1}H, but also ^{13}C and ^{15}N which can be used as labels). As opposed to powder X-ray diffraction which interacts with sample electrons, NMR is specific to atoms. By unraveling the signals, individual residues are identified. Many (10 to 50) structural models are usually found that are consistent with the data and consistent with knowledge from other methods. These structures represent the statistical uncertainty of the solutions. The best structures agree with these models at resolutions about 2 Å. The strength of NMR is that it can measure the dynamics of these inter-atomic distances. By comparing with molecular dynamics simulations, the number of structural solutions can be reduced. NMR is essentially the only way to get atomic resolution information on membrane proteins currently (although to date there are about one dozen integral membrane protein structures determined by X-ray crystallography), but the technique is limited to molecules with sizes less than about 5000 atoms. Beyond that, the uncertainties get too large. Large proteins and protein complexes are 10 to 100 times larger than this limit, and virus particles may consist of a million or more atoms

It is clear from this discussion that atomic-resolution diffraction imaging at an XFEL, while ambitious, has the potential to revolutionize atomic structure determination of biological systems. Diffraction imaging builds upon the huge image processing

Target	Composition	Diameter (Å)
Phospholipase	~130 amino acids	~40
Lysozymes	~130 amino	~40
Botulism A protease domain	~800 amino acids (400 amino acids / monomer)	~80
Nucleosome	~750 amino acids & ~450 nucleic acids	~100
Botulism B holotoxin	~1200 amino acids	~110
Anthrax lethal factor	~1500 amino acids	~120
RIBOSOME	~3500 amino acids & ~3000 nucleic acids	~200

Table 3. Selected biological models

knowledge that has been built up in the fields of crystallography and electron microscopy, and it will overcome the current barriers to noncrystalline samples, cryogenically fixed samples and NMR size limitations.

2. Research and Results

The research was carried out to determine the feasibility of XFEL diffraction imaging and to determine the further research and development needed to field the first experiments at the LCLS. The highlights of our research include: the development, improvement, and testing of a hydrodynamic model of the Coulomb explosion of particles (Hau-Riege, 2004b); the development of a model that estimates the required fluence to classify and average diffraction patterns (Huldt, 2003); the integration of those models to determine resolution limits (Hau-Riege, 2005); the development of models for X-ray-induced damage in solids; the introduction of a new algorithm for automatic reconstruction of an image from its diffraction pattern without the need for any additional low-resolution information (Marchesini, 2003a); successful X-ray diffraction imaging experiments carried out at the Advanced Light Source at LBNL (the world's first true lensless coherent diffraction image formed without a priori information, and the world's first full 3D coherent diffraction image) (Marchesini, 2003b); and the design and construction of high-stability multilayer optics for the VUV-FEL source. In addition to the Uppsala University group of Prof. Janos Hajdu, we have formed fruitful collaborations with DESY in Hamburg (Prof. Thomas Moeller, Technische Universitaet Berlin), SUNY at Stony Brook (Prof. Janos Kirz), LBNL (Dr. Malcolm Howells and Dr. Haifeng He), Arizona State University (Prof. John Spence), and The University of Melbourne (Prof. Keith Nugent and Dr. Andrew Peele). We have leveraged our LDRD-ER project to attract NSF Center for Biophotonics Science and Technology funding to the Laboratory to apply diffraction imaging techniques to cellular imaging using synchrotron sources.

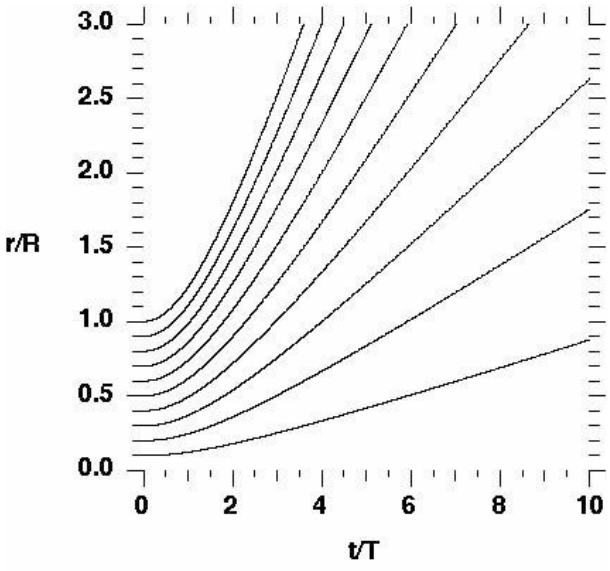

Figure 6: Trajectories of 10 radial shells. The shells originate at radii between 0.1 R and R. Time is measured in units of the characteristic time, $T = (2\pi./3\ d)^{1/2}\ R^3/Q$.

2.1. Biological Modeling

One of the first tasks of the ER was to construct structural models of biological samples to be used in detailed simulations of damage and diffraction imaging. We selected seven static models of proteins or protein/nucleic acid complexes. This set, found in the Table 3, was chosen to represent a range of sizes, function, and atomic composition.

Phospholipase, botulism toxin (and subdomains), and anthrax lethal factor represent targets of programmatic and/or biodefense interest because of their toxicity to humans. Lysozyme is a standard model for many proof of principle studies in structural biology. The nucleosome and the ribosome represent large quanternary complexes between protein and nucleic acid and contain a number of other heteroatoms. The ribosome is also the largest non-virus model in the structure database. We are currently investigating dynamic models that will lead to experimental design intended to take advantage of the pulse times of LCLS. The dynamic processes we are currently considering are the formation of thymine dimers (an important process in cancer and health effects of UV exposure) and peptide hydrolysis by Botulism zinc protease (the critical step in paralysis by the most toxic substance known).

2.2. Hydrodynamic Model for X-Ray Irradiated Biological Molecules

A key concept for X-ray imaging of small biological samples is the use of very short pulses to capture the data before damage occurs. The main goal of this part of the project

is to calculate how short the pulses must be in order to achieve a desired resolution for a given sample.

Molecular dynamics simulations of X-ray irradiated biological molecules have recently been presented (Neutze, 2000). We have developed an alternate model (Hau-Riege, 2004b) that utilizes an approximate, but computationally more efficient, hydrodynamic description of the atomic motion and includes the effects of trapped electrons and secondary ionization, which Neutze *et al* left out. The basic assumption of the hydrodynamic model is that the sample is a continuum of matter rather than individual atoms, as in the molecular dynamics approach. We further assume that the particle has spherical symmetry, reducing the mathematical model to one dimension.

In general there are two types of forces acting to explode the molecule: the Coulomb (electrostatic) force, due to the net positive charge left by escaping electrons, and the pressure force due to trapped electrons. The damage process begins with the absorption of the X-rays, predominantly by K-shell ionization of the abundant, medium weight elements (C, N and O). This produces photoelectrons of energy nearly equal to the photon energy (~10 keV). On a 10 fs time scale the inner shell holes decay primarily by emitting Auger electrons of much lower energy. If the sample is small most of the photoelectrons and even some Auger electrons escape.

When the number of trapped electrons is small, the Coulomb forces dominate. By assuming a very short X-ray pulse, an analytic result for the particle explosion can be found. We model the molecule as an initially homogeneous sphere that is conceptually partitioned into shells characterized by their initial radius, r_o. Using the energy form of the equation of motion we find an implicit solution for the trajectory of each shell:

$$t = \left(\frac{2\pi}{3} d\right)^{1/2} \frac{R^3}{Q} \frac{1}{r_o} \int_{r_o}^{r} \frac{x^{1/2} dx}{(x - r_o)^{1/2}}. \qquad (1)$$

Here t is time, d the mass density, R the initial radius, Q the charge created by photoionization and r is the radius of each shell. The solution, which can be expressed in terms of algebraic and logarithmic functions, is shown in Figure 6.

From Figure 6 we see that the motion in the pure Coulomb explosion is self-similar, i.e. all shells follow a trajectory of the same shape. We are mainly interested in small displacements, $\Delta r << R$, since we strive to determine the molecular structure at much higher resolution than its size. We concentrate on the surface layers since they move the fastest and thereby provide the most stringent constraint on the pulse length. We find in this case:

$$t = \left(\frac{2\pi}{3} d R\right)^{-1/2} \frac{A}{e f_i} \sqrt{\Delta r} = 5.3 \ \ fs \left[\left[d\left(\frac{R}{10\text{Å}}\right)\right]^{-1/2} \left(\frac{A}{7}\right) (f_i)^{-1} \ (\Delta r)^{1/2}\right] \qquad (2)$$

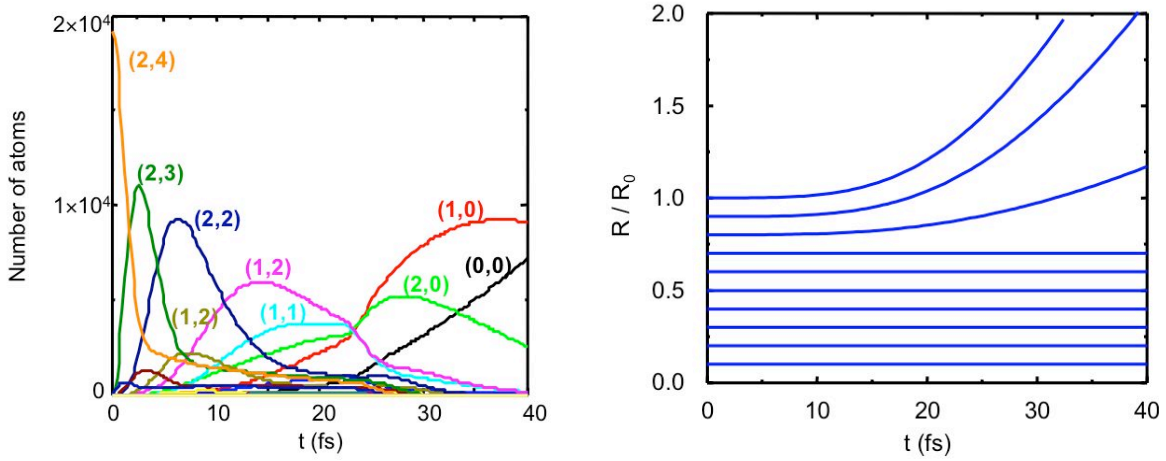

a b

Figure 7. (a) Ionization of C in a 50 Å radius protein molecule by 10 keV X-ray pulse of 1.5×10^{11} ph/fs/(100nm^2). (b) Trajectories of 10 radial shells calculated using the numerical model. The molecule radius, R_0, is 50A, the pulse length is 40fs, and the fluence is 6×10^{12} photons/100nm diameter.

where e is the electronic charge, A is the average atomic mass number, and f_i is the fraction of photoionized atoms.

The results of the analytic Coulomb model compare well to the molecular dynamics model results of Neutze (2000). The formulae are useful to see the scaling with resolution, molecular size, and degree of ionization, and have also been used to benchmark the detailed numerical model described below.

In the case of large molecules (R > 50 Å for typical parameters), only a small fraction of the electrons can escape before the remaining positive charge traps the rest. The trapped electrons generate low energy secondary electrons (which are also trapped) by collisional ionization. The trapped electrons quickly relax in energy and position to form a neutralizing cloud around the positively charged ions, similar to Debye shielding in a plasma. The molecule will assume a two-region structure with a nearly neutral interior core and a positively charged shell around the core. The transition typically extends over a Debye length.

We have developed a detailed numerical model to handle the general case of an arbitrary X-ray pulse including the effects of trapped electrons. The number and energy of trapped electrons are calculated from time dependent rate equations including photo, Auger, collisional, and three-body recombination processes. We assume that the electrons instantaneously relax to a force-free equilibrium spatial distribution, including Coulomb forces due to the ions and the electrons, and the pressure gradient of the electrons. The electron distribution is calculated at each time step by solving a 2nd order ODE. The

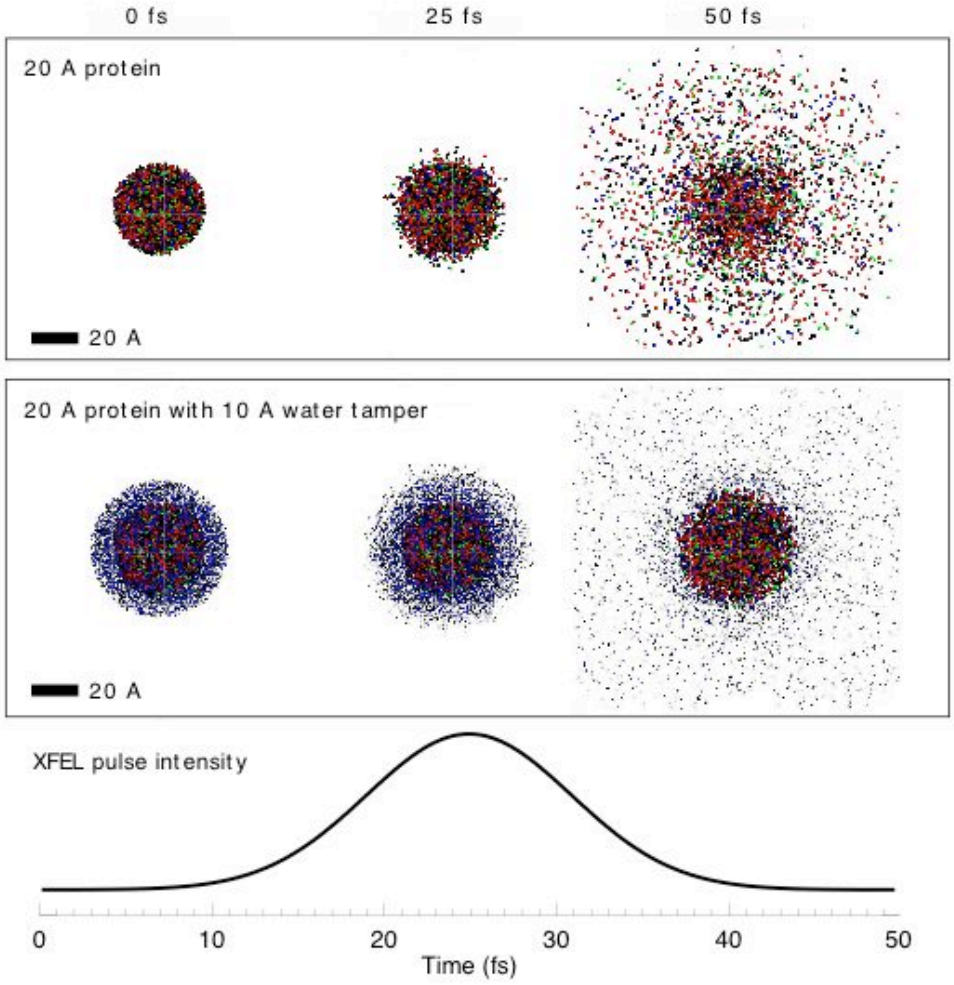

Figure 8. Protein Coulomb explosion: Explosion of a 20-A radius model protein molecule due to interaction with a 20-fs 12 keV X-ray pulse with 3×10^{12} photons in a 0.1 micron-diameter spot (top). The middle panel shows the delay of the molecule destruction when a 10 Å water tamper layer (blue) encapsulates it. Atom trajectories are computed from a hydrodynamic model. Combined with modeling of the diffraction, the hydrodynamic model predicts that atomic resolution can be achieved for pulse lengths of 20 fs and less.

atomic motion responds to Coulomb forces and is advanced in time by a 1st order finite difference method.

We illustrate results of the numerical model for the case of a 50 Å radius molecule illuminated by a 10 keV photon pulse of flux $1.5x10^{11}$ph/fs/(100nm^2). Figure 7 (a) shows the ionization of C, the most important component of biomolecules. (Similar processes occur in O, and N). We see that even though photoionization is the initial process, collisional ionization of the valence electrons dominates the early time behavior. This is due to the fact that each photoelectron has enough energy to ionize about 10^3 valence electrons. The first valence electrons get stripped in about 1 fs, while at 20 fs,

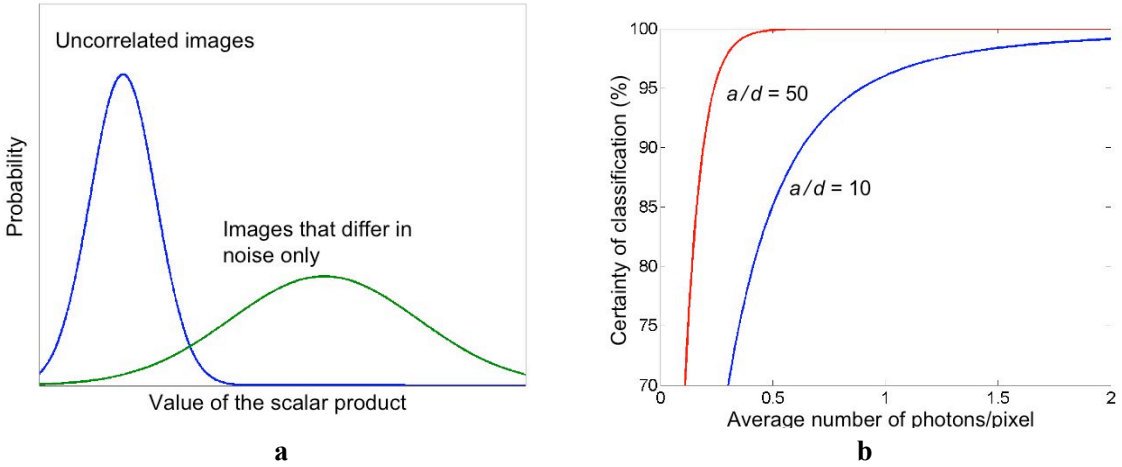

Figure 9. (a) Schematics of the distribution of the scalar product of two image vectors. The area of the overlapping sections gives the probability for misalignment. (b) Certainty of classification as a function of the average number of photons per pixel. The results depend on the ratio of the particle radius, a, and the resolution, *d*.

about 3 electrons remain on each C atom. Figure 7 (b) illustrates the motion of the atomic shells. In comparison to the results of the pure Coulomb explosion without trapped electrons (Figure 6), we see the differentiation into an outer shell that expands very quickly due to the concentrated charge and an inner core which expands more slowly from electron pressure. This picture leads to the suggestion of reducing the motion by surrounding the molecule by a low-*Z* tamper (see Figure 8).

2.3. Effect of Damage on Imaging and Classification

To achieve three-dimensional, high-resolution reconstruction, it is desirable to balance both sample damage and photon-counting noise in each image. The damage is minimized by using short pulses, low fluences, and small samples; the photon noise is small when a large number of photons is detected, which can be achieved by using high fluences and large samples. In order to estimate the pulse parameters required to achieve a desired resolution, we have folded together a large number of simulations of the effect of damage on imaging using the hydrodynamic model described above, with a theory for the effect of photon noise on resolution, developed by Huldt, Szoke, and Hajdu (2003). In the following we will first describe the resolution theory considering image classification, then discuss the resolution limit due to damage dynamics, and finally combine both results to estimate the image resolution as a function of pulse parameters and sample size.

2.3.1. Image Classification

Many molecules, in different orientations, would have to be used to obtain the three-dimensional diffraction pattern, required for the reconstruction of the electron density.

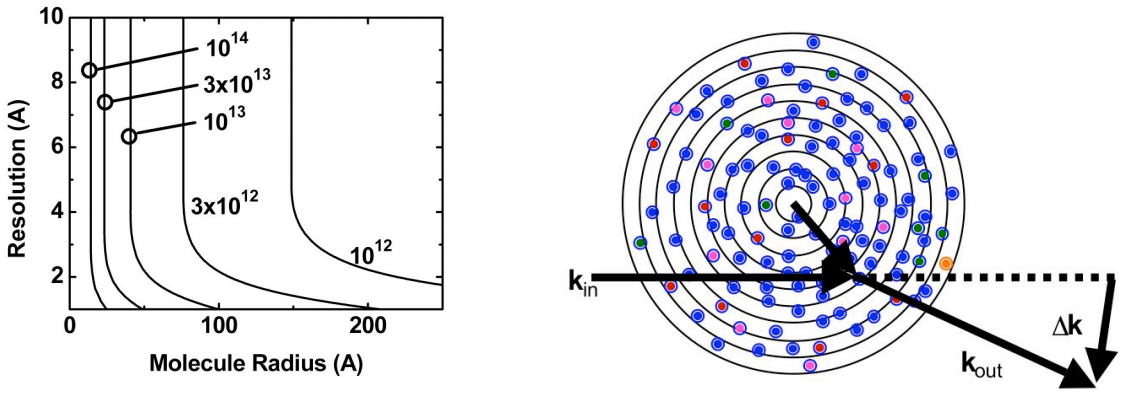

a **b**

Figure 10. (a) Classification-limited resolution as a function of particle size and fluence. (b) "Pseudo-molecule" generated by placing different atoms randomly within the boundary of the molecule according to the mass density and stoichiometry.

We analyze the case, where identical molecules are injected into the X-ray beam in random, unknown orientation and destroyed by a single pulse. The procedure envisaged is that the individual diffraction patterns will be used to find the orientation of the molecule and the diffraction images of molecules in similar orientation will be averaged to get a sufficient signal to noise ratio.

Three-dimensional image reconstruction may be possible from a collection of individual diffraction images, provided that the signal-to-noise ratio is sufficiently large for their orientation to be determined relative to each other. The signal-to-noise ratio is limited by counting statistics due to the small number of detected photons, which is necessary in order to minimize damage. However, averaging of many images can be used to enhance the signal and extend resolution in redundant data sets. A basic requirement for averaging is the ability to determine if two noisy diffraction images show the same angular view of the sample or two different views. The precision and noise tolerance of the classification procedure limit the final reconstruction. In collaboration with Uppsala University, we developed an analytical solution to this classification problem based on statistical properties of the diffraction patterns (Huldt, 2003). The solution connects the number of incident X-ray photons with the particle size and the achievable resolution.

For the purpose of classification, we divide the image into resolution elements, or pixels, each defined as an area of the diffraction pattern over which we integrate the number of detected photons. We think of an image as an *n*-dimensional vector, where *n* is the number of pixels, and each element of the vector is the photon count per pixel. The scalar product of two image vectors is a measure of the correlation of two images. To determine whether it is possible to classify images by this correlation measure, we derive the probability distributions of the scalar product for two limiting cases: (i) images that present different views of the samples, and (ii) images that present the same view of the

	Noise-Free	With Poisson Noise
μ_g	$\langle W \rangle$	$\langle W \rangle$
σ_g^2	$\langle W \rangle^2$	$\langle W \rangle^2 + \langle W \rangle$
μ_{gh}	$\langle W \rangle^2$	$\langle W \rangle^2 + \langle W \rangle$
σ_{gh}^2	$3\langle W \rangle^4$	$3\langle W \rangle^4 + 4\langle W \rangle^3 + \langle W \rangle^2$
$\mu_{gg'}$	$2\langle W \rangle^2$	$2\langle W \rangle^2$
$\sigma_{gg'}^2$	$20\langle W \rangle^4$	$20\langle W \rangle^4 + 32\langle W \rangle^3 + 13\langle W \rangle^2$

Table 4. Expectation values and variance of the product of the photon count in two pixels at the same resolution.

sample but differ in the distribution of noise. Classification will be regarded as possible if the two distributions are sufficiently distinct.

We derived the distribution of the scalar product of two image vectors for the special case where the image vectors are constructed from a single circle of high-resolution pixels. Since the scalar product is a sum of random variables, the scalar product is asymptotically normally distributed. The normal distribution is described by the mean, μ, and variance, σ^2. We obtained expressions for the expectation values and variances of the product of photon count of two pixels at a certain resolution as shown in Table I. Here, $\langle W \rangle$ is the average (classical) intensity at a certain resolution, expressed in photons per unit area. The subscript gg' indicates two images presenting the same view and differing only in noise, whereas gh indicates two noisy images presenting different views. The mean and variances of the scalar product take on higher values if the images present the same view of the sample than if they present independent views, as shown in Figure 9 (a).

We consider two distributions of scalar products of image vectors to be distinct if their overlap is smaller than a given fraction of their total area. This criterion allowed us to obtain analytical expressions for the certainty of classification as a function of the average number of photons per pixel. The solution for a ball of randomly distributed carbon atoms as a model particle is shown in Figure 9 (b). The results depend on the ratio of the radius of the particle, *a*, and the resolution, *d*. The results are surprising in that they show that classification can be done with less than one photon per pixel in the limiting resolution shell, assuming Poisson-type photon noise in the image. If we require a 90% confidence for the image classification, we can generalize this result to obtain the resolution as a function of particle size and incoming photon fluence, as shown in Figure 10 (a). The classification-limited resolution gets worse with decreasing fluence and is independent of pulse length.

2.3.2. Computer Requirements for Image Classification

The full reconstruction of the electron density from experimental data in a biomolecular imaging experiment is limited by the computational power needed for image classification. The required computational power increases with increasingly better image resolution. Through the use of hierarchical algorithms to determine equivalence

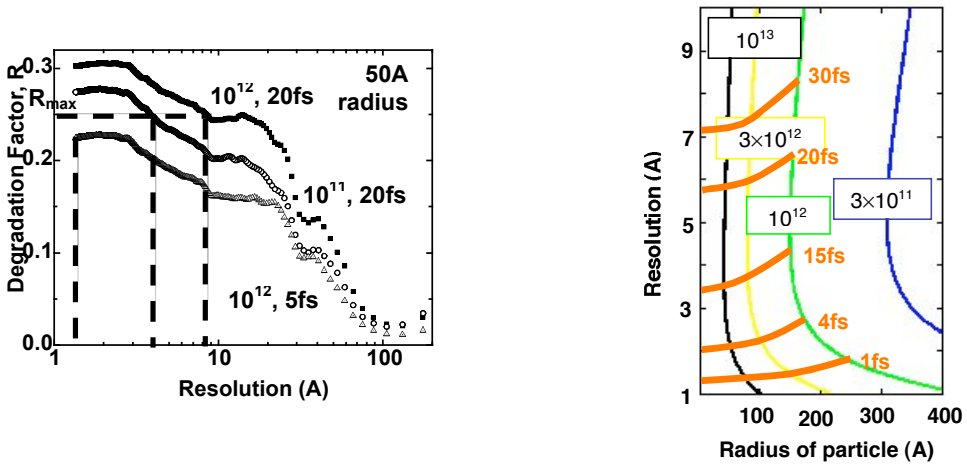

a b

Figure 11. (a) Degradation factor, R, as a function of resolution for different beam parameters. The graphs are labeled with the number of photons per 100nm diameter and the pulse length in fs. The radius of the molecule is 50A. Also indicated are the resolutions for R_{max} = 25%. (b) Pulse length as a function of particles radius, X-ray fluence, and image resolution.

classes as described in Press (1992), we were able to reduce the expense of the classification algorithm, measured by the number of floating-point operations, to $O(M N^4 \log N)$. N is the CCD array size and determines the resolution, and M is the number of patterns per class. This assumes that the molecule is somewhat oriented and is only allowed to rotate around one axis. In this case, we estimated that the calculations could be performed on a regular desktop computer. However, in order to do the full experiment without any preference in orientation, the classification problem will require a cluster of desktop computers or an ASCI-scale computer.

2.3.3. Effect of Irradiation-Induced Damage on Image Quality

The complementary source of difficulty in diffraction imaging of single molecules is their explosion during the X-ray pulse. In this calculation we neglected the finite amount of photons scattered by the sample and assumed a "perfect" diffraction image, limited only by the motion of the nuclei and the ionization of the constituent atoms. In order to assess the effect of the damage dynamics on the quality of the diffraction image, we calculated the time-integrated diffraction pattern of a *pseudo molecule*, and compared it with the diffraction pattern of a hypothetically undamaged sample. The pseudo molecule was generated by placing different atoms randomly within a spherical volume according to the stoichiometry, assumed to be $H_{49}C_{33}N_9O_9S_1$ as an "average" protein, and the mass density, which was taken to be 1.35g/cm^3. An example for the two-dimensional equivalent of this three-dimensional process is shown in Figure 10 (b).

The mean number of elastically scattered photons, $I(\mathbf{u},\Omega)$, to be detected by an idealized detector pixel of projected solid angle Ω centered at a positional vector, $\mathbf{u}$, is

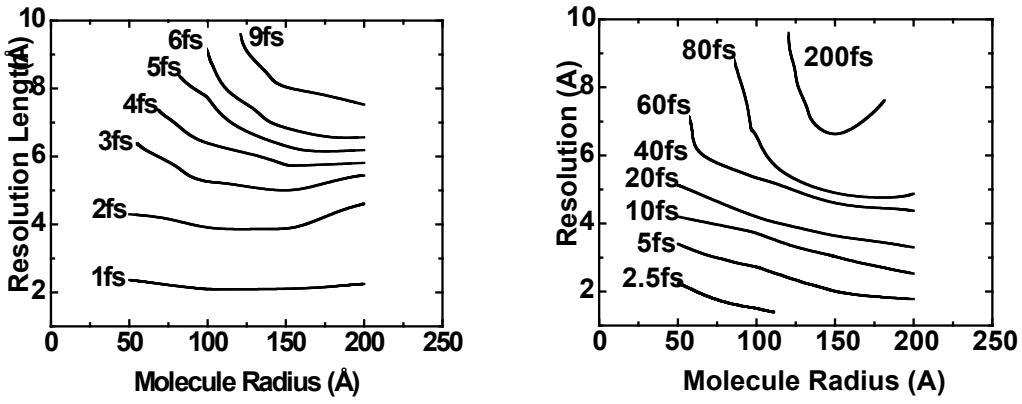

(a) (b)

Figure 12. Pulse length as a function of particle radius and image resolution for (a) three times and (b) ten times lower pulse fluence requirements.

$$I(\mathbf{u},\Omega) = \Omega r_e^2 \int_{-\infty}^{\infty} I(t) \left| \sum_j f_j(\mathbf{u},t) \exp\left(i\Delta\mathbf{k}(\mathbf{u}) \cdot \mathbf{x}_j(t)\right) \right|^2 dt, \tag{3}$$

where r_e is the classical electron radius (2.8×10^{-5}A), I(t) is the intensity of the X-ray pulse, $f_j(\mathbf{u},t)$ is the atomic scattering factor of the j^{th} atom as a function of time, $\mathbf{x}_j(t)$ is the position of this atom as a function of time, and $\Delta\mathbf{k}$ is the change in the wave vector of the X-ray photon when scattered toward the pixel centered at $\mathbf{u}$. Radiation damage interferes with $x_j(t)$ through ion movement, and with $f_j(\mathbf{u},t)$ through atomic ionization. Due to the high velocities of the trapped electrons, these electrons are treated as a homogeneous background charge.

We follow the treatment by Neutze *et al* (2000), and define a measure, R, for the effect of damage on the image quality,

$$R = \sum_{\mathbf{u}} \left| \frac{K^{-1}\sqrt{I_{real}(\mathbf{u},\Omega)} - \sqrt{I_{ideal}(\mathbf{u},\Omega)}}{\sum_{\mathbf{u}'}\sqrt{I_{ideal}(\mathbf{u}',\Omega)}} \right|, \tag{4}$$

where

$$K = \frac{\sum_{\mathbf{u}}\sqrt{I_{real}(\mathbf{u},\Omega)}}{\sum_{\mathbf{u}}\sqrt{I_{ideal}(\mathbf{u},\Omega)}}. \tag{5}$$

The scaling factor K describes the relative scattering power of the sample. We computed values for I_{real} by evaluating equation (3) from 60 snapshots of each trajectory. I_{ideal} is the diffraction pattern of an undamaged sample. An R value of 0 is ideal, and as R increases the image quality becomes poorer. For two totally random arrays, R ~ 67%, and typical R values in the protein database are about 20%.

The degradation factor, R, strongly depends on the resolution up to which the ideal and the real images are compared, as shown in Figure 11 (a). The resolution is inversely proportional to the scattering factor, $\Delta\mathbf{k}$. For given irradiation conditions (fluence and pulse length) the R-factor increases as we demand higher resolution. We also found that the R factor is strongly affected by the beam parameters. As also shown in Figure 11 (a), lower fluences or shorter X-ray pulses lead to lower R factors, and therefore higher-quality diffraction images, since the molecule is less damaged.

If the damage of the molecule is too severe, the diffraction image is insufficient to allow image reconstruction. This poses an upper limit, R_{max}, on the R factor. As indicated in Figure 11 (a), R_{max} can be used to determine the maximum achievable resolution from a damage point of view.

2.3.4. Convolution of Damage and Classification Models

Our model for image classification allows the calculation of the image resolution as a function of particle size and pulse fluence, as shown in Figure 11 (b). Bigger particles and lower fluences lead to better resolution. In this model, the resolution is independent of the pulse length. Our calculations of the effect of irradiation-induced damage on image quality provide the image resolution as a function of particle size, pulse fluence, and pulse length. From a damage point of view, smaller particles, lower fluences, and shorter pulses lead to better resolutions.

We have folded together the results from a large number of damage simulations with the results from the theory for the effect of photon noise on image resolution (classification). We adjusted the pulse length until the resolution obtained from the damage calculations matched the resolution obtained from the classification theory, shown in Figure 10 (a), assuming R_{max} = 25%. The result is shown in Figure 11 (b).

If prior information about the orientation of the molecule is available and the pulse fluence requirements can be relaxed, it is possible to use longer pulses. Figure 12 (a) and (b) show pulse length requirements when the fluence requirements are three times and ten times lower, respectively. These results show that prior information about the molecule orientation is very valuable for relaxing the X-ray beam pulse length requirements.

2.3.5. Mapping of Resolution for Different Biological Molecules

For a molecule size range of 20 to 300Å, pulse lengths of 1 to 30 fs are required to achieve resolutions of 1 to 8 Å, as indicated in Figure 11. With the original proposed experimental setup, it is difficult to image larger molecules at atomic resolution, since the X-ray fluence required for classification causes very severe damage in the sample. The root cause is the trapping of photoelectrons, which occurs earlier in the pulse for large

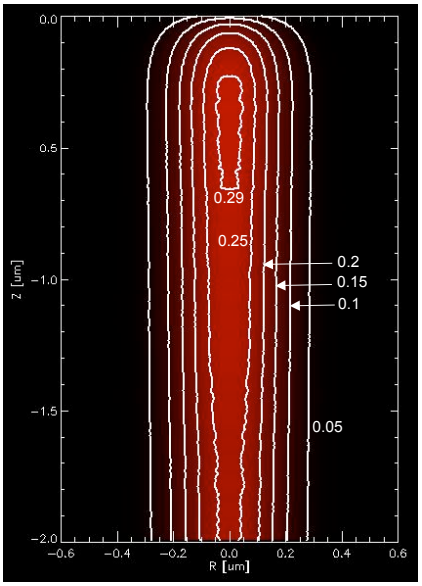

Figure 13. Contour plot of the energy density (in eV/atom) in the InSb solid. The InSb surface is located at Z=0.

samples. The trapped photoelectrons are highly-energetic and cause severe damage mainly through collisional ionization, which degrades the atomic scattering factors.

One way to image larger molecules or to be able to use longer pulses for small molecules, is to relax the pulse requirements imposed by classification. We envision schemes to pre-orient the samples either completely or limit the random orientation to one axis, both of which would require less information for the classification of the diffraction images, which, in turn, would decrease the lower fluence limit imposed due to classification requirements.

2.4. Dynamics of bulk materials

Biological imaging at XFELs will require optics to focus the intense pulses to spot sizes less than 0.1 micron. These optics will require demanding tolerances and will need to operate under extreme pulse intensities. The feasibility of XFEL imaging depends upon understanding the interaction of XFEL pulses with bulk material. In addition, studies of the dynamics of bulk material under irradiation by short X-ray pulses can help validate our models for imaging particles.

Initial short-pulse damage and dynamics experiments were performed at the SPPS at SLAC, as part of the SPPS collaboration. The collaboration performed experiments on the non-thermal melting of InSb, which showed that when a crystalline sample is rapidly heated by a short laser pulse a dense electron-hole plasma is generated which leads to disordering of the crystal lattice at timescales faster than those for attaining thermal equilibrium. By monitoring the Bragg reflections of the lattice, using the short SPPS X-ray pulses, it was shown that the dynamics of the atoms is inertial, with the atoms initially

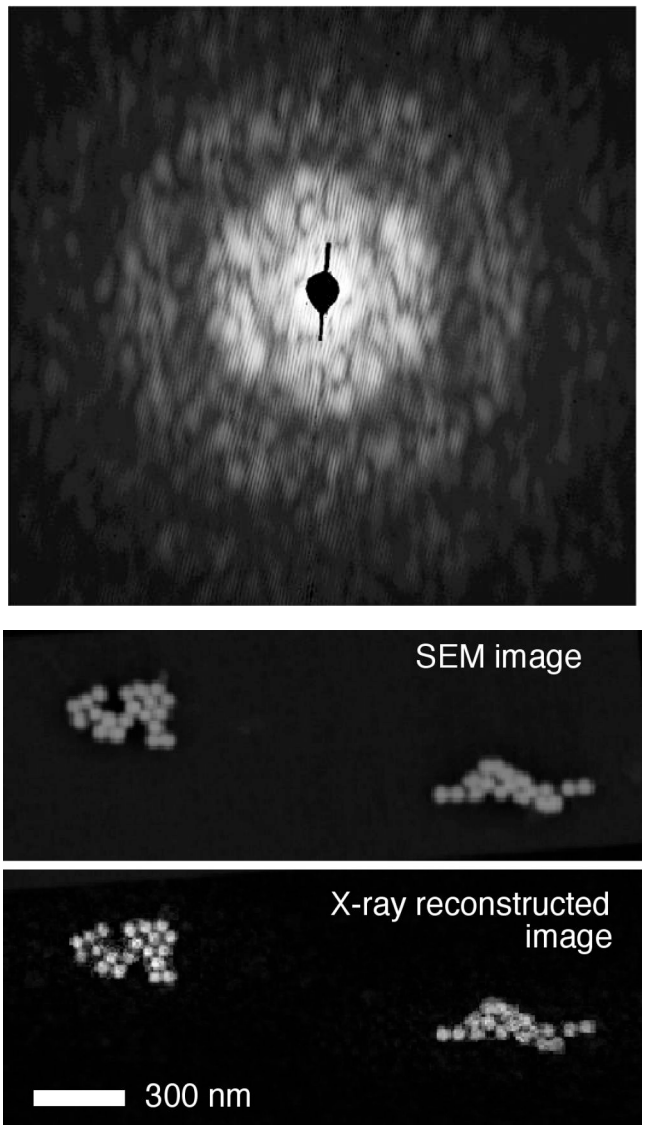

Figure 14. The first true lensless X-ray imaging of a nonperiodic specimen. A sample of 50-nm-diameter colloidal gold spheres, as imaged by an SEM (middle), and as reconstructed (bottom) from a diffraction pattern recorded at a wavelength of 2 nm (top). The X-ray image is quantitative and shows a phase shift in agreement with the optical constants of gold. This is the first demonstration of true lensless imaging, and overcomes limitations of previous work, which required detailed prior knowledge about the object.

moving freely with velocities set by the room-temperature thermodynamics velocities (Lindenberg, 2005; Cavalleri, 2005). These results show that the physics assumptions in our models of dynamics of particles are essentially correct for the short timescales considered.

To understand further the problem of damage to X-ray optics by intense X-ray pulses we developed a Monte-Carlo-type model of the X-ray material interaction. In this

Array size	Time per 3D Fourier transform	Time per 3D reconstruction
256^3	73 ms	10 min
512^3	850 ms	1.5 h
1024^3	7.9 s	14 h

Table 5. Computing times using a cluster-based Fourier transform and reconstruction code on 16 G5 dual-processor Xserve compute nodes. Fourier transform timings are wall time per individual FFT. Reconstruction timings are for a complete 3D reconstruction consisting of 2000 iterations of HIO phase retrieval complete with two FFTs per iteration plus other operations required to calculate the reconstruction.

model, X-ray photons are absorbed through photoionization, and the path and energy decay of the photoelectrons is tracked as it passes through the solid. We then compare the amount of deposited energy with an analytical estimate of the energy required to melt the solid top determine if damage will occur. For 2 to 20 keV photons, the predominant mode of X-ray interaction with the substrate is the photoelectric process. The photoelectrons tend to be ejected in the direction of the electric field vector of the incident radiation, i.e. at right angles to the direction of incidence. The passage of the photoelectron through the solid is calculated by tracking it from one scattering interaction to the next. It loses energy through inelastic scattering events and changes direction through elastic scattering. The energy loss is described by a modified version of the Bethe equation, in which the stopping power was corrected below 0.5 keV to match experimental results. The elastic scattering is described by a screened (differential) Rutherford cross section.

We applied the model to possible SPPS optics damage experiments. Taking an InSb substrate as an example, we assumed that in the experiment it is irradiated with 1.5×10^6 photons in a 0.2×0.45 μm^2 spot at 9.4 keV. These are our current best guesses for future SPPS performance. Figure 13 shows a contour plot of the deposited energy in the InSb. Interestingly, the maximum energy density of 0.30 eV/atom is not reached at the InSb surface but 0.35um below. An analytical simple estimate suggests that 0.23 eV/atom are required to melt InSb, so that melting should be achieved. We are currently investigating how other materials should behave upon X-ray irradiation.

2.5. Image Reconstruction

Each diffraction image records the diffraction pattern of the particle in one orientation. It corresponds to the square of the amplitude of the Fourier transform of the electron density of the particle on a plane (actually a sphere) perpendicular to the incident beam. The sphere is called the Ewald sphere and the space of the diffraction pattern is called reciprocal space by crystallographers. The result of successful classification and averaging is, therefore, a measured diffraction pattern on a collection of hemispheres in reciprocal space. Finding the electron density that gives rise to the diffraction pattern is called the reconstruction problem. It has to be done by computers. We pursued two

different approaches: one is called the Gerchberg-Saxton-Papoulis-Fienup iterative algorithm, the other is a real-space algorithm.

2.5.1. The Shrinkwrap Iterative Algorithm

An iterative phase-retrieval method, successful with simulated data, first appeared in 1972 (Gerchberg, 1972) followed by important theoretical advances due to Fiddy, Bates and others. The iterative algorithm was greatly improved through the introduction of feedback and compact support by Fienup around 1982 with the hybrid input-output (HIO) algorithm. (The support is the boundary of the object. For early inversions of optical data, see Cederquist, 1988 and Kamura, 1998). We have, for the first time, demonstrated the reconstruction from an experimental X-ray diffraction pattern, without the need for any extra information about the size and shape of the object whatsoever. We have done this by improving the algorithm used for reconstruction. In our process, as in others, we iterate between the image and diffraction spaces using fast Fourier transforms (FFTs), and force the reconstructed object to be zero outside a given area. A reconstruction requires 100 to 1000 iterations (with two FFTs per iteration). Our novel improvement is that the estimate for this area (know as the object support) is continually updated by thresholding the intensity of the current object reconstruction. We start from a threshold of the transform of the diffraction pattern and as the iterations progress the support converges to a tight boundary around the object. This, in turn, improves the image reconstruction, which gives a better estimate of the support. We term this algorithm "Shrinkwrap" due to the dramatic way the support shrinks around the image of the object. As described below, we demonstrated this algorithm on data we recorded at the Advanced Light Source.

Our initial development and testing of the Shrinkwrap algorithm was on experimental single-view diffraction data that we acquired from flat test objects. This gives a 2D image of the object, but our goal was to demonstrate feasibility for 3D imaging of complicated structures for XFEL applications. We expanded the Shrinkwrap algorithm to three dimensions, which posed a major computational challenge due to the size of the data files and the need to carry out thousands of fast Fourier transforms (FFTs) on that data. Our data array size was 1024^3, or approximately one billion elements. It is not practical to carry out FFTs on such array sizes on single-CPU computers. The data array occupies 8 GB of memory, and the iterative algorithm requires at least 21 GB (single precision). This necessarily required a computer cluster, however FFTs are not trivially parallelizable due to the fact that one element of an array affects all elements of its transform. We overcame the problem of efficiently calculating distributed Fourier transforms by using `dist_fft` distributed giga-element fast Fourier transform library from Apple Computer specifically written for this project by the Apple Advanced Computation Group (Crandall, 2004). This FFT library distributes the Fourier transform calculation load efficiently over many processors and has been hand-optimized to take advantage of the G5 architecture used in the Apple Macintosh line of computers and the "Altivec" single-instruction-multiple-data (SIMD) floating point vector processing unit. Distributed FFT libraries are also available elsewhere, for example in version 2 of the FFTW libraries (Frigo, 2005) but at this time these do not support SIMD vector processing extensions and proved to be slower on our platform. `dist_fft` decomposes

the input 3D data set into n_{proc} discreet data slabs each consisting of a sub-portion of the original data array. Only a distinct portion of the array resides on each CPU at any given time enabling data sets much larger than the memory of each individual node to be computed, and the distributed memory nature of the FFT is exploited through parallelization of all steps in the reconstruction code. Standard message passing interface (MPI) commands are used to communicate data between processes.

Based on the sizes of our arrays of experimental diffraction intensities we specified and acquired a 16-node 2.0 GHz dual-processor (32 processors total) Macintosh Xserve G5 cluster with 4 GB RAM per node. To maximize inter-process communication speed we used high-speed, low-latency Mellanox Infiniband interconnects to carry MPI traffic between compute nodes. We parallelized the shrinkwrap algorithm and compiled it with the `dist_fft` and MPI libraries. Using this cluster and software the processing time on a 512^3 array is 2.2 seconds per iteration using the HIO phase retrieval algorithm, and an acceptable 3D reconstruction can be produced in under 2500 iterations for a total computation time of 2.5 hours on a 512^3 grid. The individual FFT timing and total reconstruction time for typical array sizes on this cluster is given in Table 5.

2.5.2. Real-Space Algorithm

The real space algorithm is an outgrowth of our previous work on the reconstruction of electron density in crystallography. In crystallography, the number of measurable diffraction intensities is limited by the Bragg condition. Consequently, there is not enough information for a unique reconstruction of the electron density, but *a priori* information has to be utilized for that. It was realized by Sayre (1980) that in continuous diffraction images one can "oversample" the intensities and that should make unique reconstruction possible. Our crystallographic program, EDEN (Szoke, 1993) uses external information explicitly and, theoretically, it should be able to use oversampling information optimally. It was modified for using experimental data that does not satisfy the Bragg conditions and renamed SPEDEN (Hau-Riege, 2004a) short for "Single particle electron density". It is now being tested on both artificial and experimental data. We expect that its theoretical advantage will eventually show up in problems with incomplete and noisy data, and that it will be used to refine solutions determined by Shrinkwrap to give optimal reconstructions based on all available data and prior knowledge.

2.6. ALS Experiments

In collaboration with Dr. Malcolm Howells (LBNL) and Prof. John Spence (U. Arizona) we performed X-ray diffraction imaging experiments at the Advanced Light Source (ALS) synchrotron at LBNL. The aim of the experiments was to test our image reconstruction algorithms on samples that are analogues of single molecules, as well as to develop the experimental technique to acquire multiple-view diffraction tomography data and to perform the first full 3D reconstructions. The results from these experiments were significant to the field, since we were able to demonstrate, for the first time, true lensless X-ray imaging (Marchesini, 2003a; 2003b) (see Figure 14), and then extend that to the first full high-resolution 3D lensless X-ray image.

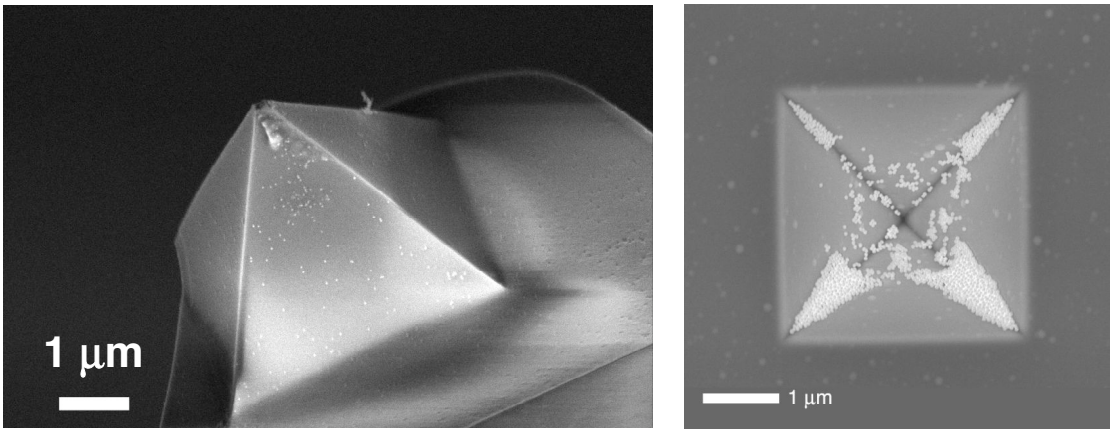

Figure 15. Three-dimensional test objects fabricated for X-ray diffraction imaging. The left picture shows a SEM perspective image of a silicon nitride pyramid membrane, and the right picture shows a top view of a similar pyramid that has been decorated with 50 nm diameter gold spheres. The silicon nitride is 100 nm thick, and the pyramid is hollow. These objects are ideal for testing since they can be well characterized in the SEM, have extent in all three dimensions, and can be treated as an analogue to a molecule. The samples were fabricated at the LLNL Microtechnology Center, following a suggestion by Ray Mariella.

At the LLNL Microtechnology Center, we fabricated samples consisting of 50 nm colloidal gold spheres deposited on a silicon nitride window. We used an AFM to arrange the spheres in an optimal distribution of a few micron extent and with a limited number of spheres. This manipulation on the submicron scale opens up the technique of X-ray diffraction imaging to a larger range of samples. This is because the required condition of an isolated object can be strictly enforced (for example for a group of cells). Holographic methods can be employed by placing a reference-wave scatterer (a gold sphere) at an optimal position relative to the object of interest, which will lead to an enhanced signal to noise ratio. The implications of these experiments are discussed in He *et al*. (2003). In addition to two-dimensional samples of gold spheres on a flat membrane, we spent considerable effort in fabricating three-dimensional samples. For the ALS detector geometry, wavelength, and resolution, we required an object no larger than 2 μm in all three dimensions. This was achieved by fabricating a silicon nitride membrane pyramid in a silicon-framed window, following a suggestion by Ray Mariella (LLNL). The process is to anisotropically etch a pyramid into a silicon wafer, grow nitride on the surface with the pyramid pit, then etch away the silicon from the back. The pyramid was then coated with colloidal gold spheres with the AFM method. A SEM image of a sample is shown in Figure 15.

We then carried out coherent X-ray diffraction imaging of the three-dimensional pyramid. The images were processed using the parallelized “shrinkwrap” algorithm and SPEDEN program, and a 3D reconstruction of the pyramid was obtained as shown in Figure 16. Although the reconstruction of images from experimental coherent X-ray diffraction patterns has been previously demonstrated, all work to date has required detailed and high-resolution images to provide real-space boundary constraints for the reconstruction algorithms. These real-space maps of the object boundary have all been

determined from images acquired in X-ray microscopes at near the resolution required in the final reconstruction. Such a stringent requirement would render single-particle imaging in XFELs all but useless. Our algorithm requires absolutely no prior knowledge about the spatial distribution of the sample, and does not require a secondary image. Instead, our simple but extremely powerful advance is to use the current estimate of the image to give a guess of the real-space boundary constraint. A comparison of our reconstructed image, of a field of gold balls on a flat membrane, with an SEM image of the sample shows the fidelity of the imaging technique (Figure 14). This is a significant advance in the field, which has clearly established our dominance and demonstrates the feasibility of lensless diffraction imaging of single-molecules.

3. Exit Plan

The exit plan from the outset of this Exploratory Research project was to determine the feasibility of XFEL atomic-resolution imaging, its benefit to the Laboratory and, if appropriate, go forward with a Strategic Initiative project to secure LLNL participation in the LCLS experiments in Biological Imaging, and bring new science and technology opportunities to the Lab in the areas of high-energy density science, X-ray imaging, and biology. LCLS is not a User facility, and Laboratory participation in these experiments (as opposed to acting as a vendor for facility optics and diagnostics) must be as a member of the teams selected for first experiments. Throughout the period of the project we have managed to become an influential part of such a team. We accomplished this through a focused and persistent effort of organizing workshops and informal meetings, initiating collaborations, and establishing a high-quality publication record.

There are advantages to the Lab to continue a focus of research in bio-imaging at LCLS. In particular, the bio-imaging research on LCLS has the following attributes:

a) It has the highest scientific visibility
b) It encompasses multiple experimental, theoretical and technological aspects relevant to programmatic work on LCLS itself,
c) It maintains and develops skills generally needed by the Laboratory
d) It provides the high possibility of external funding

The LCLS bio-imaging research has the most stringent experimental requirements (extreme focusing, alignment, temporal compression, sample manipulation, diagnostics, etc). Understanding the associated Coulomb explosion of the sample implies an understanding of the intermediate regimes of optics damage and warm dense matter. It encompasses most aspects of all the other LCLS experiments, and it requires and further develops the unique Laboratory strengths in photon-material interactions, diagnostics and optics.

During the ER project we successfully worked towards the exit plan that we laid out in 2002. Early in the project we became a part of the pre-existing LCLS bio-imaging team, lead by Prof. Janos Hajdu who is the originator of the LCLS bio-imaging concept. Our recognition in the community grew with our world firsts in 3D lensless X-ray imaging,

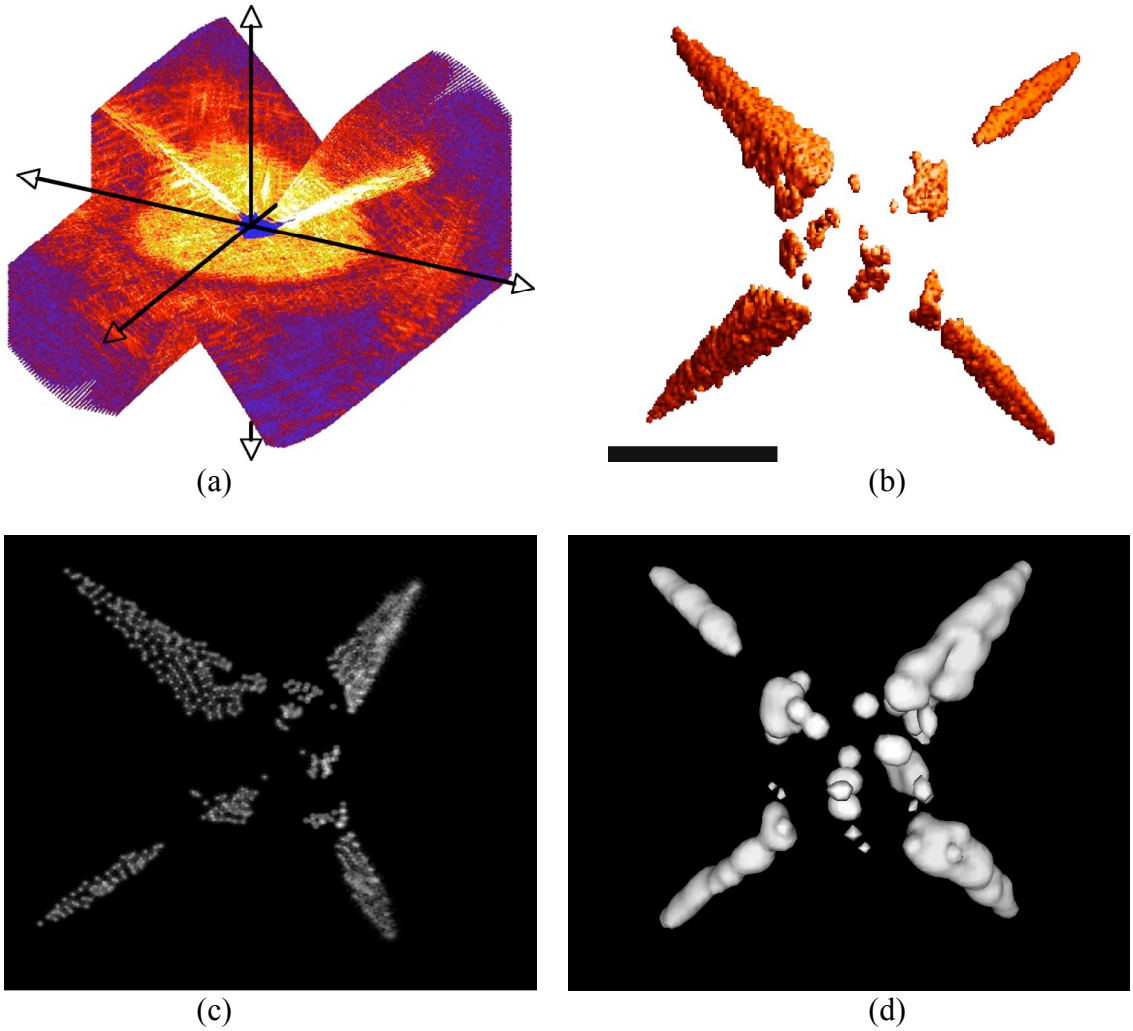

Figure 16. Highest-resolution 3D X-ray image of a non-periodic object. (a) A rendering of the 1024^3-element 3D diffraction dataset (with a quadrant removed for visualization) recorded at a wavelength of 1.6 nm at ALS from the test object shown in Figure 15. (b) A rendering of the 3D image, reconstructed with a 3D version of our "Shrinkwrap" algorithm. Scalebar is 1 micron. The reconstructed resolution is 10 nm in all three directions. (c) A two-dimensional reconstruction of a single-view diffraction pattern using the "shrinkwrap" algorithm. Artifacts can be seen due to the propagation of X-rays through the thickness of the object. Such artifacts are overcome by 3D reconstruction as in (b). (d) A three-dimensional reconstruction using the SPEDEN program.

and unique capabilities in modelling the XFEL-matter interaction. The culmination of this step was our organizing and leading the International Workshop on Instrumentation Development for Biological Imaging at the LCLS, held March 15-16, 2004, at SLAC, which led to our submission of a Letter of Intent (LOI) for an experimental station to be built at LCLS (see Appendix C). The LOI unambiguously places LLNL as a leading institution of the bio-imaging team, and confirms our standing in the international community.

In preparation for the SI project to follow the ER, we leveraged funding from the NSF Center for Biophotonics Science and Technology, and were successful in winning proposals for first-year beamtime at the DESY VUV-FEL: the world's first X-ray FEL, that began operating in the last months of 2005 (although with a 6-nm wavelength this will unable to achieve atomic resolution). We proposed experiments to perform the first X-ray diffraction imaging experiments on an XFEL, including 2D images that break the radiation-damage resolution limit of X-ray microscopy, and 3D images of unsupported free-falling samples. In another series of experiments on the VUV-FEL we propose to directly measure, via X-ray scattering of aerosols, the Coulomb explosion of particles irradiated by the XFEL pulse. Each one of the experiments will be groundbreaking and a world first, promising publication in *Nature* or *Science*. Our proposals for the VUV-FEL beamtime were judged by DESY, against international competitors, on the basis of scientific payoff and technical feasibility. The DESY committee ranked our proposals A1, the highest ranking in both categories. On the basis of winning this beamtime our Uppsala collaborators have made a strong proposal for European Union Framework 6 funding to partially cover costs of the VUV-FEL experiments.

In addition to the Uppsala group, led by Prof. Janos Hajdu who is a co-investigator on this project, we have formed fruitful collaborations with DESY in Hamburg (Dr. Thomas Moeller), SUNY at Stony Brook (Prof. Janos Kirz), LBNL (Dr. Malcolm Howells and Dr. Haifeng He), Arizona State University (Prof. John Spence), and the University of Melbourne (Prof. Keith Nugent and Dr. Andrew Peele). One of us (Henry Chapman) is also part of the working group on XFEL physics, run by Prof. Claudio Pellegrini of UCLA. The groups mentioned here represent the leading expertise in the fields of diffraction imaging, short pulse photon material interactions, and XFEL sources and optics. The collaborations that we have fostered will be built upon in the SI, and will lead to capabilities and new knowledge well beyond what would be achieved in isolation.

Summary

New tools, x-ray free-electron lasers are being developed. As with the introduction of synchrotron x-ray sources, these new x-ray lasers will revolutionize the life sciences by making it possible to determine the atomic structure of macromolecules, protein complexes, and virus particles without the need for crystallization. It will be possible to achieve this with sub-picosecond time resolution in order to understand the dynamics of these molecules. In this research project we determined the feasibility of XFEL diffraction imaging and defined the R&D needed to perform the initial demonstration experiments at the LCLS. We demonstrated experimental capability to reconstruct ab *initio* 3D images from multiple-view single-shot data obtained using existing light sources, achieving the world's first full 3D coherent diffraction image and the highest resolution 3D x-ray image of a non-periodic object. We developed and published a new continuum dynamics model of XFEL-matter interactions, which includes more physics than existing molecular dynamics simulations and which can simulate large particles such as protein complexes and viruses. The estimate for the required pulse length to achieve atomic resolution is less than originally predicted by MD simulations, but shows the

feasibility of the technique with pulse durations less than 10 fs. However, preliminary analysis indicates that longer pulse durations could also be used, by utilizing sample preparation techniques, such as weakly orienting the molecules, using symmetric samples such as nanocrystals, and by using a water tamper around the molecule. In collaboration with Uppsala University we proposed and designed experiments to be carried out at the VUV-FEL, the shortest-wavelength FEL, which begins operation in 2005. Our proposal to the VUV-FEL facility was the highest ranked in an international competition. These experiments will help validate our dynamics models and will be used to design the imaging experiments at the LCLS.

Our team has fast become a leading world authority in XFEL imaging, based on the strength of our theoretical and experimental results, and the lead we will take in the VUV-FEL experiments. We have secured an influential position for LLNL as a Science Team Leader on the LCLS Ultrafast Science Instrumentation project, and as such we will define the necessary R&D required for XFEL imaging, as well as provide LLNL early access to the unique capabilities that LCLS will provide. In doing so we will bring to the Lab enhanced capabilities in high-energy-density science, biophysics, and X-ray imaging and metrology.

Acknowledgements

This work was performed with a large number of generous collaborators, many of whom have been named in this report. We would like to thank the staff of the Advanced Light Source, and the support of Janos Kirz (Stony Brook University and LBNL) and Chris Jacobsen (Stony Brook University) for the use of the excellent diffraction apparatus at beamline 9.0.1. We would also like to thank Keith Hodgson of SLAC, who consistently encouraged this work and guided us towards future opportunities. We gratefully acknowledge Richard Crandall and the Advanced Computations Group (Apple Computer, Inc.) for the development of the `dist_fft` software. In the course of this work we interacted with and depended upon many at LLNL, including Sherry Baker, Cindy Larson, John Taylor, Jim Brase, Jim De Yoreo, Alex Artyuhkin, Shannon Ward, Rick Levesque, Jackie Crawford, Cheryl Stockton, Ray Mariella (who gave use the idea of the silicon nitride test object), Giles Graham, Dennis Matthews, and Steve Lane.

References

Bilderback, D., I. Bazarov, K. Finkelstein, S. Gruner, G. Krafft, L. Merminga, H. Padamsee, Q. Shen, C. Sinclair, M. Tigner, Synchrotron Radiation News **14**, 12 (2001).

Cavalleri, A. L. et al., Phys. Rev. Lett., **94**, 114801 (2005)

Cederquist, J. N., Fienup, J.R., Marron, J.C. & Paxman, R.G. Phase Retrieval from Experimental Far-Field Speckle Data. *Opt. Lett.* **13**, 619-621. (1988).

Cornacchia, M., J. Arthur, K. Bane, P. Bolton, R. Carr, F.J. Decker, P. Emma, J. Galayda, J. Hastings, K. Hodgson, Z. Huang, I. Lindau, H.D. Nuhn, J.M. Paterson, C. Pellegrini, S. Reiche, H. Schlarb, J. Stohr, G. Stupakov, D. Walz, and H. Winick, "Future possibilities of the Linac Coherent Light Source," J. Synchr. Rad. **11**, 227-238 (2004).

Crandall, R., E. Jones, J. Klivington, and D. Kramer. Gigaelement FFTs on Apple G5 clusters. Technical report, Advanced Computation Group, Apple Computer, http://images.apple.com/acg/pdf/20040827_GigaFFT.pdf (2004).

Frigo, M. and S. G. Johnson. The design and implementation of FFTW3. *Proceedings of the IEEE*, 93(2):216–231, (2005)

Gerchberg, R. & Saxton, W. Practical Algorithm for Determination of Phase from Image and Diffraction Plane Pictures. *Optik* **35**, 237-246 (1972)

Hajdu J. and E. Weckert (2001), "TESLA Design Review, Life Science Applications," http://tesla.desy.de/new_pages/TDR_CD/start.htm

Hau-Riege, S. P., London, R. A., and Szoke, A., Phys. Rev. E, **69**, 51906, (2004a)

Hau-Riege, S. P., R. A. London, and A. Szoke. Dynamics of biological molecules irradiated by short x-ray pulses. *Phys. Rev. E*, 69:051906, (2004b)

Hau-Riege, S. P., R. A. London, G. Huldt, and H. N. Chapman. Pulse requirements for x-ray diffraction imaging of single biological molecules. *Phys. Rev. E*, 71:061919, (2005)

He, H., S. Marchesini, M. Howells, U. Weierstall, G. Hembree and J. C. H. Spence, Experimental lensless soft-X-ray imaging using iterative algorithms: phasing diffuse scattering, Acta Cryst. A59, 143-152 (2003).

Henderson, R., "Cryoprotection of protein crystals against radiation damage in electron and X-ray diffraction," Proc. R. Soc. London Sci. Ser. B **241**, 6-8 (1990).

Henderson, R. "The potential and limitations for neutrons, electrons and X-rays for atomic resolution microscopy of unstained biological molecules," Quarterly Rev. Biophys. **28**, 171-193 (1995).

Huldt, G., A. Szoke, and J. Hajdu. Diffraction imaging of single particles and biomolecules. *Journal of Structural Biology*, 144:219–227, (2003)

Kamura, Y. & Komatsu, S. Phase retrieval microscope for quantitative imaging of a weak phase object. *Jpn. J. Appl. Phys*. **37**, 6018-6019 (1998).

Lindenberg, A. M. et al. Science **308**, 392–395 (2005).

Marchesini, S. et al. Phys. Rev. B **68**, 140101(R) (2003a).

Marchesini, S., He, H., Howells, M., Weierstall, U., Chapman, H., Hau-Riege, S. & Spence, J.C.H., Opt. Expr. 11, 2344-2353 (2003b).

Miao, J. and D. Sayre, Acta Cryst. **A56**, 596 (2000).

Nuhn H.-D. and J. Rossbach, Synchrotron Radiation News **13**, 18 (2000).

Pellegrini, C. and J. Stoehr, Beam Line **32**, 32 (2002).

Press, W. H., S. A. Teukolsky, W. T. Vetterling, and B. P. Flannery, Numerical Recipes in C, Cambridge University Press, 2nd Edition (1992).

Sayre, D. Acta Cryst. **5**, 843 (1952).

Sayre, D. Image processing and coherence in Physics. Springer Lecture Notes in Physics 112, Ed. M. Schlenker, 229-235 (1980).

Sayre, D. and H. N. Chapman, *Acta. Cryst.*, **A51**, 237-252 (1995).

Shen, Q., CHESS Technical Memo 01-002 (2001). Available at http://erl.chess.cornell.edu/papers/ERL_CHESS_memo_01_002.pdf

Siwick, B.J., J.R. Dwyer, R.E. Jordan, and R.J.D. Miller, "Ultrafast electron optics: Propagation dynamics of femtosecond electron packets," J. Appl. Phys. **92**, 1643-1648 (2002).

Solem, J.C., and G. C. Baldwin, Science, **218**, 229 (1982).

Solem, J.C. and G. F. Chapline, Opt. Eng., **23**, 193 (1984).

Spence, J.C.H. and R.B. Doak, "Single molecule diffraction," Phys. Rev. Lett. **92,** 198102 (2004).

Szoke, A. Holographic Methods in X-ray Crystallography .II. Detailed Theory and Connection to Other Methods of Crystallography. Acta Cryst. A49, 853-866 (1993).

A. Publications from the Project

A.1. Papers to Peer-Reviewed Journals

1. "X-ray image reconstruction from a diffraction pattern alone," S. Marchesini, H. He, H. N. Chapman, S. P. Hau-Riege, A. Noy, M. R. Howells, U. Weierstall, and J. C. H. Spence, Phys. Rev. B **68**, 140101 (2003) (UCRL-JC-153571)
2. "Single particle diffraction imaging: image classification," G. Huldt, A. Szoke, J. Hajdu, J. Struct. Biol. **144**, 219-227 (2003) (UCRL-JC-154036)
3. "SPEDEN: Reconstructing single particles from their diffraction patterns," S.P. Hau-Riege, A. Szoke, H. N. Chapman, and H. Szoke, Acta Cryst. A (in press, 2004) (UCRL-JC-154574)
4. "Unique phase recovery for non-periodic objects," K. A. Nugent, A. Peele, and H. Chapman, Phys. Rev. Lett. **91**, 203902 (2003) (UCRL-JC-152722)
5. "Coherent X-ray diffractive imaging: applications and limitations," S. Marchesini, H. N. Chapman, S. P. Hau-Riege, R. A. London, A. Szoke, H. He, M. R. Howells, H. Padmore, R. Rosen, J. C. H. Spence, U. Weierstall, Opt. Express **11**, 2344 (2003) (UCRL-JC-155105)
6. "Inversion of x-ray diffuse scattering to images using prepared objects," H. He, S. Marchesini *et al*., Phys. Rev. B **67**, 174114 (2003) (UCRL-JC-151664).
7. "Mo:Y multilayer mirror technology uitlized to image the near-field output of a Ni-like Sn laser at 11.9 nm," J. Nilsen, S. Bajt, H.N. Chapman, F. Staub, and J. Balmer, Opt. Lett. **28**, 2249-2251 (2003) (UCRL-JC-152269).
8. "Taking X-ray diffraction to the limit: Macromolecular structures from femtosecond X-ray pulses and diffraction microscopy of cells with synchrotron radiation," J. Miao, H.N. Chapman, J. Kirz, D. Sayre, and K.O. Hodgson, Ann. Rev. Biophys. And Biomol. Structure **33**, 157 (2004) (UCRL-JP-200184)
9. "Dynamics of X-ray irradiated biological molecules," S.P. Hau-Riege, R.A. London, and A. Szoke, Phys. Rev. E 69, 051906 (2004). Also published in the Virtual Journal of Ultrafast Science, June (2004). (UCRL-JC-155565)
10. "Extended and Prepared Reference Objects in Experimental Fourier Transform X-Ray Holography," H. He, M.R. Howells, S. Marchesini, H.N. Chapman, U. Weierstall, H.A. Padmore, J.C.H. Spence, Appl. Phys. Lett. **85** 2454–2456, (2004) (UCRL-JRNL-204107)
11. "Phasing diffuse scattering. Application of the SIR2002 algorithm," B. Carrozini, G. L. Cascorano, L. De Caro, C. Giacovazzo, S. Marchesini, H. N. Chapman, M. R. Howells, H. He, J. S. Wu, U. Weierstall, J.C.H. Spence, Acta Cryst. A **60** 331-338 (2004) (UCRL-JRNL-203071)
12. "Diffraction with Wavefront Curvature: a Path to Unique Phase Recovery," K. A. Nugent, A.G. Peele, H.M. Quiney, and H. N. Chapman, Acta Cryst. A. **61** 373-381 (2005) (UCRL-JRNL-211569).
13. "Atomic-scale visualization of inertial dynamics," A. Lindenberg, J. Larsson, K. Sokolowski-Tinten, K. Gaffney, C. Blome, O. Synnergren, J. Sheppard, C. Caleman, A. MacPhee, D. Weinstein, D. Lowney, T. Allison, T. Matthews, R. Falcone, A. Cavalieri, D. Fritz, S. Lee, P. Bucksbaum, D. Reis, J. Rudati, D. Mills, P. Fuoss, G. Stephenson, C. Kao, D. Siddons, R. Pahl, J. Als-Nielsen,

S. Dusterer, R. Ischebeck, H. Schlarb, H. Shulte-Schrepping, T. Tschentscher, J. Schneider, O. Hignette, F. Sette, H. Chapman, R. Lee, T. Hansen, S. Techert, J. Wark, M. Bergh, G. Huldt, D. van der Spoel, M. Timneanu, J. Hajdu, D. von der Linde, R. Akre, E. Bong, P. Emma, P. Krejcik, J. Arthur, S. Brennan, K. Luening, J. Hastings, Science, **308**, 392–395 (2005) (UCRL-JRNL-210233).

14. "Clocking femtosecond X-rays," A. L. Cavalieri, D. M. Fritz, S. H. Lee, P. H. Bucksbaum, D. A. Reis, D. M. Mills, R. Pahl, J. Rudati, P. H. Fuoss, G. B. Stephenson, D. P. Lowney, A. G. MacPhee, D. Weinstein, R. W. Falcone, R. Pahl, J. Als-Nielsen, C. Blome, R. Ischebeck, H. Schlarb, T. Tschentscher, J. Schneider, K. Sokolowski-Tinten, H. N. Chapman, R. W. Lee, T. N. Hansen, O. Synnergren, J. Larsson, S. Techert, J. Sheppard, J. S. Wark, M. Bergh, C. Calleman, G. Huldt, D. van der Spoel, N. Timneanu, J. Hajdu, E. Bong, P. Emma, P. Krejcik, J. Arthur, S. Brennan, K. J. Gaffney, A. M. Lindenberg, J. B. Hastings, Phys. Rev. Lett., **94**, 114801 (2005) (UCRL-JRNL-207122).

A.2. Invited Presentations

1. "Hydrodynamic model of X-Ray Irradiated Biological Molecules," S. Hau-Riege, X-ray science with coherent radiation, San Francisco, August 2003 (UCRL-PRES-15272)
2. "Prospects for Single-Particle Imaging with XFELs," H. Chapman et al, Second International Workshop on Noncrystallographic Phase Retrieval, Palm Cove (Australia), July 2003 (UCRL-PRES-154182)
3. "Dynamics of X-Ray Irradiated Molecules," S. Hau-Riege, DESY (UCRL-PRES-151688)
4. "Hydrodynamic model of short pulse X-ray imaging," R. London, Uppsala, 2002 (UCRL-PRES-149846).
5. "Instrument development workshop for biological imaging experiments at LCLS," H.N. Chapman, Instrument development workshop for biological imaging experiments at LCLS, March 15-16, 2004 (UCRL-PRES-203061).
6. "The role of damage in x-ray imaging of biological molecules," S. P. Hau-Riege, Instrument development workshop for biological imaging experiments at LCLS, March 15-16, 2004 (UCRL-PRES- 207385)
7. "Diffraction imaging with x-rays and electrons," H.N. Chapman, First Workshop on Ultrafast Electron Diffraction, Pleasanton CA, April 2004 (UCRL-PRES-204134).
8. "Prospects for single-particle imaging at XFELs," H.N. Chapman, IEEE-LEOS Summer Topicals Meeting on Biophotonics, June 2004 (UCRL-PROC-203932)

A.3. Other Presentations

1. "X-ray microscopy by phase-retrieval methods," M. Howells, H. Chapman, *et al*, J. De Physique IV **104**, 557-561 (2003) (UCRL-JC-151355)
2. "Imaging without lenses," S. Marchesini et al, *Second International Workshop on Noncrystallographic Phase Retrieval*, Palm Cove (Australia), July 2003 (UCRL-PRES-153586)

3. "Hydrodynamic Model of X-Ray Irradiated Nano-Particles," R. London et al, SPIE conference on *X-Ray optics for fourth-generation x-ray sources,* San Diego, August 4, 2003 (UCRL-PRES-151328)
4. "Compression of X-ray FEL Pulses with Volume Diffraction Elements," H. N. Chapman, S. Bajt, K. A. Nugent, E. M. Gullikson, and A. Aquila, SPIE conference on *X-Ray optics for fourth-generation x-ray sources,* San Diego, August 4, 2003 (UCRL-PRES-151222).
5. "Normal incidence multilayer coatings for 6 to 12 nm wavelength region," S. Bajt, H.N. Chapman, B. Kjornrattanawanich, J. Alameda, J. C. Robinson, SPIE conference on Advances in mirror technology for X-rays, San Diego, August 2003 (UCRL-PRES-151205)

A.4. Records of Invention

1. "Method for Characterizing Mask Defects Using Image Reconstruction from X-Ray Diffraction Patterns", S. P. Hau-Riege, IL-11154.
2. "A high-efficiency spectral purity filter for EUV lithography," H. N. Chapman, August 12, 2003. IL-
3. "Method for Reconstructing Single Particles from Their Diffraction Patterns," S. P. Hau-Riege, H. Szoke, A. Szoke, H. N. Chapman, IL-11302
4. "A Tamper to Delay the Motion of a Sample During Irradiation by Short Intense X-Ray Pulses," R. A. London, A. Szoke, S. P. Hau-Riege, H. N. Chapman, IL-11271

A.5. Technical Reports

1. "An extraordinarily bright idea," R. Bionta and H. N. Chapman, Science and Technology Review, December 2003 (UCRL-52000-03-12)
2. S. P. Hau-Reige, "Pulse requirements for electron diffraction imaging of single biological moleculels," UCRL-TR-207533
3. H. N. Chapman, "Estimates of signals in LCLS diffraction imaging experiments," UCRL-TR-210230

B. VUV-FEL Proposals and Review

A package of three proposals was submitted to the Hamburg Synchrotron Radiation Laboratory (HASYLAB), DESY, for consideration for beamtime at the VUV-FEL. The proposals were submitted as a collaboration between ourselves and University of Uppsala. The acceptance letter of the proposals from J. Schneider, Director of HASYLAB, is given below, followed by our proposal package.

Deutsches Elektronen-Synchrotron DESY

Prof. Dr. Jochen R. Schneider
Director of Research

DESY
Hamburg

Prof. J. Hajdu, University of Uppsala
Structural and Computational Biophysics
Box 576, 751 23 UPPSALA, Sweden

Dr. H. Chapman
L-395, LLNL
Livermore, CA 94550
USA

Extension: -3815
Fax: -4475
Email: jochen.schneider@desy.de
http://www-hasylab.desy.de/

Hamburg, December 16, 2002

Your proposal II-**02-039 FEL,** formerly chapters 10 and 11 of proposal II-02-049 FEL
Projectleader: **J. Hajdu, H. Chapman**
Project title: "Coulomb explosion and diffraction imaging of biological samples"

Dear Professor Hajdu, dear Dr. Chapman,

it is a pleasure to inform you that the above proposal has been accepted as a research project for the VUV FEL at DESY-HASYLAB. The project review panel has recommended that the experiments on biological samples you proposed (chapters 10 and 11 of proposal II-02-049 FEL) should be considered as a separate proposal. Consequently, your proposal has been assigned project number II-02-039 FEL with project leaders J. Hajdu and H. Chapman and the project title "Coulomb explosion and diffraction imaging of biological samples". For your information, the panel also recommended that the proposal originally assigned II-02-039 FEL, project leader V.E. Fortov, should join the "plasma consortium" instead and participate in the proposed effort of proposal II-02-049 FEL.

Due to the unique situation that the VUV FEL in the TTF II phase is a new and yet untested source, the project review panel has characterized the research projects by two criteria: scientific content and feasibility in accordance with the FEL characteristics and photon diagnostics expected to be available in 2004 as well as the status of the proposed experimental apparatus. The scientific content of all research projects is ranked from A to C in descending order or the proposal is rejected (ranking D). In addition, several proposals, which are considered to be of major importance for technical development of VUV FEL diagnostics, are ranked T. The feasibility is ranked from 1-3; 1 most easily realisable, 2 requires the completion of more complex diagnostics, in particular the monochromator, and 3 considered difficult at a first stage. On this basis beamtime will be allocated.

Your project has been ranked: A1

Letters: D-22603 Hamburg
Phone: +49 40 8998-0
Fax: +49 40 8998-3282
Address: Notkestrasse 85, D-22607 Hamburg

Locations of DESY are Hamburg and Zeuthen/Brandenburg

Directorate: Prof. Dr. R. Klanner, Ch. Scherf, Dr. H. von der Schmitt, Prof. Dr. J. R. Schneider, Dr. D. Trines, Prof. Dr. A. Wagner (Vorsitzender)
Representative of the Directorate in Zeuthen: Dr. U. Gensch

At the current planning stage, projects ranked A1 will receive two weeks of beamtime in 2004, proposals ranked A2 one week. Two experiments are expected to be set up in parallel and share the VUV FEL during their appointed beamtime. Projects ranked T will receive beamtime during the time allocated to FEL driven R&D independent of user beamtime. Other projects will be appointed beamtime upon availability. At this early stage, the proposed beamtime allocations are subject to change according to the availability of the system. The HASYLAB team will keep you informed on the status of the FEL as much as possible.

I would like to thank you for your engagement at such an early stage of the VUV FEL project. The research proposals offer a very strong case for the VUV FEL and we are looking forward to many exciting new results.

Let me finally mention that we need copies of all publications and reports resulting from this work as well as a list of all collaborations, and your contribution to the HASYLAB annual report.

Yours sincerely,

J. Schneider

Jochen R. Schneider
Director HASYLAB
Hamburg Synchrotron Radiation Laboratory

B.1. Biological Imaging in the VUV-FEL (Overview)

X-ray FELs promise to revolutionize the life sciences, by allowing atomic resolution imaging of virtually any macromolecule, protein complex, or virus. Such an ability will have a profound impact on structural biology and medicine, and could eventually lead to solving the entire proteome—the complete structure of every protein that can be expressed by a genome. The technique that will enable this is single-molecule diffraction. By using pulses of X-rays that are intense enough and short enough in duration, a diffraction pattern could be recorded from a single molecule. The molecule will subsequently Coulomb-explode, but if the timescale for structural change (at the Angstrom scale) is longer than the pulse duration then the diffraction pattern will represent the undamaged molecule. A complete three-dimensional atomic-resolution structure determination requires many diffraction patterns made at different molecule orientations. These will be obtained by injecting single molecules into the beam and recording one pattern per pulse.

Although the shortest wavelength of the VUV-FEL precludes atomic resolution imaging, this source will provide crucial information regarding the dynamics of the Coulomb explosion, the effects of high fields on the scattering factors of atoms, and in validating the diffraction-based imaging technique. In addition, it will enable X-ray microscopy to be performed on living systems beyond the current resolution limited by radiation damage. The VUV-FEL experiments will also enable us to develop the necessary sample handling techniques in which single molecules or clusters can be injected into the pulsed beam. Obtaining the intensities required to record high-resolution diffraction data will require the use of X-ray optics that will provide extremely concentrated X-ray beams, and understanding the lifetime and performance of such optics in high-intensity beams is a priority. We propose experiments to examine these fundamental questions so that we will be fully prepared for future experiments at XFELs. The experiments include an investigation of the dynamics of the Coulomb explosion by small-angle scattering, high-resolution diffraction imaging of biological samples, and an investigation of damage in X-ray optics. Proposals for these experiments follow.

B.2. Coulomb Explosions of Biological Samples

Abstract

X-ray FELs will offer the opportunity to image single molecules and virus particles, at atomic resolution, without the need for crystallization. The imaging method relies upon overcoming the steady-state radiation-damage resolution limit by using pulses short and intense enough to be able to scatter enough photons from the particle before the damage processes have begun to modify its structure. In this flash-imaging regime, the damage will be the ionisation of atoms in the sample and the subsequent Coulomb explosion of the molecule. Recent molecular dynamics calculations have shown that in the femtosecond time domain, diffraction to high resolution may be observable for single virus particles and nanocrystals or nanoclusters of proteins (a nanocrystal of 5×5×5 lysozyme molecules is predicted to diffract to atomic resolution). The limitations and XFEL pulse requirements of single-molecule diffraction imaging crucially depend on the dynamics of the Coulomb explosion. Experiments have not been carried out to validate models due to the lack of a suitably bright source. Experiments on the VUV-FEL will provide data on the progression of the explosion over the duration of the pulse and longer, for particles similar in composition to biological materials. The experiments will measure the size of particles as they explode by measuring the FEL scattering pattern from a gas of particles (similar to visible-light Mie scattering from aerosol particles) as a function of X-ray fluence. Pump-probe experiments will also be carried out where both the pump and the probe are split from the same soft-X-ray FEL pulse. The use of a water-drop tamper will be investigated as a way to slow down the damage of the particle. The experiments will give direct and compelling evidence on the viability and capabilities of the imaging technique of single molecule X-ray diffraction.

Scientific Background

One of the most impressive and far-reaching XFEL experiments envisioned is atomic resolution imaging of single molecules, single virus particles, or nanocrystals. The method relies on being able to record the large-angle diffraction pattern of single particles, which will require incident fluences greater than 10^{12} photons/0.1 μm^2 [1]. Although this is about five orders of magnitude greater than the steady-state radiation-damage fluence limit with macroscopic samples it is possible to obtain the diffraction data if the X-ray pulse is shorter than the time for structure degradation at the Angstrom scale. This will require pulse lengths of 100 fs or less, and the damage in this case will be the ionization of atoms in the sample and the subsequent Coulomb explosion of the molecule. The limitations and XFEL pulse requirements of single-molecule diffraction crucially depend on the dynamics of this Coulomb explosion. Although molecular dynamics [1] and hydrodynamics [2] modeling has been carried out which suggests that atomic-resolution diffraction patterns could be obtained, it has not been possible to carry out experiments to verify those models due to the lack of a suitable source. It is the goal of the experiments proposed here to measure the progress of a Coulomb explosion using soft X-rays, over the duration of the interaction with a FEL pulse.

Molecular dynamics calculations have been carried out on a number of molecules of a range of sizes [1]. The calculations assume a single-photon cross-section for photoionization, and the photo- and Auger electrons are taken to infinity. The positively charged atoms then repel each other and the molecule explodes. The results have shown that 12 Å resolution can be achieved with XFEL pulses of 8×10^{11} photons/0.1 μm^2 and 50 fs duration for a cluster of 125 lysozyme molecules. Higher resolution can be achieved with larger samples. For example a resolution of 2.5 Å can be achieved with 10 fs pulse duration for tomato bushy stunt virus samples. There are many effects that still need to be added to the models. Auger electrons will cause a cascade of secondary electrons over a volume that is comparable to a large molecule or virus [3]. Most of the Auger and secondary electrons will be trapped in the molecules by the net positive charge left behind by the escaped photoelectrons. The trapped electrons will affect the explosion, both by shielding the charge in the core of the molecule and also by providing a quasi-neutral plasma pressure. We expect the outer layers of the molecule will by expelled by the coulomb forces, which the inner part will undergo a pressure-driven explosion. High electric fields from the X-ray pulse may considerably modify the scattering factors and absorption cross sections. Two-photon absorption cross-sections are not known. While modeling efforts continue to be refined, we require experiments in a FEL to validate our models.

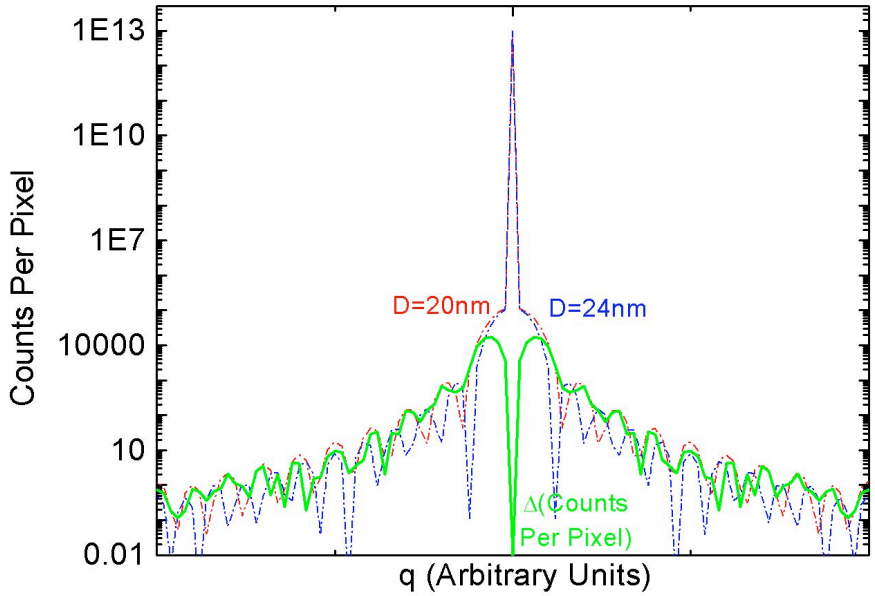

Figure CEBS 1. Computed diffracted intensities at a wavelength of 6 nm for a 20 nm diameter protein sphere before Coulomb explosion (red) and after the sphere has expanded in diameter by 20% (for which the density has dropped by 32%). Shown in green is the expected difference in counts per pixel for these two cases. The areal density of spheres for the calculation was 25 per μm^2 and the beam energy was 0.3 mJ, or 10^{13} photons. The large central spike is the zero order that would pass through the hole in the detector. The calculation follows a method used to estimate scattering strength of colloidal gold in dark-field X-ray microscopy [4].

In order to record the dynamics of the explosion over the very short duration of the pulse, we propose to measure small-angle scattering of the particles. The particles will be sprayed into the vacuum to intersect with the beam, and just as in visible-light diffraction from aerosol particles, or diffraction from randomly positioned identical particles, the diffraction pattern will be the incoherent sum of diffraction patterns of single particles. In this way, the signal to noise of this experiment will be large due to the high particle density of the spray (up to 10^6 particles interacting with the beam) and the SNR can be increased further by summing measurements over many pulses. We propose the use of 20 to 50-nm diameter latex spheres, this material being chosen for the availability of mono-dispersed colloidal suspensions of such spheres, and their compositional similarity to biological materials. Actual biological samples, including benign virus particles, will also be used. From the scattering pattern we will determine the size distribution of the particles, and this will be measured as a function of pulse fluence. Undamaged spheres will diffract 6-nm wavelength light to angles of 7 to 17 degrees, and larger (exploding) particles will diffract to smaller angles. The fluence will be varied simply by moving through focus of the beamline focusing optics. In the simplest experiment the size distribution will be measured, integrated over the duration of the pulse. The fluence will be varied over values that bracket the expected damage threshold of about 1 J/cm^2. For the 0.3 mJ beam of the VUV-FEL, this threshold occurs when the unattenuated beam is

focused to a 200-μm diameter spot. As the fluence exceeds the damage threshold and the particle expands, the diffraction pattern will change. For example, for a pure coulomb explosion, the continuum model predicts that the outer radius of the particle will grow quadratically with time and the density inside will drop uniformly. The diffracted energy scales as the inverse-square of the radius. When the particle grows by 20% in radius, the density will drop by a factor of 2. The diffraction pattern of the exploded particle is predicted to be 20% as large in angle, but 0.7 times as strong. For a beam energy of 0.3 mJ and 25 identical particles per square micron in the beam, we expect a signal level $>3\times10^6$ photons/steradian, adequate for considerable better than a 20 % measurement of the particle size (see Figure CEBS 1).

Note that as the fluence is varied, the average detected signal in the experiment will remain constant (for non-exploding particles). This is because the signal depends only on the areal density of particles. The diffracted signal of a single particle depends on the number of photons per unit area, and as this fluence decreases, by increasing the beam area, the number of particles in the beam increases in proportion.

An experiment that will provide more information on the speed at which the explosion develops is a pump-probe measurement where both the pump and probe are split from the same FEL pulse. A fraction of the pulse energy is split from the beam and delayed. This beam can be considered as a backlighter that will be used to record scattering from the Coulomb-exploding particles. In other measurements, we will record the dependence of the explosion on particle size, and on particle structure (for example, we will study the effectiveness of water as a tamper to the explosion).

Experimental Plan

The experiments proposed here are similar to the Coulomb explosions of atomic clusters carried out by Dr. Thomas Moller, and experiments will be carried out in the same chamber as those experiments. The existing diagnostics of time of flight mass and electron spectrometers, and fluorescence detector, will be employed in these experiments. A direct detection back-illuminated CCD will be provided to record the scattering patterns, and a new sample injection and collection apparatus will be added that can handle particles diameters from 20 nm to 2 μm. An attenuator will be required in the beamline to enable alignment of the CCD and particle injection. The split and delay will be identical to that used in the optics damage experiments (see description in proposal "X-ray interaction with matter: optics damage") and will be provided in a separate chamber. This optical system will not be needed for the initial experiments.

The direct-detection soft X-ray CCD will be supplied by LLNL and is the same equipment that will be developed for the diffraction imaging experiments. The detector will have a hole in the center for the direct beam to pass through (this will be achieved by tiling four CCD chips). The detector must never be exposed to the full-power FEL beam, and so an attenuator will be required for the initial alignment of the CCD. The sample handling equipment is currently under development at LLNL (see Figure CEBS 2). The system can produce a spray of single particles into vacuum and can be used on monodispersed particle diameters ranging from 0.02 μm to 2 μm. A solution with a colloidal suspension of particles is sprayed into sub-micron sized droplets with an atomizer. The water drops contain mostly either no particles or one particle. The drops are passed through a dryer and finally a neutralizer, before the particles are sprayed through a small orifice into the vacuum. The velocity of the particles is about 30 m/s. The spray fans out by about 5 degrees, and so it should be easy to align it to the X-ray beam. The areal density of particles in the spray, projected along the direction of the beam can be controlled by setting the distance of the orifice to the beam, and the concentration of the suspension. The unexposed particles of the spray will be collected in a cold trap. The injection system has been tested on 0.5-μm diameter silicon dioxide spheres, but could be used with latex spheres, colloidal gold particles, spores, virus particles, or nanocrystals. The evaporator and neutralizer can be turned off to spray sub-micron diameter water drops, or particles inside water drops. The particle injection system is compatible with Dr. Möller's atomic cluster chamber, and it should be possible to use the same orifice (or same mounting hardware for a similar orifice) to inject the particles as is used to produce atomic clusters.

It is expected in a Coulomb explosion that the particle increases in size whilst maintaining a uniform density throughout its volume. The width of the central diffraction peak will be inversely proportional to the mean particle size, integrated over the pulse duration. This width will be measured as fluence is varied, which will be achieved by moving the spray through the focus of the beamline optics, and employing a gas-cell attenuator. The samples will initially consist of 20-nm to 50-nm diameter latex spheres,

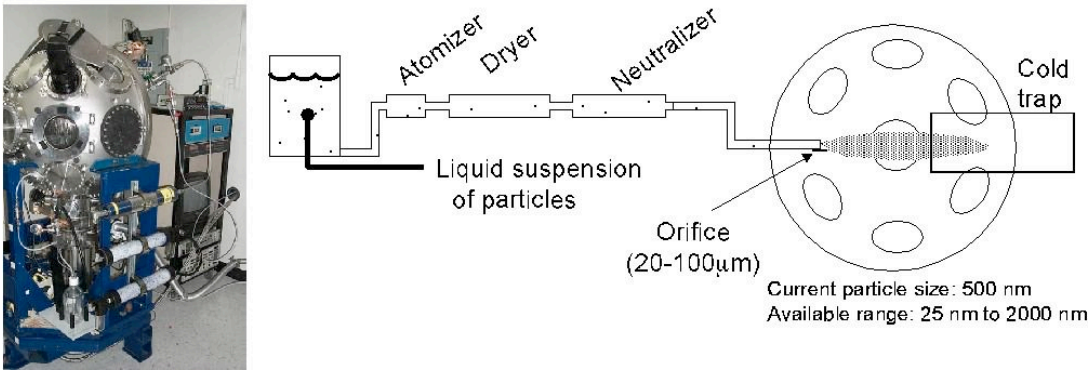

Figure CEBS 2: Particle sprayer system currently under development at LLNL. The system sprays single particles through a small orifice with particle velocities of about 30 m/s. The particles are essentially neutral, but could be made charged if we wished to manipulate their trajectories with electric fields.

and other materials, such as SiO_2 microspheres, protein, and water, will be used to verify the models. The expected diffraction signal from 20-nm protein spheres, with a single pulse, is shown in Figure CEBS 1. The areal density of spheres was 25 per μm^2. As can be seen, at this density there will be over 1000 counts per pixel at the half maximum of the central (non-zero-order) peak where the FWHM will be computed.

A further experiment will be to determine if a water-drop tamper will delay the damage of a latex or SiO_2 particle. Here we wish to work at an X-ray energy where water is transparent so that the diffraction pattern primarily relates to the size distribution of the particle. At an X-ray wavelength of 6 nm, a volume of silicate should scatter about 100 times more strongly than the same volume of water.

Pump-probe experiments will be carried out by splitting and delaying the FEL pulse. The initial intense pulse will be used to initiate the Coulomb explosion, and the delayed pulse will be used to record the scattering pattern. The optical components for the split and delay will be supplied by LLNL and will be located in a separate chamber. These optics will be the same as used in the optics damage experiments and are described in more detail in that proposal. The exact experimental scheme has not yet been decided. The possible schemes are to split the two beams by wavelength using a coarse grating (into first and a harmonic) or by intensity (both beams the same wavelength). In the former case, a filter will be placed at the detector so that only the scattering from the probe (the second or third harmonic) is recorded. In the second case, a part of the beam can be selected either using a large-area free-standing multilayer or a small finger mirror. The finger mirror has the disadvantage that it will cause a lot of scattering. The probe beam will be incident on the sample at a different angle than the pump beam, and so the diffraction patterns of the two beams would be separated in angle. In this case the particles will need to be confined to a narrow region in the direction of beam propagation, since the delay between the two beams will vary as a function of distance along this direction and as the sine of the included angle of the beams.

The expected scattering strength is quite large, and we do not foresee any difficulties in recording a pattern. Experiments will be carried out at LLNL to develop the sample injection and collection system to make sure that the beamline is not contaminated with particles. Another technical challenge is in protecting the X-ray CCD and we will develop attenuator filters that can allow reduced intensity illumination of a small area of the detector.

It is expected that these experiments will require two campaigns. The initial experiments will not include pump-probe measurements. Those experiments can be attempted after the split and delay optics have been proven in the optics damage experiments. We will require two weeks of beamtime per each campaign (total of four weeks beamtime). Each campaign will require three days of setup time and half a day to dismount the experiment. We will be ready to carry out the first campaign in the second half of 2003 and the second campaign early in 2004.

Experimental Requirements

The requirements for this experiment are:

1. Single FEL pulses, ideally at a wavelength of 6 nm. We would also like to use harmonics. We can utilize no more than 10 Hz repetition rate. Pulses need not be monochromatized, but they do need to be filtered from the spontaneous background.
2. Attenuator (10^{-4}) and shutter.
3. Focusing optics to achieve ~10 μm minimum spot, variable to 200 μm by translation of the target chamber.
4. Target chamber with particle injection system, soft-X-ray CCD, intensity monitor, and TOF mass- and electron-spectrometers.
5. Target (particle spray) alignment capability, with real-time viewing of luminescence.
6. Split and delay optics (in separate chamber).

Contributors

The list of involved individuals and their affiliations are:

Henry Chapman, Stefan Hau-Riege, Jaroslav Kuba, Richard Lee, Richard London, Abraham Szoke, Jim Trebes, and Alan Wootton, Lawrence Livermore National Laboratory, USA.

Janos Hajdu, Beata Ziaja, David van der Spoel, Remco Wouts, and Gösta Huldt, University of Uppsala, Sweden.

Richard Neutze, Chalmers University of Technology, Sweden.

Thomas Möller and Jacek Krzywinski, DESY, Germany.

Correspondence should be directed to:

Henry Chapman, L-395, LLNL, Livermore CA, 94550, USA.
chapman9@llnl.gov, fax: +1 925 423 1488

References

1. R. Neutze, R. Wouts, D. van der Spoel, E. Weckert and J. Hajdu, Nature, **406**, 757 (2000).
2. R. London and A. Szoke, in preparation.
3. B. Ziaja, D. van der Spoel, A. Szoke and J. Hajdu, Phys. Rev. B, **64**, 214104 (2001).
4. H. N. Chapman, C. Jacobsen, S. Williams, Ultramicros. **62**, 191—213 (1996).

B.3. Diffraction Imaging of Biological Samples

Abstract

X-ray FELs promise to revolutionise the life sciences, by allowing atomic resolution imaging of virtually any macromolecule, protein complex, or virus. Such an ability will have a profound impact on structural biology and medicine, and could eventually lead to solving the entire proteonome—the complete structure of every protein that can be expressed by a genome. The technique that will enable this is single-molecule diffraction. By using pulses of X-rays that are intense enough and short enough in duration, a diffraction pattern could be recorded from a single molecule before the radiation damage destroys it. A complete three-dimensional atomic-resolution structure determination requires many diffraction patterns made at different molecule orientations. These will be obtained by injecting single molecules into the beam and recording one pattern per pulse. Although the shortest wavelength of THE VUV-FEL precludes atomic resolution imaging, this source will be used to validate the diffraction-based imaging technique and to enable X-ray microscopy to be performed on living systems beyond the current resolution limited by radiation damage. The VUV-FEL will also enable us to develop the necessary sample handling techniques in which single molecules or clusters can be injected into the pulsed beam. We propose here groundbreaking experiments on the VUV-FEL to perform two-dimensional flash imaging of wet biological structures at resolutions approaching the X-ray wavelength, and high-resolution three-dimensional imaging performed on a set of individual particles.

Scientific Background

The extremely high brightness and short pulse duration of VUV- and X-FELs will allow a new regime of X-ray microscopy to be explored. On current synchrotron-based X-ray microscopes, where optics have steadily been improving, the highest resolution that can be achieved on living systems has reached a limit imposed by radiation damage. This resolution limit is about 20 nm or less, and is caused mainly by chemical changes, diffusion, and local heating over timescales greater than microseconds [1]. This barrier to resolution can be removed (or substantially reduced) by using intense X-ray pulses, of duration shorter than any process that causes structural changes over the resolution length of interest [2]. This concept of flash imaging can be extended all the way to atomic resolution [3] where it seems possible that single molecules could be imaged. The experimental method of choice to perform high resolution imaging, from resolutions of 20 nm to below 0.2 nm, is single-particle diffraction [4,5]. While there are other methods that require less dose (and hence induce less damage) for a given resolution [6], diffraction imaging does not require any optics and hence does not impose any technological limit to the resolution.

Case for Performing Experiments at the VUV-FEL

The method of diffraction-based imaging can be applied almost universally for X-ray microscopy of whole cells to atomic-resolution imaging of molecules. Learning acquired in groundbreaking experiments performed in X-ray microscopy of cells in a VUV-FEL can directly be applied to atomic-resolution imaging of single molecules in an X-FEL. The experiments proposed here on the VUV-FEL will result in the first single-pulse high-resolution images obtained in a XFEL. The experiments will validate methods and equipment for sample injection into the pulsed beam, and will help determine the effects of damage on the achievable image resolution. The experiments will also help validate methods to classify and average diffraction patterns, and to reconstruct the three-dimensional structure from a diffraction dataset (recorded on reproducible samples, where a new object can be used for each exposure).

It is clear that the sample will not survive the interaction with the beam, and so we can consider two classes of experiment: two-dimensional imaging of test objects and biological cells; and three-dimensional imaging of identical structures, such as spores. In the first case, the diffraction pattern will be recorded with a single pulse. The sample will be destroyed and so no further views will be obtained. A high-resolution two-dimensional image will be reconstructed, and this will be the first time that high-resolution diffraction imaging will be achieved with a single pulse. The sample will initially consist of a test structure, lithographically patterned on a thin membrane such as silicon nitride, and as such can be extensively characterized by electron microscopy. The structure will have feature sizes down to 10 nm, and so will provide the opportunity to collect diffraction data out to large scattering angles, with 6 nm X-rays. Following these experiments will be the imaging of biological cells. Candidate samples include diatoms, which are single-celled organisms that have very intricate silicate skeletons of various morphologies, yeast cells (wet or dry), and wet living cells, and wet chromosomes. First

experiments will be carried out in vacuum, on dry samples. In the case of wet biological samples, imaging would best be carried out using the second harmonic of the FEL, tuned to the water window (between the carbon and oxygen *K*-edges). In these experiments, the extreme fluence and short pulse duration of the VUV-FEL will enable us to go beyond the radiation-damage resolution limit in X-ray microscopy of about 20 nm. These results will firmly establish the usefulness of FELs over other sources for X-ray microscopy.

In the second class of experiments, three-dimensional imaging of identical particles, we will inject particles into the vacuum to intersect with the FEL pulse. Diffraction patterns will be recorded from different particles injected at a rate at which the X-ray area detector can be read out. Particles can be injected in a controlled manner from an initial sample of a suspension of particles in a solution, by spraying with an atomizer and passing through a dryer and finally a neutralizer. The samples may include purified solutions of spores, polystyrene latex spheres, silicate spheres, or colloidal clusters. Each injected drop will contain a cluster of only a few particles, with a very narrow distribution of size ranges. It should be quite easy to distinguish the number of particles from the diffraction pattern itself, and so we will obtain sets of diffraction patterns of various cluster sizes. Each diffraction pattern in a particular set will be at a different random orientation. By post-processing the data we will determine the orientation with respect to all others and then reconstruct the three-dimensional structure of the cluster. Algorithms to do this will be adapted from single-particle tomography in high-resolution electron microscopy. These experiments will obviously be groundbreaking since they are a direct analog to single-molecule imaging in a XFEL. This will be the first time that the methods of classifying and orienting diffraction patterns will be experimentally verified, and the first time with X-rays that three-dimensional reconstruction will be carried out on a set of individual particles. This experiment absolutely requires diffraction patterns to be recorded with single pulses, which requires doing this at the VUV-FEL. In the experiments we will vary the VUV fluence to determine effects of damage on the diffraction patterns and the reconstruction.

Experimental Plan

The two classes of experiment listed above have different needs in terms of the experimental chamber, sample handling equipment, and diagnostics. The most cost-effective way to carry out the first experiments is to use the existing chamber built by Dr. Jacek Krzywinski (see “Free Electron Laser - Interaction with Solids” proposal Fig. 1 for diagram). In this will be placed a sample holder and manipulation stage and a VUV CCD (supplied by LLNL). We will require beamline focusing optics to illuminate the sample with the highest intensity. It is desirable that the intensity distribution in the focus be reasonably uniform and of flat phase, since the illuminating complex amplitude multiplied by the object’s complex transmittance will be reconstructed. The sample will be prealigned using a long working distance microscope. A scintillating screen will be placed at the sample position (in the microscope focus and field of view), and the position of the microscope image of the X-ray beam would be noted. The sample will then be brought into this same position relative to the microscope. This fine adjustment of the

sample position will be carried out using the attenuated X-ray beam. To check and refine the positioning of the sample in the beam we could record low-resolution scattering of the attenuated beam. The attenuation must be great enough to reduce the sample dose to below the continuous exposure radiation-damage limit (of 10^9 photons/μm^2 for 200 eV photons), but this must be done in such a way as to not move the beam spot by more than 0.2 μm. We require a shutter that can select a single pulse, which will expose the sample at full power and diffract onto the CCD. The CCD would be directly exposed (the chip would be back illuminated) and must not see the direct beam. A beam stop located near the surface of the CCD may cause too much scatter, so the best solution would be to have a hole in the CCD through which the direct beam can pass. This could be achieved by tiling four CCD chips. The diagnostics available in Dr. Krzywinski's chamber, such as the time-of-flight mass spectrometer, will be used to determine the scale of the damage to the sample. After exposure, the sample holder will be translated to expose a fresh sample. The samples will be mounted (or manufactured) on thin membranes such as silicon nitride in small windows in a silicon wafer. The sample may consist of hundreds of such windows, and damage of one window due to the FEL exposure should not affect the other windows (debris will be directed away from the sample holder in a strong electric field).

Wet samples can be sandwiched between two silicon nitride windows. Since the area of the windows will be small, these windows will be able to withstand an atmosphere pressure differential, and so the sample holder can remain in the vacuum.

The three-dimensional experiments require a different sample manipulation strategy. Samples will be injected into the chamber and will drift a short distance through vacuum before intersecting the beam. The experiment is actually an extension of the experiment described in the proposal "Coulomb explosions of biological samples", and will be carried out in the same chamber (built by Dr. Thomas Möller). The sample injection system, illustrated in Figure DIBS 1, will be the system developed by LLNL for particles in the size range from 0.02 μm to 2 μm. In this system a solution with a colloidal suspension of particles is sprayed into sub-micron sized droplets with an atomizer. The water drops contain either no particles or one particle, although conditions can be found to produce a cluster of two or more particles. The drops are passed through a dryer and finally a neutralizer, before the particles are sprayed through a small orifice into the vacuum. The velocity of the particles is about 30 m/s. The spray fans out by about 5 degrees, and so it should be easy to align it to the X-ray beam. The areal density of particles in the spray, projected along the direction of the beam, can be controlled by setting the distance of the orifice to the beam and the concentration of the suspension. We will set this to slightly less than one per beam diameter (eg, one particle per 100 μm^2) to minimise the number of multiple-cluster hits. The unexposed particles of the spray (ie almost all) will be collected in a cold trap. The injection system has been tested on 0.5-μm diameter silicon dioxide spheres, but could be used with latex spheres, colloidal gold particles, spores, or nanocrystals. The main difference in practice with this experiment and the Coulomb explosions of biological materials, is that here we wish to record the diffraction patterns of single particles. This will require the FEL beam to be focused to 0.5 micron or better. The optics to achieve this will be provided by LLNL, but some

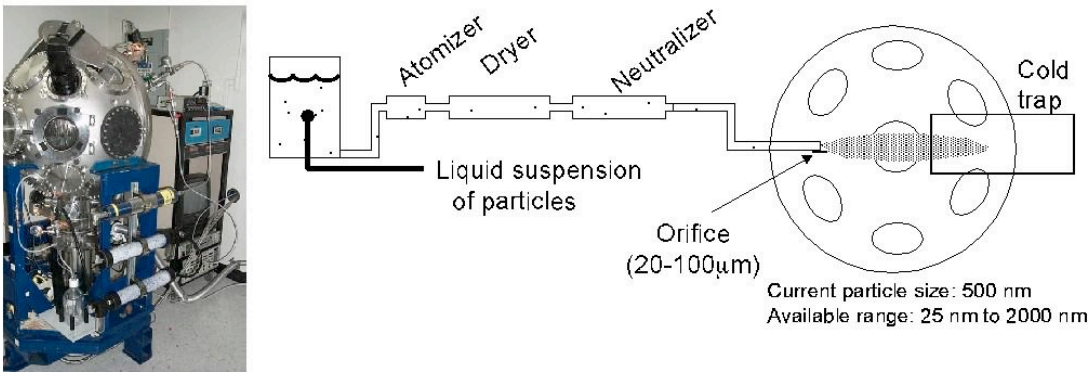

Figure DIBS 1: Particle sprayer system currently under development at LLNL. The system sprays single particles through a small orifice with particle velocities of about 30 m/s. The particles are essentially neutral, but could be made charged if we wished to manipulate their trajectories with electric fields.

development and testing time will be required on the VUV-FEL to qualify these optics for the diffraction experiments.

In the diffraction experiment we expect to get useful data on each pulse, although the repetition rate will be determined by the readout time of the CCD detector. We expect to collect thousands of diffraction patterns of a particular type of sample. The CCD detector, and other components of the experiment, will be identical to those for the two-dimensional imaging experiments and the Coulomb explosions of biological materials experiments. An attenuator is required for the initial alignment of the CCD to the beam, and the microscope may be useful in the initial alignment of the spray.

The two classes of experiments are to be carried out in separate chambers and require separate experimental runs separated by several months. We will be ready to perform the two-dimensional imaging experiments in the second half of 2003. These will be the first experiments to use the tiled CCD detector at the FEL, and three days will be required to align and characterize it. The imaging experiments will then require two sets of two week runs (the second in early 2004). The three-dimensional single-particle imaging experiments will naturally follow the Coulomb explosion experiments after advanced focusing optics have been tested. We expect to be ready to perform the 3D imaging experiments in late 2004, and will require two runs of two weeks each (the second in early 2005).

The main technical challenge for the two-dimensional imaging experiments will be in reducing stray scattering from reaching the detector. We plan to perform synchrotron experiments with the samples to be used here in order to overcome some of these problems. For the three-dimensional imaging experiments, the biggest challenges are in producing optics of high enough quality and in obtaining the operating conditions of the particle spray. Again, these issues will be tested at synchrotrons, as much as is practical, prior to FEL experiments.

Experimental Requirements

The requirements for this experiment are:

1. Single FEL pulses, ideally at a wavelength of 6 nm. We would also like to use harmonics. We can utilize no more than 10 Hz repetition rate. Pulses need not be monochromatized, but they do need to be filtered from the spontaneous background.
2. Attenuator (10^{-4}) and shutter.
3. Focussing optics to achieve ~10 μm minimum spot, and higher performance optics to achieve ~0.1 μm minimum spot. The latter to be installed in target chamber.
4. Target chamber with sample translation and rotation stage, soft-X-ray CCD, intensity monitor, and visible-light microscope for sample alignment.
5. Target chamber with particle injection system, soft-X-ray CCD, and intensity monitor.

Contributors

The list of involved individuals and their affiliations are:

Henry Chapman, Stefan Hau-Riege, Jaroslav Kuba, Richard Lee, Richard London, Abraham Szoke, Jim Trebes, and Alan Wootton,
Lawrence Livermore National Laboratory, USA.

Janos Hajdu, Beata Ziaja, David van der Spoel, Remco Wouts, and Gösta Huldt,
University of Uppsala, Sweden.

Thomas Möller and Jacek Krzywinski, DESY, Germany.

Correspondence should be directed to:

Henry Chapman, L-395, LLNL, Livermore CA, 94550, USA.
chapman9@llnl.gov, fax: +1 925 423 1488

References

1. G. Schneider, Ultramicros. **75**, 85 (1998).
2. L. B. Da Silva *et al* Science **258**, 269 (1992).
3. R. Neutze, R. Wouts, D. van der Spoel, E. Weckert and J. Hajdu, Nature, **406**, 757 (2000).
4. D. Sayre, in *Springer Lecture Notes in Physics* volume **112**, M. Schlenker *et al* Eds. p. 229 (1980).
5. J. Miao, J. Kirz, D. Sayre, Acta Cryst D **56** 1312 (2000).
6. D. Sayre and H. N. Chapman, Acta Cryst. A **51**, 237 (1995).

B.4. X-Ray Interaction with Matter: Optics Damage

Abstract

We propose to perform investigations of the interaction of intense ultrashort XUV pulses with solid matter. We would like to focus on structural changes and disintegration processes of solids as a function of intensity of irradiating pulses. The subject is essential for the development of optics for short wavelength FELs, as well as for the planning of any future experiments with solid samples that interact with XUV FEL light. The investigation of ablation processes in the new regime of photon energy will be also important for the development of nanotechnology and nanomachining. The experiments will cover measurements of energy spectra of the particles emitted from the sample (photons, electrons, ions and clusters), and the time evolution of materials parameters in pump and probe measurements (reflectivity, fluorescence, and scattering). The proposed experiments will be based on the experimental setup constructed and successfully used in the Phase I of the VUV-FEL-FEL project.

Scientific Background

X-VUV FEL based sources will deliver radiation in femtosecond pulses with peak powers in the order of a few gigawatts. Since there is very little experience with the interaction of intense, ultra-short VUV pulses with matter the understanding of such processes is of key importance for all future experiments that will apply such sources. Therefore, it is very important to study the problem both theoretically and experimentally in an early stage of the FEL development. Also the reaction of matter to short wavelength radiation is of great importance for nanotechnology and nanomachining.

The interaction of intense X-VUV radiation with matter differs from conventional laser-matter interaction. The main difference is the photon energy. With new generation X-VUV sources it will be possible, for the first time, to excite directly deep lying electron states in the atomic time scale (inverse of Debye frequency). The high photon density is expected to lead to new kinds of matter excitations such as collective motion of inner atom shells [1] or nonlinear process due to interactions of highly excited states (e.g. hollow atoms). Also the role of non-thermal phenomena such as Coulomb explosions, photo-induced bond breaking and ionization excited by multi-high-energy-photon absorption can be studied for the first time. Gaining an understanding of such process will be indispensable for the prediction of damage of optical components and reaction of samples in experiments exploiting the high intensity of new generation sources.

Scientific Case

The main goal of the proposed experiment is to investigate structural changes and disintegration processes of solids as a function of intensity of irradiating X-VUV pulses. We would like to focus on the following measurements:

1. Time dependent reflectivity measurements with sub-picosecond resolution. The change of the reflectivity will give an insight in the electron excitation and relaxation

process (e.g. electron concentration changes in the conduction band of insulators and semiconductors). It can also provide a probe for a dynamics of phase transitions, and these measurements will be invaluable for developing X-ray optics for XFELs.
2. Fluorescence spectral and time depended measurements will provide information on the change of certain excitation states as a function of irradiation intensity. Results of preliminary experiments done with 90 nm FEL radiation have shown a dramatic decrease of the fluorescence decay time at intensities close to the damage threshold (with respect to the value measured at low intensities).
3. Energy/mass spectra of desorbed ions and clusters as a function of intensity. This measurement can provide information about non-thermal process of damage (e.g. Coulomb explosion, bond breaking) and final states of the disintegration processes.
4. Photoelectron energy spectra can provide information on changes of electronic states due to irradiation.
5. Post-irradiation structural, chemical and morphological changes will be studied by differential-phase contrast microscopy, AFM, sputter-Auger analysis, X-ray microdiffraction and Raman microbeam analysis.

We plan to investigate simple elemental samples such as Si, C, Al, and Mo in order to check our unerstanding of physics of the interactions, as well as more complicated systems (e.g.multilayer optics or organic compounds) to obtain data as early as possible to be able to solve practical questions connected with the design of future experiments. The results of the proposed investigations will provide experimental data of radiation interacting with solids, over a range of parameters which is unexplored but which we need to understand in order to fully utilize future XFEL sources.

Description of the Experiment

It is planned that, after some modifications, the experiment will be performed on the setup built for the Phase I of the VUV-FEL (see Fig. 1). This setup is based on vacuum chamber, in which all other equipment is mounted. The chamber can be translated parallel to the beam focused by the ellipsoidal mirror. This motion, in and out of focus, allows the beam area, and hence the intensity of radiation on the sample surface, to be varied without changing any other parameter in the setup. The samples are placed on a holder that is mounted on a manipulator with movement along three axes with micrometer accuracy, together with the capability of rotation around one axis. The sample holder allows sample temperature to be controlled up to 900 °C. The reflected and scattered radiation will be detected by the XUV detectors, located inside the chamber, which can be rotated around the illuminated spot. The electrons as well as the ions emitted from the sample surface will be detected by a Time of Flight (TOF) spectrometer equipped with a high-pass voltage filter. The spectrum of the XUV radiation emitted from the sample will be measured by a spectrograph, while its time structure will be measured by a streak-camera. The setup is equipped with a video microscope for in-situ inspection of surface damage. There are also optical ports for the pump and probe experiments that use the optical laser beam. Evaporation cells, mounted inside the chamber, allow for preparation of fresh surface layers of various thicknesses.

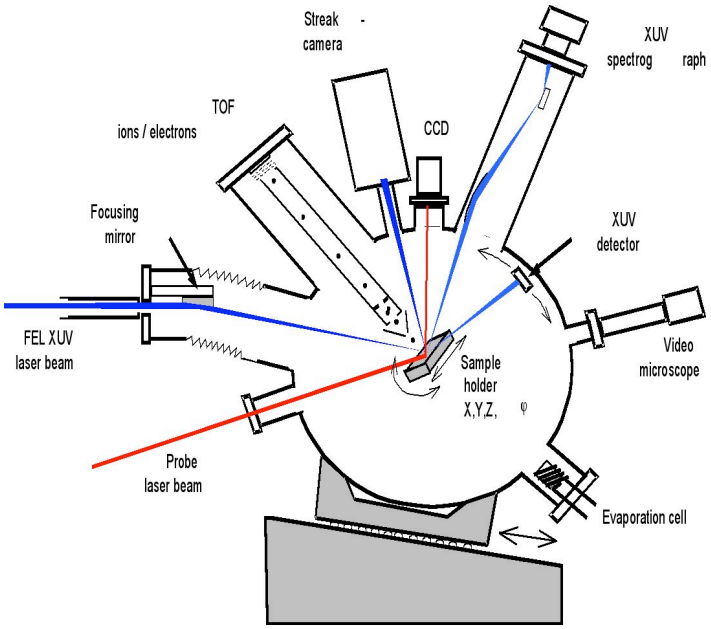

The layout of the experiment

Sample surfaces will be illuminated by the VUV-FEL pulse at various pulse fluences, and various properties will be recorded, such as mirror specular reflectivity, fluorescence, and emitted ions and electrons. Some samples will subsequently be examined for structural changes by AFM, differential-phase contrast microscopy, sputter-Auger analysis, and microdiffraction. In the case of measuring reflectivity, the sample will be positioned at grazing incidence, or near-normal incidence in the case of multilayer-coated optics. The study of multilayer coated optics allows many materials of various optical properties to be examined, and the design of the coating allows a range of energy absorbencies to be studied. The multilayer mirrors will include Si- and C-based optics, such as Mo-Si or Ru-C.

Time-resolved measurements of the reflected probe beam, fluorescent of scattered light will be made using an ultra-fast streak camera with 100-fs resolution (such cameras are being developed at LBNL in the USA, and should be available within a year). A trail of low intensity pulses would enable us to diagnose the reflectivity development on a time scale after the first damage pulse. The reflected pulse(s) will be compared on a shot-to-shot basis with the original pulse, a small portion of which will be sent directly to the streak camera. In order to compare the reflected and original beams on a shot-to-shot basis within the temporal window of the streak camera, the optical paths of the reflected and original beams will be equalized to ~100-ps precision (~ 3 cm) using a timing slide. We plan to use a femtosecond probe laser to measure the dynamics of the ablation front.

The FEL beam focal spot will be imaged by a high resolution imaging system similar to that developed recently for the COMET laser [4]. This scheme will allow us to evaluate the intensity profile on the target, and to calibrate the spot size (and hence intensity) as a function of the distance between the focusing optics and the target.

Experimental Requirements

The requirements for this experiment are:

- Single FEL pulses and pulse trains, ideally at a wavelength of 6 nm. We would also like to use harmonics. Pulses need not be monochromatized, but they do need to be filtered from the spontaneous background.
- Focussing optics to achieve ~10 μm minimum spot.
- Target chamber with sample translation and rotation stage, CCD, intensity monitor, and visible-light microscope, streak camera, TOF spectrometer (all provided).
- Optical laser pulse synchronized to FEL pulse for pump-probe experiments.
- Split and delay optics.

We will require two weeks of beam time every six months, for three years. We will be ready to perform experiments as soon as the user facility becomes operational.

Contributors

J. Krzywiński[1], A. Andrejczuk[2], J.B. Pełka, Institute of Physics, Polish Academy of Sciences.

H. Fiedorowicz, Institute of Optoelectronics, Military University of Technology, Poland.

L. Juha, Institute of Physics, Czech Academy of Science.

J. Kuba, A. Wootton, R. London, and H. N. Chapman, Lawrence Livermore National Laboratory, USA.

V. N. Shlyaptsev, University of California at Davis, USA.

J. Hajdu, B. Ziaja, D. van der Spoel, and R. Wouts, University of Uppsala, Sweden.

[1]Also at HASYLAB at DESY

[2]Also at University of Białystok, Poland

Summary of Results of Initial Experiments

A number of bulk materials (Si, Cu, Au, PMMA, PTFE, YAG, SiO_2, Al_2O_3, MgF_2), as well as 10-200 nm thick films deposited on Si substrates (Au, Al, graphite), were irradiated during the "Phase I" experiment at VUV TESLA Test Facility Free Electron Laser (the VUV-FEL) at DESY, Hamburg [2]. The VUV FEL delivered a radiation of quantum energy centered around 12 eV, in short pulses of only 30-100 femtoseconds and of peak power up to 1 GW [3]. The power levels were sufficient to induce material damage involving ablation and plasma creation. The FEL VUV beam was focused on sample surfaces to a spot of size 10-200 μm. Ions and electrons emitted from surfaces have been analyzed by the time-of-flight method (TOF) as a function of radiation power

density. The range of the changes induced by irradiation on sample surfaces was determined by means of differential-phase contrast microscopy and AFM. The results were correlated with measured ion TOF spectra (e.g. cluster desorption, plasma formation) and with the applied irradiation fluences. Different morphological structures have been observed such as selective film evaporation and light-induced periodic structures (LIPS). The study of details of the structural changes induced by the FEL ultra-short VUV pulses are under way (AMF, X-ray microdiffraction, Raman microbeam analysis). Preliminary analysis shows that, in case of the VUV radiation interacting with insulators and semiconductors, the damage threshold is much more correlated with optical constants measured at low intensities than it is in the visible range. Other experiments that are relevant to this work include damage of optics induced by 100-fs optical pulses at the LLNL JanUSP laser facility. In experiments in early 2001, clearly observable irreversible damage at fluences as low as ~0.1 J cm^{-2}, with no dependence on intensity (the pulse duration was varied more that 100 while keeping the energy constant; the damage onset fluence remained unchanged). This onset fluence is 50 times lower than those predicted theoretically! This unexplained result was first ascribed either to unknown surface effects, or an unknown experimental setup problem. However, a German group has now repeated our experiment and found the same results [5], with no explanation. R. London, S. Rubenchik, and M. Feit of LLNL are currently developing a theoretical explanation. Our results, and data and ideas discussed at numerous workshops and conferences (e.g. 'New opportunities in ultra fast science using X-rays', held in Napa, March 2002) clearly demonstrate that the field of photon-matter interaction is far from understood.

References

[1] M.Brewczyk, K. Rzazewski, " Interaction of a multi-electron atom with intense radiation in the VUV range: beyond the conventional model for harmonic generation," J. Phys. B At. Mol. Opt. 34 (9): L289-L296 (2001).

[2] A. Andrejczuk, U. Hahn, M. Jurek, J. Krzywinski, J.B. Pelka, H. Reniewicz, E.A. Schneidmiller, W. Sobala, R. Sobierajski, M.V. Yurkov and TTF FEL team; „Investigations of damage thresholds of optical components at the VUV TESLA FEL Phase I"; Hasylab Annual Report 2001, ed. R. Gehrke, U. Krell, J.R. Schneider, Hamburg 2002, pp. 117-120

[3] Ch. Gerth, B. Faatz, T. Lokajczyk, R. Treusch, J. Feldhaus; "Photon diagnostics for the study of electron beam properties of a VUV SASE-FEL"; Nucl. Instr. Meth. in Phys. Res. A 475 (2001) pp.481-486.

[4] J. Dunn, R. F. Smith, J. Nilsen, J. R. Hunter, T. W. Barbee, Jr., V. N. Shlyaptsev, J. Filevich, J. J. Rocca, M. C. Marconi, H. Fiedorowicz, and A. Bartnik: Recent X-ray Laser Experiments on the COMET Facility, SPIE conference 4505, 62 (2001).

[5] J. Bonse *et al.*, 'Femtosecond laser ablation of silicon – modification thresholds and morphology', Appl. Phys. A74, 19 (2002).

C. LCLS 2004 Letter of Intent

The Letter of Intent, given below, was submitted on June 21, 2004, to the Science Advisory Committee of the LCLS. This was in response to a call for letters of intent, the details of which can be found at http://www-ssrl.slac.stanford.edu/lcls/users/index.html. As explained at the LCLS website:

> This call for LOIs is the first step in the process of defining the initial scientific program of the LCLS. LOIs will be submitted to SSRL/LCLS. Based on review of the LOIs by the LCLS SAC and their recommendations, SSRL/LCLS will authorize the formation of teams for the development of a limited number of full proposals for the detailed R&D, engineering and construction of LCLS experimental stations and associated science programs. Full proposals developed by authorized teams will be reviewed by the LCLS SAC. Again based on SAC recommendations, full proposals approved by SSRL/LCLS may then be submitted to DOE or other agencies for funding.

Letter of Intent (Category A): Imaging of Single Particles and Biomolecules at the Linac Coherent Light Source (LCLS)

SPOKESPERSON: Janos Hajdu, Molecular Biophysics, Institute of Cell and Molecular Biology, Uppsala University, Husargatan 3 (Box 596), SE-751 24 Uppsala, Sweden, Tel: 46-18-4714449, Fax: 46-18-511755, E-mail: janos@xray.bmc.uu.se
CO-PIs: Henry Chapman, Tel: 925-423-1580, Fax: 925-423-1488, chapman9@llnl.gov
Keith Hodgson, Tel: 650-926-3153, Fax: 650-9264100, hodgson@ssrl.slac.stanford.edu

THE PROJECT TEAM:

Accelerator-Based Light Sources and Synchrotron Sources

Stanford Synchrotron Radiation Laboratory, Stanford Linear Accelerator Center, 2575 Sand Hill Road, Menlo Park, California
- Keith Hodgson, Tel: 650-926-3153, Fax: 650-926-4100, hodgson@ssrl.slac.stanford.edu
- John Miao, Tel: 650-926-5168, Fax: 650-926-4100, miao@slac.stanford.edu

DESY - Deutsche Elektronen-Synchrotron, Notkestr. 85, D-22607 Hamburg, Germany
- Jochen Schneider, Tel: 49-40-89983815, Fax: 49-40-89984475, Jochen.Schneider@desy.de
- Edgar Weckert, Tel: 49-40-89984509, Fax: 49-40-89984475, Edgar.Weckert@desy.de
- Ivan Vartaniants, Tel: 49-40-89982643, Fax: 49-40-89984475, Ivan.Vartaniants@desy.de
- Christian Schroer, Tel: 49-40-89982643, Fax: 49-40-89984475, Christian.Schroer@desy.de

VUV-FEL, Deutsche Elektronen-Synchrotron, Notkestr. 85, D-22607 Hamburg, Germany
- Josef Feldhaus, Tel: 49-40-8998-3901, Fax: 49-40-8998-2787, E-mail: feldhaus@desy.de
- Elke Plönjes Tel: 49-40-8998-2602, Fax: 49-40-8998-2787, Email: elke.ploenjes@desy.de

Advanced Light Source, Lawrence Berkeley National Laboratory, Berkeley, CA 94720, USA
- Janos Kirz, Tel: 510-486-6692, Fax: 510-486-4960, jkirz@lbl.gov

Advanced Photon Source, Argonne National Laboratory, 401-B3157, 9700 S. Cass Avenue, Argonne, IL 60439, USA
- Ian McNulty, Tel: 630-252-2882, Fax: 630-252-9303, mcnulty@aps.anl.gov

VUV Laser Facilities

Service des Photons Atomes et Molecules, Commissariat à l'Energie Atomique, Centre d'Etudes de Saclay, 91191 Gif sur Yvette, France
- Hamed Merdji, Tel: 33-1-69085163, Fax: 33-1-69081213, merdji@drecam.cea.fr

Laboratoire d'Optique Appliquée, Chemin de la Hunière, 91761 Palaiseau, France
- Philippe Zeitoun, Tel: 33-1-69319703, Fax: 33-1-69319898, Philippe.Zeitoun@ensta.fr

Universities and Research Institutes

Molecular Biophysics, Institute of Cell and Molecular Biology, Uppsala University, Husargatan 3 (Box 596), SE-751 24 Uppsala, Sweden
- Janos Hajdu, Tel: 46-18-4714449, Fax: 46-18-511755, janos@xray.bmc.uu.se
- David van der Spoel, Tel: 46-18-4714205, Fax: 46-18-511755, spoel@xray.bmc.uu.se
- Nicusor Timneanu, Tel: 46-18-4714451, Fax: 46-18-511755, nicusor@xray.bmc.uu.se
- Martin Svenda, Tel: 46-18-4714954, Fax: 46-18-511755, martin-s@xray.bmc.uu.se
- Gosta Huldt, Tel: 46-18-4714642, Fax: 46-18-511755, huldt@xray.bmc.uu.se
- Carl Caleman, Tel: 46-18-4714642, Fax: 46-18-511755, calle@xray.bmc.uu.se
- Magnus Bergh, Tel: 46-18-4714642, Fax: 46-18-511755, magnus@xray.bmc.uu.se
- Sara Lejon, Tel: 46-18-4714451, Fax: 46-18-511755, sara@xray.bmc.uu.se
- Alexandra Patriksson, Tel: 46-18-4714914, Fax: 46-18-511755, alexandra@xray.bmc.uu.se

*Department of Physics, Cornell University, 5*24 Clark Hall, Ithaca, New York 14853, USA
- Veit Elser, Tel: 607-255-2340, Fax: 607-255-2643, ve10@cornell.edu

The Institute of Optics, University of Rochester, Wilmot 410, R.C., Rochester, New York 14627-0186, USA
- James Fienup, Tel: 585-275-8009, Fax: 585-271-1027, fienup@optics.rochester.edu
- Lukas Novotny, Tel: 585-275-5767, Fax: 585-271-1027, novotny@optics.rochester.edu
- Pascal Anger, Tel: 585-275-5767, Fax: 585-271-1027, panger@optics.rochester.edu

Division for Electricity and Lightning Research, Department of Engineering Sciences, Uppsala University, Box 524, SE - 751 21 Uppsala, Sweden
- Jan Isberg, Tel: 46-18-4715821, Fax: 46-18-4715810, jan.isberg@hvi.uu.se

Department of Physics and Astronomy, Stony Brook University, Stony Brook, NY 11794-3800, USA
- Chris Jacobsen, Tel: 631-632-8093, Fax: 631-632-8101, jacobsen@xray1.physics.sunysb.edu
- David Sayre, Tel: 908-595-6854, Fax: 631-632-8101, Sayre@xray1.physics.sunysb.edu
- David Shapiro, Tel: 631-632-8002, Fax: 631-632-8101, dshapiro@ xray1.physics.sunysb.edu
- Enju Lima, Tel: 631-632-8002, Fax: 631-632-8101, lima@xray1.physics.sunysb.edu,
- Huije Miao, Tel: 631-632-8002, Fax: 631-632-8101, hmiao@xray1.physics.sunysb.edu

Department of Biomedical Engineering, Stony Brook University, Stony Brook, NY 11794-3800, USA
- Helmut Strey, Tel: 631-632-1957 Fax: (631)-632-8577, helmut.strey@stonybrook.edu

Department of Chemistry & Bioscience, Chalmers University, Box 462, 40530 Gothenburg, Sweden
- Richard Neutze, Tel: 46-31-7733974, Fax: 46-31-7733910, neutze@molbiotech.chalmers.se
- Arjan Snijder, Tel: 46-31-7733974, Fax: 46-31-7733910, arjan.snijder@chembio.chalmers.se
- Susanna Tornroth, Tel: 46-31-7733974, Fax: 46-31-7733910, susanna.tornroth@chembio.chalmers.se

Department of Physics, University of Illinois at Urbana-Champaign, 1110 West Green Street, Urbana, IL 61801-3080 USA
- Ian Robinson, Tel: 217-244-2949, Fax: 217-244-2278; robinson@mrl.uiuc.edu, ikr@uiuc.edu

Department of Physics, University of California Berkeley, CA 94720-7300, USA
- Roger Falcone Tel: 510-642-8916, Fax: 510-643-8497, rfalcone@socrates.Berkeley.EDU

Lawrence Berkeley National Laboratory, MS 10-100, Berkeley, CA 94720, USA
- Musahid Ahmed, Tel: (510) 486-6355 Fax: (510) 486-531, mahmed@lbl.gov

Institute for Atomic Physics and Teacher Training, Technical University Berlin, Hardenbergstrasse 36, D-10623 Berlin, Germany
- Thomas Möller, Tel: 49-30-31423712, Fax: 49-30-31423018, thomas.moeller@physik.tu-berlin.de
- Christoph Bostedt, Tel: 49-30-31423712, Fax: 49-30-31423018, christoph.bostedt@desy.de

Department of Physics and Astronomy, Arizona State University, P.O. Box 871504, Tempe, Arizona 85287-1504, USA
- John C.H. Spence, Tel: 602-965 6486, Fax: 602-965 7954, spence@asu.edu

Grupo de Lasers e Plasmas, Centro de Fisica dos Plasmas, Av. Rovisco Pais 1, 1049-001 Lisbon, Portugal
- Martha Fajardo, Tel: 351-21-8419202, Fax: 351-21-8464455, marta.fajardo@ist.utl.pt
- Nelson Lopes, Tel: 351-21-8419202, Fax: 351-21-8464455, nmcl@alfa.ist.utl.pt
- Joao M Dias, Tel: 351-21-8419202, Fax: 351-21-8464455, jmdias@alfa.ist.utl.pt
- Goncalo Figueira, Tel: 351-218419329, Fax: 351-21-8464455, gonf@ist.utl.pt
- Luis Silva, 351-21-8413379, Fax: 351-21-8464455, luis.silva@ist.utl.pt
- Ricardo Fonseca, Tel: 351-21-8419202, Fax: 351-21-8464455, pcl36688@mail.ist.utl.pt
- Fabio Peano: Tel: 351-21-8419379, Fax: 351-21-8464455, fabio.peano@alfa.ist.utl.pt

Department of Theoretical Physics, The Henryk Niewodniczanski Institute of Nuclear Physics, Radzikowskiego 152, 31-342 Krakow, Poland
- Beata Ziaja, Tel: 48-12-6628-448, Fax: 48-12-6628458, beataz@beata.ifj.edu.pl
Research Institute for Solid State Physics and Optics, H 1525 Budapest, P.O. Box 49, Hungary

- Gyula Faigel: Tel: *36-1-392-2222/337*, Fax: 36-1-392-2219, gf@power.szfki.kfki.hu

The School of Physics, The University of Melbourne, Victoria, 3010, Australia
- Keith Nugent, Tel: 61-3-83445446, Fax: 61-3-93474783, K.Nugent@physics.unimelb.edu.au
Department of Chemistry, Cambridge University, Lensfield Road, Cambridge, CB2 1EW, UK

- Carol Robinson, Tel: 44-1223-763846, fax: 44-1223-762829, cvr24@cam.ac.uk

Center for Biophotonics Science and Technology, UC Davis, 225 Hunt Hall, Davis, CA 95616, USA
- Eugene Ingerman, Tel: 530-754-5256, Fax: 530-754-5309, eugening@ucdavis.edu

Lawrence Livermore National Laboratory, 7000 East Avenue, Livermore CA 94550, USA
- Henry Chapman, Tel: 925-423-1580, Fax: 925-423-1488, chapman9@llnl.gov, L-210
- Stefan Hau-Riege, Tel: 925-423-5892, Fax: 925-423-1488, hauriege1@llnl.gov, L-210
- Hope Ishii, Tel: 925-422-7927, Fax: 925-423-5733, ishii2@llnl.gov, L-210
- Stefano Marchesini, Tel: 925-422-0648, Fax: 925-423-1488, smarchesini@llnl.gov, L-210
- Rodney Balhorn, Tel: 925-422-6284, Fax: 925-422-3915, balhorn2@llnl.gov, L-448
- Henry Benner, Tel: 925-422-7363, Fax: 925-422-1488, benner2@llnl.gov, L-233
- Matthias Frank, Tel: 925-423-5068, Fax: 925-424-2778, frank1@llnl.gov, L-211
- Aleksandr Noy, Tel: 925-4246203, Fax: 925-422-3160, noy1@llnl.gov, L-234
- Anton Barty, Tel: 925-424-4815, Fax: 925-423-1488, barty2@llnl.gov, L-210
- Brent Segelke, Tel: 925-424-4752, Fax: 925-422-2282, segelke1@llnl.gov, L-448
- Abraham Szoke, Tel: 925-4231467, Fax: 925-423-9969, szoke1@llnl.gov, L-030
- Peter Young, Tel: 925-422-5478, Fax: 925-424-3874, peyoung@llnl.gov, L-479
- Richard Lee, Tel: 925-422-7209, Fax: 415-520-0580, dicklee@physics.berkeley.edu, L-399
- Richard London, Tel: 925-4232021, Fax: 925-423-9969, rlondon@llnl.gov, L-030
- Daniel Barsky, Tel: 925-422-1540, Fax: 925-424-3130, barsky@llnl.gov, L-448

INTRODUCTION

Much of what we know about the detailed structure of biomolecules, including proteins, DNA, and RNA, has come through the use of X-ray diffraction. Conventional synchrotron radiation catalyzed revolutionary advances in this field during the past two decades, enabling the study of larger and more complex systems at increasingly high levels of resolution and on smaller (often micron-sized) crystals. The key to this great success has been the use of Bragg diffraction from the millions of oriented copies of molecules that are aligned in a single crystal. However, there are classes of proteins (as well as many other types of materials) that are difficult or impossible to crystallize, including membrane proteins and many glycoproteins, for which structure determination at atomic resolution or even near-atomic resolution would be invaluable.

Theoretical studies and simulations predict that with a very short, very intense coherent X-ray pulse, a single diffraction pattern may be recorded from a large macromolecule, a virus, or a cell without the need for crystalline periodicity (Neutze *et al*., 2000; Jurek *et al*., 2004a,b; Hau-Riege *et al*., 2004). A three-dimensional data set could be assembled from such patterns when copies of a reproducible sample are exposed to the beam one by one (Huldt *et al*. 2003). The over-sampled diffraction pattern (for a recent review see Miao *et al.*, 2004) should permit phase retrieval and hence structure determination (Miao *et al*., 2001; 2002; 2003; Robinson *et al*., 2001; Marchesini *et al*., 2003a,b). However, the challenges in carrying out such an experiment are formidable, and will engage an interdisciplinary approach drawing upon structural biology, atomic and plasma physics, mathematics, statistics, and XFEL physics. The potential for breakthrough science is great with impact not only in the biological areas but wherever structural information at or near atomic resolution on the nanoscale is valuable.

In this Letter of Intent (LOI), we propose a seven-year program of research, diagnostic, and instrument development that will be carried out between now and the beginning of LCLS operation in 2008 and continue into the initial three years of the operations phase of LCLS. The specific aim is to develop, build, and commission a bioimaging experimental station on LCLS. This will be followed by operations to obtain the first significant results in this emerging new approach in bioimaging.

SCOPE OF WORK

It should be noted that while the conceptual design of the experiment has been studied extensively, the performance and X-ray pulse requirements of these imaging experiments will not be accurately known until validation experiments can be carried out on sources such as the DESY VUV-FEL and the LCLS itself. Therefore the initial work at the LCLS will be model-validation todetermine the dynamics of the interaction of molecules and clusters with XFEL pulses, destroying the sample in the process. We will also do proof-of-concept single-shot two-dimensional (2D) imaging experiments at considerably lower than atomic resolution (yet still beyond the radiation damage limit of steady-state X-ray microscopy performed at current 3rd generation synchrotron sources). This work can be carried out with the nominal baseline LCLS pulse parameters. The research program following these initial studies will be geared toward pushing X-ray imaging to higher and higher resolution, moving from the more straightforward experiments on colloidal particles and atomic clusters, toward the most challenging experiments on single molecules, viruses and protein complexes. Our present (not yet experimentally validated) models show that atomic resolution by diffraction from single macromolecules will require XFEL pulse durations much shorter than the LCLS nominal parameters, probably less than 10 fs, while the pulse requirements for inorganic high-*Z* clusters may be somewhat relaxed. It is our intention to work with the SSRL/LCLS accelerator and X-ray physics efforts on reducing pulse durations by X-ray optical methods and source modification, but we will also be pursuing a path of improving resolution by several innovativeX-ray imaging approaches that we propose to develop. A major component of the program will be in implementing and testing containerless sample handling technology and in applying particle orientation methods. These methods will be initially applied to atomic-resolution imaging of inorganic clusters and nanostructures. The

ultimate goal is to bring together all the components to image the large single biomolecules within about three years after the beginning of LCLS operations in 2008.

CONCEPTUAL DESIGN OF THE EXPERIMENTS

The experiment will consist of an apparatus to perform coherent X-ray diffraction imaging, or image reconstruction by phasing oversampled diffraction patterns. The apparatus will include optics to focus the beam onto the sample to provide the necessary X-ray fluence, and, if necessary, pulse compression optics. X-ray diffraction will occur in an ultra-high-vacuum chamber that will house sample manipulation and injection hardware, diagnostics, and a pixellated detector to record the diffraction pattern. In most experiments, a diffraction pattern will be recorded in a single pulse and the sample subsequently destroyed. A large number of diffraction patterns will be recorded, from a supply of identical or equivalent samples, and stored on a computer to be processed into a three-dimensional (3D) diffraction dataset. This dataset will be processed (phased) to obtain a 3D image of the sample. The design of the apparatus will be an evolution of chambers that we have already used for current coherent X-ray diffraction imaging experiments at SSRL/SPring8 and Stony Brook/ALS. We will also incorporate into the design of the LCLS experimental chamber the experience that we will gain at the DESY VUV-FEL high-brightness beamline, in experiments being carried out by our team between 2005 and 2008.

Components of the experiment

Optics: The beam from the LCLS must be focused to a spot diameter on the order of 0.1 to 10 microns, depending on the overall sample size and desired X-ray fluence at the sample (initial dynamics experiments can use larger beam diameters, including the unfocussed beam). This requirement could be achieved by a Kirkpatrick-Baez mirror pair, and is best carried out in the far experimental hall to allow larger aperture optics and hence reduced fluence on the optical surfaces. The pulse duration will eventually need to be shortened, which could be achieved by X-ray pulse compression (strained crystal diffraction (Chapman and Nugent, 2002), asymmetric multilayer grating pair) or by source modifications. Our current estimates are that < 10 fs pulses with > 10^{11} photons per pulse are required for realistic single-particle imaging.

Sample Handling: The main complexity and scientific challenge of the instrument will be in sample introduction and control. Since the quantities of material of the sample under study will be minute, there should be very little other matter in the beam. When imaging single molecules, the sample cannot be held on a substrate, since scattering from the atoms of the substrate will overwhelm the signal of the molecule itself. Therefore, the sample (and indeed the entire optics and experimental apparatus) must be at ultra-high vacuum (pressure ~10^{-9} Torr, similar to cryo-EM). Particles, such as macromolecules or virus particles, will be injected from the outside into the X-ray beam in such a way that single particles intersect with the brief XFEL pulses. Ideally, one fresh, single particle is injected into every focused pulse at a 120 Hz rate in the LCLS. To achieve this, the trajectories of the particles must be controlled both in space (< 1 micron) and time (< 10 ns), so that each one of them will be well aligned with the focused X-ray pulse. Present sample injection and particle manipulation techniques need to be significantly refined in order to position individual particles with sufficient precision. Initial experiments on particle dynamics will use clouds of particles without stringent requirements, achievable with current methods. These will be improved upon, by first injecting short, concentrated bursts of particles into the beam focus area and relying on statistical positioning of individual particles. Such experiments require shot-to-shot diagnostics to determine whether a particle was indeed hit by the X-ray beam. Such diagnostics could be provided, *e.g.*, by fluorescence detectors and by a mass spectrometer that analyzes the fragments of the particle after the shot passes through. More advanced techniques of particle introduction and manipulation techniques include the injection of a few or even single particles into the beam at the proper times with well-controlled velocities, or trapping single particles at the XFEL beam focus using optical, electrostatic, or electromagnetic methods.

We will explore electrospray ionization (ESI) and related ink-jet spraying techniques as methods for introducing large molecules or small particles, such as viruses, into the gas phase (Gaskell, 1997). Those spraying techniques have been refined in recent years for their application in mass spectrometry of large proteins, supramolecular complexes, such as intact ribosomes (Rostom, *et al*. 2000), and even whole viruses (Tito, *et al*., 2000). The charge imparted onto a particle by the ESI process is convenient for manipulating the particles in the gas phase by electrostatic forces (Bogan and Agnes, 2002). If necessary, a charge reduction scheme based on the recently developed charge-reduction electrospray method (Stephenson and McLuckey, 1998) can be used to reduce the charge on electrosprayed molecular ions or particles to one or few elementary charges in a controlled way. For the particle introduction into ultra-high vacuum, we will expand on the aerodynamic lens or nozzle techniques used for single-particle mass spectrometry (Gard, *et al*., 1997, Suees and Prather, 1999) and bioaerosol mass spectrometry developed at LLNL by some of us.

Prior to LCLS operations we will develop particle orientation control methods as a means to enable single-particle imaging with less stringent pulse requirements. The ASU group will shortly perform experimental measurements of the degree of molecular alignment possible in a molecular beam by a polarized laser (Spence and Doak, 2004). They plan to use a small electron gun for diffraction to measure this degree of alignment. Simulations (Spence, submitted) show that an RMS alignment of about five degrees is needed to resolve secondary structure in proteins about 10 nm long at 4 K in liquid helium drops.

For initial experiments, large particles such as nanocrystals of membrane-bound proteins or other materials, and cells, will be supported in vitreous ice and manipulated directly into the beam by visual microscopy. This handling of these types of samples will be upgraded to completely containerless by using a simple electrostatic system or in-vacuum laser tweezers. This method would be ideal for diffraction imaging of membrane nanocrystals, but must be automated to enable collection of diffraction from thousands of individual crystals. In Göteborg the Neutze group has numerous on-going membrane protein crystallisation projects, and will provide nanocrystals of membrane proteins of known structure (to validate the method) and unknown structure (to achieve new science). This group will also develop the abovementioned containerless handling system.

Detectors: The diffraction pattern will be recorded on a pixellated detector subtending a solid angle dependent on the desired resolution, and a hole in the middle to avoid the direct beam. The required number of pixels of the detector depends on the ratio of the sample (or unit cell) diameter to the resolution distance, generally not less than 1000 x1000. The detector size should be approximately 50 mm x 50 mm, in order to reduce the path from sample to detector. Other desired parameters are a read-out speed per frame of 120 Hz (maximum speed, LCLS baseline parameters) or 60 Hz (min); dynamic range ~10^8 for entire pattern for large single particles such as viruses; dynamic range locally of ~1000 (a dynamic range of 10^8 could be achievable with two detectors, each with 10^6 range where the response of the second detector measuring the strong forward scattering component is reduced with an absorber on its surface). The detector PSF must be non-zero at highest required frequency at detector plane. Diffraction data may be supplemented by a lower-resolution image of the sample obtained with a zone plate as this could prove valuable in enhancing the robustness of the oversampling phasing algorithms.

Many of these requirements are in line with general directions currently driving the development of X-ray area detectors for synchrotrons and other experiments planned for the LCLS. The reduced size-requirement in single particle/molecule imaging alleviates some of the difficulties in developing faster detectors needed for our studies. The team represented by this LOI will not be developing the diffraction detector, but we will collaborate with laboratories and companies who will do so.

Image Reconstruction: As in crystallography, the computer is a major instrument component and algorithms are required to generate images from the measurements. Single-shot 2D

diffraction patterns of 1 to 10 micron diameter objects such as cells, at resolutions above the radiation damage limit, will be reconstructed straightforwardly using methods proven by many of us and for which references have been provided in the Introduction. Three-dimensional imaging will take place in two distinct stages. In the first stage, a large number of noisy 2D diffraction patterns must be given relative orientations to each other in 3D reciprocal space and then merged into a single 3D diffraction data set (Huldt *et al*., 2003). The difficulty in this is much reduced if the particle orientation can be controlled, or if membrane or nanocrystal diffraction data is indexed. In the second stage, phases are derived from the 3D diffraction pattern using an iterative algorithm, essentially identical to the 2D case. This approach has been described by Miao *et al*. (2001). The main computational burden in the entire process is in first stage, especially if orientations are initially unknown. While methods for classification of images that have been developed for cryo-EM (Frank, 1996; van Heel *et al*., 2000) could be applied here, a new method has been proposed (Elser, 2004) which determines the relationship in the continuous Euler angle space of each diffraction pattern as it is acquired. This method could in principle be applied in real time using a distributed computer cluster, and has the ability to determine when a complete dataset has been collected (*i.e*., when to stop collecting data). For the second stage, methods will be developed in applying oversampling techniques to phasing diffraction from 2D and 3D nanocrystals, and in applying *a priori* information that may be available in the diffraction of clusters and aligned particles.

RESEARCH PLAN

Before LCLS becomes operational in 2008, we plan to conduct experimental measurements at two other linear accelerator based X-ray sources: the VUV-FEL at DESY and the Sub-Picosecond Photon Source (SPPS) at SLAC. In developing the LCLS biological imaging experiment, we will thus be building upon our experience on these sources, as well as on preparatory work at synchrotron facilities and in our laboratories. Several groups on our team have been granted beamtime at the VUV-FEL through a competitive call for proposals and approval of a proposal that received a very high ranking. The VUV-FEL program of research has been designed to confront the experimental challenges of single-particle imaging at the LCLS, and to carry out the first possible validations of models to enable us to plan and design the LCLS instrumentation. Briefly, the experiments at the Hamburg VUV-FEL will include: measurement of the Coulomb explosion of inorganic and biological particles irradiated by ultrashort VUV pulses; demonstrations of single-shot diffraction imaging of biological samples at resolutions beyond the steady-state X-ray damage limit; and demonstrations of 3D diffraction imaging of reproducible test samples. In addition, diagnostics to measure pulse structure will be tested and applied to studies on the control of explosions using dual pulses. By the end of the third year of VUV-FEL experiments, in 2007, we will have demonstrated techniques to inject clouds of particles, and single particles, into an FEL beam and measure their coherent diffraction patterns; tested ideas to trap and orient particles; determined methods to work with fully spatially coherent beams (*e.g*. to eliminate coherent noise and parasitic scattering from beamline components and gas molecules); tested sample preparation concepts to boost diffraction signal levels; and have an understanding of the required pulse parameters for LCLS experiments.

Timeline at LCLS and Expected Results

Experiment	Description	Timeline
Dynamics of particles and clusters	Determine damage rates and test damage control strategies	2008-2011
2D single-shot imaging	Zone-plate and diffraction imaging beyond radiation damage resolution limits	2008-2009
Imaging inorganic clusters	Diffraction imaging inorganic colloids and clusters	2009-2010
3D imaging of membranes	Diffraction imaging of membrane nanocrystals	2010-2011
3D imaging of particles	Diffraction imaging of aligned and non-aligned particles, including viruses	2010-2011

A summary of experiments is given in the above table. The experimental program at LCLS will roughly follow the order of the VUV-FEL experiments due to the progression in complexity and the dependencies of the experiments. Also, the timeline is driven by the development of diagnostics, sample handling such as particle orientation alignment, and X-ray optics or source upgrades for reduction of the pulse duration. The broad timeline and description of experiments is as follows:

2008: Dynamics of particles and clusters. Atomic-resolution imaging of single particles depends crucially on the rate of damage induced by photoionization by the XFEL pulse. Until we perform experiments at LCLS, there will be no validation of models in the high-energy density regime and required imaging conditions. The results from these measurements will guide the imaging experiments that follow. Initial dynamics experiments will measure XFEL diffraction from a cloud of particles, as a function of pulse parameters (most importantly, pulse fluence). The diffraction pattern will give the time-integrated structure factor of a single particle, modulated by speckle due to the random positions of the clusters or particles. Initially we are primarily interested in the average structure factor, which will give us information on the size and density profile of the particles. These initial measurements will be performed with an off-axis detector (*i.e*. to avoid the direct beam). As we reduce particle density we will record a full diffraction pattern that can be phased by oversampling (to get an image of one or several particles). We will study mechanisms to slow down the explosion, such as the use of a helium-drop tamper (Hau-Riege *et al.*, 2004), or a modified pulse structure. Theoretical studies on the control of the dynamics of the explosion of hydrogen clusters by ultra-intense laser pulses (Peano *et al*., 2004) suggest that the relative intensities and delays between two pulses could be used to create "designed" expansion geometries and times. In addition to collecting the diffraction data we will perform TOF mass spectrometry on the fragments of the particles or clusters. The outcome of these experiments will give an improved knowledge of the explosion of X-ray irradiated samples and help in developing approaches to control the rate of these events. While searching for the optimal conditions for biological X-ray diffraction imaging, we will be inspecting unprecedented interaction regimes, with tremendous application potential in atomic physics and high energy-density science.

2008-2009: 2D single-shot imaging. Initial imaging experiments will be performed at low resolution and low photon energy and fluence, using a zone plate lens. These experiments will be primarily to commission the LCLS instrument and beamline, to characterize beam intensity profile and coherence, and to eliminate sources of unwanted scattering. The sample will be on a membrane in a cryo-holder and will be positioned in the beam with a visible microscope system. Note that –the cryogenic sample holder is not for radiation protection, just a convenient way to mount the sample. In 2009 experiments will move to higher fluence, where the sample will be destroyed on irradiation, and to higher resolution, using diffraction imaging. The initial goal is to achieve better than 10 nm resolution on cellular materials. This is at or slightly better resolution than what could be achieved with steady-state X-ray microscopy of cryogenic biological samples (Miao, 2004). We then plan to continue resolution improvements on smaller samples as we move to shorter pulses in the next phase of experiments.

2009-2010: Imaging inorganic clusters. The geometric structure of clusters is of fundamental importance for the understanding of many other properties e.g. their electronic structure, reactivity, magnetic, and optical properties. Most information on the geometric structure of clusters comes from indirect methods e.g. mass spectroscopy (Haberland, 1993, Martin *et al*., 1990) flow tube measurements (Jarrold, 1991) and from theoretical work (Röthlisberger *et al*., 1994). The LCLS biological imaging experiment will allow atomic-resolution X-ray diffraction analysis, which could not be applied as yet since the particle density of cluster in a beam is very low. The pulse requirements for imaging high-*Z* materials may be much less stringent (our simulations estimate ~50 fs pulses in a 300 nm diameter spot) than for biological materials, due to the increased scattering cross section and certain translational symmetry and crystallinity that results in very intense Bragg-like diffraction peaks. We will therefore be able to develop the sample handling and image reconstruction techniques that are required for biological imaging at

these relaxed pulse parameters. We will perform initial demonstrations of the classification and reconstruction from coherent diffraction at unknown orientation, which will be achieved first at lower resolution on electrosprayed and evaporated drops of colloidal particles (sorting the diffraction data depending on the number of particles in the residual clump—*e.g*. all two particle clumps can be treated as identical structures).

Particularly interesting are studies on clusters which undergo structural phase transitions like gold clusters (Cleveland *et al*., 1997) or alloyed clusters which could provide an opportunity to observe the competition between atomic segregation and stoichiometric mixtures as the function of size and temperature (Maier-Borst *et al*., 1999). Depending on the geometrical structure, the size and of the temperature of the clusters different vibrational modes can be studied. This will be particularly interesting for systems that show strong variations of the melting temperature with size like S_n clusters (Shvartsburg and Jarrold, 2000). Furthermore, time-resolved structural studies will allow following the pathway of photo-induced reactions in real space. The advent of direct time-resolved structural probes will certainly open new scientific opportunities in this field which had to rely in the past mainly on indirect measurements.

2010-2011: Imaging biological nanocrystals. The pulse-length requirements for atomic-resolution imaging of biological materials can be much relaxed by using methods of imaging molecules in parallel. One such parallel method is to diffract from arrays and crystals of particles, and in particular XFEL diffraction of membrane nanocrystals would significantly impact structural biology. Membrane proteins govern energy transduction, import and export processes, and signalling within biological cells. Whereas 25% of the human proteome encodes membrane proteins, only 1% of the available structural information relates to membrane proteins. The LCLS experiments will be performed using the automated nanocrystal manipulation techniques described above. The 8 keV photon-energy LCLS beam will be focused to a 1-micron diameter spot or smaller, and diffraction recorded from a single membrane protein nano-crystal (destroying the crystal in the process). The image reconstruction techniques will be analogous to the single-particle case, and will require thousands of diffraction patterns from randomly oriented crystals to obtain a complete dataset. The orientation of the crystal will not be preset, but will be determined in part by indexing the diffraction pattern. Once the entire 3D diffraction pattern is assembled, individual Bragg truncation rods can be phased using iterative methods as demonstrated by Spence *et al.* (2003). In the X-ray diffraction case where a 2D image is not available, phase relationships of the truncation rods may possibly be determined by a highly redundant fit of a 2D sinc-function expansion of the phased rods to weak off-Bragg diffraction (dependent on crystal shape).

The scientific impact of a "short cut" to better resolution X-ray structures of membrane proteins is absolutely tremendous for science and medicine. In particular, the LCLS will significantly out-perform conventional micro-focus synchrotron beamlines, which themselves have been absolutely essential for the recent progress in membrane protein structural biology.

2010-2011: 3D imaging of biological particles. Another method of parallel imaging to relax XFEL pulse requirements is diffraction imaging from a gas of aligned molecules. The diffraction pattern from this gas would be the continuous molecular transform of a single molecule, modulated by speckle that will be of higher spatial frequency than the detector pixel pitch and not be detected. That is, single-particle oversampling techniques can be applied without modification to reconstruct images. While such methods could be applied with long integration times with continuous sources such as a synchrotron or an electron gun (Spence and Doak, 2004), the LCLS offers the opportunity to perform time-resolved studies on molecules that are not constrained in a crystal. The initial experiments will be performed with a 1-micron diameter beam and particles will be injected into the focal volume (1 mm depth of focus). These experiments will progress to smaller numbers of particles per pulse as the pulse duration is reduced down to 10 fs, and eventually to single-molecule imaging without the requirement of optical alignment. In 2011 we aim to perform diffraction imaging experiments on single non-aligned virus particles, such as the cow-pea mosaic virus (Wang, 2002).

By the conclusion of these experiments, and with development of pulse compression techniques or source upgrades, we will have an instrument that will be capable of determining atomic- or near-atomic resolution of 3D structures from nanocrystals and large single biomolecules. When successful, this will truly have a large impact on structural biology, allowing structures to be acquired of materials that have not been amenable to crystallization or other methods. It will also open new approaches to study of dynamics through synchronization of structural studies with laser-initiated reactions.

OVERVIEW OF THE PROJECT TEAM, MANAGEMENT, AND FUNDING

The applications of X-ray free-electron lasers (XFELs) have been examined in a series of workshops and reports both in the USA and abroad. References and details of the many workshops and reports related to the scientific cases for the two major X-ray FEL projects in the world can be found on the www sites of these two facilities at www.ssrl-slac.stanford.edu/lcls/ and http://xfel.desy.de/content/e169/index_eng.html A number of new scientific opportunities have been identified and elaborated, several of which are in the area of structural biology. The concept for atomic-resolution imaging using X-ray pulses from an X-ray FEL like LCLS arose from the convergence of the ideas of coherent X-ray diffraction imaging and overcoming the limitations of the radiation damage by the method of "flash imaging" with very short and very intense X-ray pulses. These ideas came together in the forums defining the scientific cases for the LCLS and TESLA XFELs, held in the mid-to-late 1990's, where the experimental concepts were initially defined. In parallel, concepts such as methods for delivering particles into the beam and classifying diffraction patterns of particles of unknown orientation have also evolved. A comprehensive view of biological imaging experiments at the LCLS and the R&D needs were developed at a recent workshop ("Instrument Development Workshop for Biological Imaging at the LCLS", held at SLAC in March 2004). The research proposed in this LOI is based on these efforts, and focuses a specific set of goals to achieve the ultimate success of single molecule imaging with the LCLS.

Roles and Responsibilities of Team Members. The LCLS biological imaging program has been guided by a steering committee consisting of Professor Janos Hajdu (Chair, University of Uppsala), Dr. Henry Chapman (LLNL), Professor Carol Robinson (Cambridge University) and Professor Keith Hodgson (SSRL and Stanford). The Table below lists the expertise and individual role of all participants in

NAME	INSTITUTE	ROLE / EXPERTISE
Janos Hajdu	UPPSALA	PI, theory, diffraction imaging, sample preparation
Keith Hodgson	SSRL/SLAC	Co-PI, phasing, imaging, FEL-science, detectors, SPPS
Henry Chapman	LLNL	Co-PI, optics, diffraction imaging
John Miao	SSRL/SLAC	Phasing, imaging, nanocrystals
Jochen Schneider	DESY	FEL-science, VUV-FEL, detectors, clusters
Edgar Weckert	DESY	Coulomb explosions, detectors, FEL-science, VUV-FEL
Ivan Vartianiants	DESY	diffraction physics, reconstruction, coherence
Christian Schroer	DESY	micro focussing optics, X-ray imaging, microfluoresensce
Josef Feldhaus	DESY-VUV-FEL	FEL-science, lasers, VUV-FEL experiments
Elke Ploenjes	DESY-VUV-FEL	FEL-science, lasers, VUV-FEL experiments
Ian McNulty	APS	Optics, Imaging
Janos Kirz	LBNL	Imaging

Musahid Ahmed	LBNL	Sample preparation and injection, mass spectrometry
Hamed Merdj	CEA	Soft X-ray lasers tests
Philippe Zeitoun	LOI	Soft X-ray lasers tests
David van der Spoel	UPPSALA	Theory, damage, clusters, software
Nicusor Timneanu	UPPSALA	Theory, damage, clusters, software
Martin Svenda	UPPSALA	Sample preparation
Gosta Huldt	UPPSALA	Imaging and image reconstruction
Carl Caleman	UPPSALA	Damage models, timing, imaging
Magnus Bergh	UPPSALA	Damage models, laser experiments
Sara Lejon	UPPSALA	Sample selection and injection, diffraction imaging
Alexandra Patriksson	UPPSALA	Theory, software, laser experiments
Veit Elser	CORNELL	Image reconstruction, phasing, software development
James Fienup	ROCHESTER	Phasing
Lukas Novotny	ROCHESTER	Sample trapping and orientation
Jan Isberg	UPPSALA	Damage, electron cascades in covalent carbon structures
David Sayre	STONY BROOK	Phasing
Chris Jacobsen	STONY BROOK	Imaging, instrumentation
David Shapiro	STONY BROOK	Imaging, instrumentation
Huije Miao	STONY BROOK	Imaging, instrumentation
Enju Lima	STONY BROOK	Imaging, instrumentation
Richard Neutze	CHALMERS	Nanocrystal diffraction and preparation
Arjan Snijder	CHALMERS	Nanocrystal diffraction and preparation
Susanna Tornroth	CHALMERS	Nanocrystal diffraction and preparation
Ian Robinson	URBANA	Imaging, nanocrystal diffraction
Roger Falcone	BERKELEY	Carbon nanotubes, damage studies, imaging
Thomas Möller	BERLIN	Imaging of clusters, damage models
Christoph Bosted	BERLIN	Imaging of clusters, damage models
John Spence	ASU	Sample injection, orientation, imaging
Martha Fajardo	LISBON	Clusters, damage studies, Soft X-ray lasers,
Nelson Lopes	LISBON	Clusters, damage studies, Soft X-ray lasers,
Joao M Dias	LISBON	Clusters, damage studies, Soft X-ray lasers,
Goncalo Figueira	LISBON	Clusters, damage studies, Soft X-ray lasers,
Luis Silva	LISBON	Software development, explosion control
Ricardo Fonseca	LISBON	Theory, explosion control
Fabio Peano	LISBON	Theory, explosion control
Beata Ziaja	KRAKOW	Theory, cascades, damage control
Gyula Faigel	BUDAPEST	Holographic techniques, phasing, damage studies
Keith Nugent	MELBOURNE	Optics, Imaging
Carol Robinson	CAMBRIDGE	Sample selection, injection, diagnostics
Stefan Hau-Riege	LLNL	Coulomb explosions, damage control
Hope Ishii	LLNL	Damage, imaging, diagnostics
Stefano Marchesini	LLNL	Diffraction imaging
Abraham Szoke	LLNL	Holographic techniques, phasing, imaging
Peter Young	LLNL	Laser education, Coulomb explosions

Richard Lee	LLNL	Coulomb explosions, clusters
Richard London	LLNL	Coulomb explosions, clusters
Rodney Balhorn	LLNL	Sample preparation
Henry Benner	LLNL	Sample selection, injection, orientation
Matthias Frank	LLNL	Sample selection, injection, orientation
Aleksandr Noy	LLNL	Carbon nanotubes, sample preparation
Anton Barty	LLNL	Diffraction imaging and instrumentation
Brent Segelke	LLNL	Sample preparation, diffraction imaging
Daniel Barsky	LLNL	Theory, sample injection

Management, Funding, and Financial Considerations. This experimental program on single particle imaging of biomaterials engages an existing team of about 65 collaborating scientists from 9 countries as listed in the beginning of this LOI. The effort of this instrument development team (IDT) will be coordinated and managed through a steering committee with representation from Uppsala University (Hajdu, PI), LLNL (Chapman, co-PI), SSRL (Hodgson, co-PI) and Oxford (Robinson) and manpower will be expanded as the effort ramps up. It is anticipated that our IDT will interface with SSRL/LCLS to obtain appropriate support in developing detailed designs and engineering to ensure that the experimental system will be fully compatible with, and integrated into, the LCLS experimental program. As a result of the workshop described above on the LCLS bioimaging experiment, we have developed a preliminary conceptual instrument concept and cost. The major elements of this are listed below and for each is given an overall capital/operations cost and a manpower estimate. The estimates are for ***total effort over the 7 year period*** and manpower includes engineering/design, scientific and technical/assembly and operations: The 6 elements are: 1. X-ray optics and experimental front end – includes final focusing, zone-plate imaging, and pulse compression - R&D, $1,500K, 14 FTE; 2. Sample injection and handling – includes R&D and methods for particle and nanocrystal preparation and injection, orientation (magnetic and optical) - $2,900K, 47 FTE; 3. Chamber and Diagnostics – includes R&D at the VUV-FEL and SPPS, equipment for beam characterization and monitoring, pulse diagnostics, integrated visible microscope, mass spectrometer, electron spectrometer, and sample stages - $3,700K, 35 FTE; 4. Detectors – includes two 2D pixel array detectors and associated readout electronics - $2,000K, 2 FTE; 5. Simulations and theory – includes effort for reconstruction development, software and integration, and compute and storage subsystems - $350K, 66 FTE; 6. Other – includes laboratory equipment for sample preparation (visible and electron microscopes, centrifuge, cold room), fs-pulsed laser (microJ/pulse) - $2,600K, 3 FTE. Elements 1. through 6. sum to $13.05M and 167 FTEs over 7 years.

We anticipate building upon funding that is already being committed (or sought in pending applications) for aspects this imaging program by the participating institutions. SSRL, through core research funds and grants (new and pending) from NIH and DOE-BER will contribute $1.27M and 42FTEs. The University of Uppsala will contribute 56 FTEs through existing and submitted Swedish and EU grant applications. We anticipate collaborations with LCLS and with DESY to lead to the detector, but include 2 FTE in this project cost for integration. This leaves $9.78M in equipment/other costs and 69 FTEs. Assuming an average cost of $200K/FTE, this gives a remaining total needed over the seven years of $23.6M ($9.8M + $13.8M). LLNL is seeking strategic laboratory initiative (internal) funds for $5M of this total. The remainder will be sought through the development and submission of DOE proposals of $18.6M (~$12.5M to DOE-BES and ~$6.1M to DOE-BER). Alternative sources of funding could include the NSF or private 3rd party investments.

REFERENCES

References and details of the many workshops and reports related to the scientific cases for the two major X-ray FEL projects in the world (LCLS at Stanford and the European XFEL at DESY)

can be found on the www sites of these two facilities at www.ssrl-slac.stanford.edu/lcls/ and http://xfel.desy.de/content/e169/index_eng.html.

Bogan, M.J. and G.R. Agnes, "MALDI-TOF-MS analysis of droplets prepared in an electrodynamic balance:"wall-less" sample preparation", *Anal. Chem*., **74**, 489-496 (2002).

Chapman, H.N and K. A. Nugent, "X-ray pulse compression using strained crystals," *Opt. Comm.* **205**, 351—359 (2002).

Cleveland, C. L., U. Landman, T. G. Schaaff, M. N. Shafigullin, P. W. Stephens, and R. L. Whetten, "Structural evolution of smaller gold nanocrystals: The truncated decahedral motif," *Phys. Rev. Lett.*, **79**, pp. 1873-1876 (1997).

Elser, V., private communication (2004).

Fajardo, M., Zeitoun, P., Gauthier, J.-C.: "Hydrodynamic simulation of XUV laser-produced plasmas," *Euro. Phys. Journal D*, **29**, 69 (2003).

Gard, E., J.E. Meyer, B.D. Morrical, T. Dienes, D.P. Fergenson, K.A. Prather, "Real-time analysis of individual atmospheric aerosol particles: desing and performance of a portable ATOFMS", *Anal. Chem.* **69**, 4083-4091 (1997).

Gaskell, S.J., "Electrospray: Principles and Practice", *J. Mass Spectrom.*, **32**, 677-688 (1997).

Goodman, J.W., *Statistical Optics* John Wiley, New York (1985).

Haberland, H. *Clusters of Atoms and Molecules*, **52**, Berlin: Springer, (1993).

Hau-Riege, S.P., R.A. London, and A. Szoke, "Dynamics of X-Ray Irradiated Biological Molecules," *Phys. Rev. E* **69**, 051906 (2004). Also published in the Virtual Journal of Ultrafast Science, June (2004).

Hirano, K. and A. Momose, "Investigation of the phase shift in X-ray forward diffraction using an X-ray interferometer," *Phys. Rev. Lett*., **76**, 20, p373 (1996).

Huldt, G., Szoke, A., Hajdu, J., "Diffraction imaging of single particles and biomolecules." *J. Struct. Biol.* **144**, 219–227, (2003).

Martin, T. P., T. Bergmann, H. Göhlilch, and T. Lange, "Observation of electronic shells and shells of atoms in large Na clusters," *Chem. Phys. Lett.*, **172**, pp. 209-213, (1990).

Jarrold, M.F., "Nanosurface chemistry on size-selected silicon clusters," *Science* **252**, 1085-1092 (1991).

Jurek, Z. G. Faigel, and M. Tegze, "Dynamics in a cluster under the influence of intense femtosecond hard X-ray pulses", *Euro. Phys. J. D* **29**, 217 (2004a).

Jurek, Z., G. Oszlanyi and G. Faigel, "Imaging atom-clusters by hard X-ray free electron lasers", *Europhys Lett.*, **65**, 491-497, (2004b). Laarmann, T., H. Wabnitz, J. Schulz, A.R.B. de Castro, P. Gürtler, W. Laasch, T. Möller, "Interaction of argon clusters with intense VUV-laser radiation: The role of electronic structure in the energy deposition," *Phys. Rev. Lett.* **92**, 143401 (2004).

Maier-Borst, M., D. B. Cameron, M. Rokni, and J. H. Parks, "Electron diffraction of trapped cluster ions," *Phys. Rev. A*, **59**, pp. R3162, (1999).

Marchesini, S., Chapman, H. N., Hau-Riege, S. P., London, R. A., Szoke, A., "Coherent X-ray diffractive imaging: applications and limitations," *Opt. Express* **11** (19), 2344–2353, (2003a).

Marchesini, S., He, H., Chapman, H. N., Hau-Riege, S. P., Noy, A., Howells, M. R., Weierstall, U., Spence, J. C. H., "X-ray image reconstruction from a diffraction pattern alone," *Phys. Rev. B* **68** (114), 140101, (2003b).

Miao, J., Hodgson, K., Sayre, D., "An approach to three-dimensional structures of biomolecules by using single-molecule diffraction images." *Proc. Natl. Acad. Sci. USA* **98** (12), 6641–6645, (2001).

Miao, J., Ishikawa, T., Johnson, B., Anderson, E. H., Lai, B., Hodgson, K. O., "High resolution 3D X-ray diffraction microscopy," *Phys. Rev.* **89**, 088303, (2002).

Miao, J., Hodgson, K. O., Ishikawa, T., Larabell, C. A., LeGros, M. A., Nishino, Y., "Imaging whole *Escherichia coli* bacteria by using single particle X-ray diffraction," *Proc. Natl. Acad. Sci. USA,* **100** (1), 110–112, (2003).

Miao, J., H.N. Chapman, J. Kirz, D. Sayre and K.O. Hodgson, *Annu. Rev. Biophys. Biomol. Struct*. **33**, 157 (2004).

Neutze, R. Wouts, D. van der Spoel, E. Weckert, and J. Hajdu, "Potential for biomolecular imaging with femtoscond X-ray pulses," *Nature*, **406**, pp. 752-757, 2000.

Peano, F. Fonseca, R., Silva, L., "Dynamics and control of shock shells in the coulomb explosion of very large deuterium clusters," submitted to *Phys. Rev. Lett.* (2004).

Robinson, I. K., Vartanyants, I. A., Williams, G. J., Pfeifer, M. A., Pitney, J. A., "Reconstruction of the shapes of gold nanocrystals using coherent X-ray diffraction," *Phys. Rev. Lett.,* **87** (19), 195505, (2001).

Rostom, A.A., P. Fucini, D.R. Benjamin, R. Jueneman, K.H. Nierhaus, F.U. Hartl, C.M. Dobson, C.V. Robinson, "Detection and selective dissociation of intact ribosomes in a mass spectrometer", *Proc. Natl. Acad. Sci. USA*, **97**, 5185 (2000).

Röthlisberger, U., W. Andreoni, and M. Parinello, "Structure of nanoscale silicon clusters," *Phys. Rev. Lett.*, **72**, pp. 665-668, (1994).

Shvartsburg A. A. and M. F. Jarrold , "Solid clusters above the bulk melting point," *Phys. Rev. Lett.*, **85**, pp. 2530, (2000).

Spence, J.C.H, U. Weierstall, T.T. Fricke, R.M. Glaeser, and K.H. Downing, "Three-dimensional diffractive imaging for crystalline monolayers with one-dimensional compact support," *J. Struct. Biol.* **144**, 209-218 (2003).

Spence, J.C.H and R.B. Doak, "Single molecule diffraction," *Phys. Rev. Lett*. 92**,** 198102 (2004).

Stephenson, J.L. and S.A. McLuckey, "Charge manipulation for improved mass determination of high-mass species and mixture components by electrospray mass spectrometry", *J. Mass Spectrom*. **33**, 664-672 (1998).

Suess, D.T., K.A. Prather, "Mass Spectrometry of Aerosols", *Chem. Rev.* **99**, 3007-3035 (1999).

Tito, M. A., Tars, K., Valegard, K., Hajdu, J., Robinson, C V. "Electrospray Time-of-Flight Mass Spectrometry of the Intact MS2 Virus Capsid," *J. Am. Chem. Soc.* **122**, 3550-3551 (2000).

Wabnitz, H., L. Bittner, R. Döhrmann, P. Gürtler, A.R.B. de Castro, T. Laarmann, W. Laasch, J. Schulz, A. Swiderski, K. von Haeften, T. Möller, B. Faatz, A. Fateev, J. Feldhaus, C. Gerth, U. Hahn, E. Saldin, E. Schneidmiller, K. Sytdev, K. Tiedtke, R. Treusch, and M. Yurkov, "Multiple ionisation of atom clusters by intense soft X-rays from a free-electron laser radiation," *Nature,* **420**, 482 (2002).

Wang, Q., T.W. Lin, L. Tang, J.E. Johnson and M.G. Finn, *Angew. Chem. Int. Ed.* **41**, 459 (2002).